Contributions of Metallo-β-Lactamase Domain Containing Protein 1 (MBLAC1) to
the Neurobiological Actions of Ceftriaxone

By

Cassandra Lynn Retzlaff

Dissertation

Submitted to the Faculty of the

Graduate School of Vanderbilt

University in partial fulfillment of the

requirements for the degree of

DOCTOR OF PHILOSOPHY

in

Neuroscience

December 16, 2017

Nashville, Tennessee

Approved:

Randy D. Blakely, Ph.D.

Roger Colbran, Ph.D.

Tina Iverson, Ph.D.

Brian Wadzinkski, Ph.D.

TABLE OF CONTENTS

To family, friends, and science enthusiasts.

ACKNOWLEDGEMENTS

LIST OF TABLES

LIST OF FIGURES

LIST OF ABBREVIATIONS

ALS	Amyotrophic Lateral Sclerosis
AMPA	α-amino-3-hydroxy-5-methyl-4-isoxazolepropionic acid receptor
BBB	Blood brain barrier
BSI	Backscattering interfermometry
BSO	Buthinone sulfoximine
CCD	Charged Coupled Device
Cas9	CRISPR associated enzyme
Cef	Ceftriaxone
CephC	Cephalosporin C
CNBr	Cyanogen bromide
CRISPR	Cluster regularly interspersed short palindromic repeat
Ctx	Cortex
Cys	Cysteine
DA	Dopamine
DAT	Dopamine transporter
EAAT	Excitatory Amino acid transporter
GAPDH	Glyceraldehyde 3-phosphate dehydrogenase
γ-GCL	γ-glutamylcysteine ligase
γ-GCLC)	γ-glutamylcysteine ligase catalytic unit
γ-GCLM	γ-glutamylcysteine ligase modifier unit
GFAP	Glial fibrilary acid protein
GLAST	Glutamate/aspartate transporter

Gln	Glutamine
Glu	Glutamate
GLT-1/EAAT2	Primary Astrocytic glutamate transporter
Gly	Glycine
GPCR	G coupled protein receptor
GSH	Glutathione
GST	Glutathione-s-transferase
HAGH	Hydroxyacylglutathione hydrolase
IACUC	Institutional Animals Care and Use Committee
iGluRs	Ionotropic glutamate receptors
IPTG	Isopropyl β-D-1-thiogalactopyranoside
KAR	Kainate Receptor
KO	Knockout
MBL	Metallo-β-lactamase
MBD	Metallo-β-lactamase domain
MBLAC1	Metallo-β-lactamase domain containing protein 1
mGluRs	Metabotropic glutamate receptors
NHEJ	Non-homologous end joining
NMDA	*N*-methyl-D-aspartate receptor
NMDG	*N*-methyl-D-glucamine
RI	Refractive Index
SOD1	Super oxide dismutase 1
SSRI	Selective serotonin reuptake inhibitor

SWIP	Swimming induced paralysis
TBI	Traumatic brain injury
TBST	TBS with 0.01% Tween
TET	Tetracycline
T-REx	HEK Flp-In T-REx-293 cells
[^{3}H]Glu	Tritated (radioactive) Glutamate
WT	Wild type
X_c^-	System X_c^- transporter
#80	#4980 MBLAC1 antibody
#79	#4979 MBLAC1 anitbody

CHAPTER 1

INTRODUCTION

Glutamate and its role in the central nervous system

From the mid-twentieth century on, it has been clear that the common amino acid, glutamate (Glu), participates in the excitation of neurons. Seminal work by Curtis and Watkins details the ability for Glu to depolarize neurons[1]. It is now well recognized that Glu is essential for both the development and function of the brain.[2, 3] Glutamatergic neurons account for about 85% of the neurons in the human neocortex neurons, and over 85% of brain synapses.[4] Glu releasing neurons are present throughout the brain in all major regions from the cortex to the cerebellum to the thalamus, and can be released from a variety of cell types including pyramidal neurons, granule cells, and astrocytes.[5-7]

The release of Glu at synapses via vesicular fusion is similar to that of most Ca^{2+}-dependent neurotransmitter release, where vesicle fusion machinery relies on an influx of Ca^{2+} from presynaptic Ca^{2+} channels to initiate the vesicle fusion process, by which the contents are released into the synaptic cleft.[8] Subsequently, Glu can bind and activate either ionotropic Glu receptors (iGluRs) or the metabotropic Glu receptors (mGluRs) on the postsynaptic neuron.[9] Much of the synaptically released Glu is quickly transported into surrounding astrocytes by a glial expressed Glu transporter (GLT-1 (mouse), EAAT2 (humans)).[10] Glu taken up into astrocytes by GLT-1 is converted into glutamine (Gln) by the enzyme glutaminase, where it can be transported out of astrocytes via system N transporters. When in the extracellular space, neurons expressing system A transporters,

can transport the Gln into neurons where it is rapidly converted back to Glu, and packaged into synaptic vesicles (Figure 1).[11, 12]

As previously mentioned, when neurons release Glu, the neurotransmitter signals through glutamate receptors, iGluRs and mGluRs, of which there are multiple subtypes. First, the iGluRs consist of three main subtypes, α-amino-3-hydroxy-5-methyl-4-isoxazolepropionic acid receptor (AMPA), *N*-methyl-D-aspartate receptor (NMDA), and kainate receptor (KAR), all named after the exogenous agonists that led to the discovery of these receptors (Figure 2A).[9] All subtypes are multi-subunit membrane embedded protein complexes that form a functional ion channel with the binding of Glu. Typically these receptors allow for the passage of positively charged ions, such as Na^+ and Ca^{2+}, with varying permeability to each depending on receptor and subunit combinations.[9, 13, 14] AMPA receptors, located primarily on the postsynaptic neuron, are key torapid Glu induced membrane depolarization in these neurons.[15] AMPA receptors are tetrameric receptors, with each subunit containing four transmembrane domains. These receptors allow the passage of Na^+ ions, and sometimes Ca^{2+} ions, depending on the subunit makeup of the receptor complex. For example, the GluR2 subunit makes any multimeric complex impermeable to Ca^{2+}.[9] The influx of ions is critical for neuronal depolarization, and downstream signal propagation, as this lowers the membrane potential, permitting the activation of NMDA receptors. At resting state, the NMDA receptors need a two-step mechanism to be fully active and allow the passage of positive ions. First, the receptor requires the appropriate ligand (i.e. Glu) and second, the membrane needs to be depolarized slightly to dislodge a Mg^{2+} ion that blocks the channel. NMDA receptors are more permeable to Ca^{2+}, which activates many
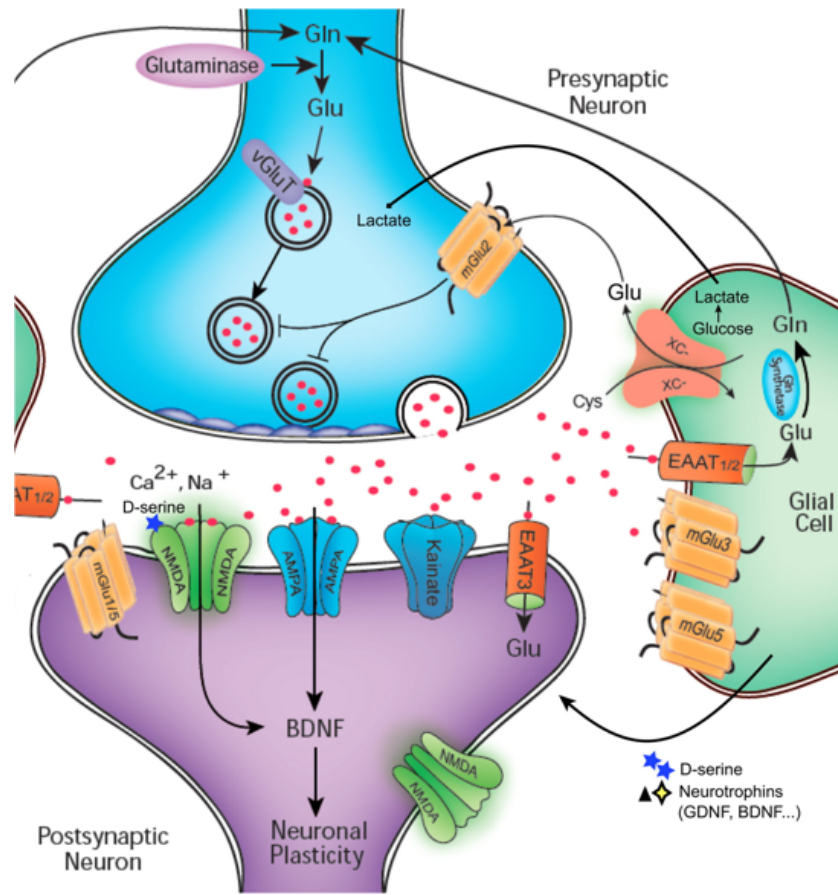
Figure 1. Depiction of glutamatergic synapse. Cycle of Glu from the presynaptic release sites and back. Image modified from Sanacora and Banasr. Biol Psychiatry. 2013 Jun 15;73(12):1172-9.

downstream Ca^{2+}-dependent signaling cascades to evoke acute, as well as lasting, changes within the postsynaptic neurons.[15] The ability for plastic changes are thought to be the underlying mechanisms for learning and memory.[15, 16] Excess Ca^{2+} transported through NMDA receptors is also thought to be the primary culprit in mediating excitotoxicity and cell death due to over excitation (discussed in more detail below).[17] KARs, though less abundantly expressed and studied, pass ions similarly to AMPA and NMDA, due to the similar architecture across the ionotropic receptors families. Studies have shown KARs to be able to signal through G-proteins similar to mGluRs (discussed below). This signaling has been shown to modulate neurotransmitter release, depolarization of the postsynaptic neuron, and participate in the developing nervous system to support proper circuitry formation.[18, 19]

The other class of Glu receptors are the mGluRs, which act through activated effector proteins, as opposed to the channel-like properties of the iGluRs (Figure 2B). The mGluRs consist of three main subtypes of GPCRs. The type I (mGluR1 and 5) are G_q-coupled and activate phospholipase C signaling cascades, type II/III (mGluR2 and 3) are $G_{i/o}$-coupled and inhibit adenylyl cyclase, whereas type IV (mGluR4, and 6-8) are Gs-coupled and activate adenylyl cyclase signaling pathways.[14] The actions of these receptors are important for the more modulatory effects of Glu. Due to the nature of GPCRs, the signaling is on a slower time scale than their iGluR counterparts. The location of these receptors also contributes to the type of signaling they participate. For example, mGluR2 and 3 are primarily located on the presynaptic neuron, and exert inhibitory control over Glu synaptic release.[20] Conversely, mGluR5 is predominantly located extra-synaptically on the postsynaptic neuron where it can modulate AMPA receptor expression

A

AMPA or Kainate

Na$^+$

Glu

Na$^+$

K$^+$

NMDA

Na$^+$

Ca^{2+}

Mg^{2+}

Glu

Zn^{2+}

Gly

PCP

Mg^{2+}

K$^+$

B

Glu

Receptor

G protein

P
P
P

Effector
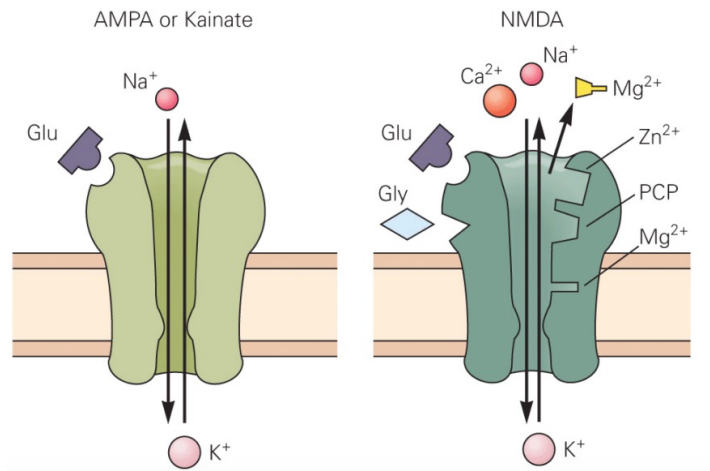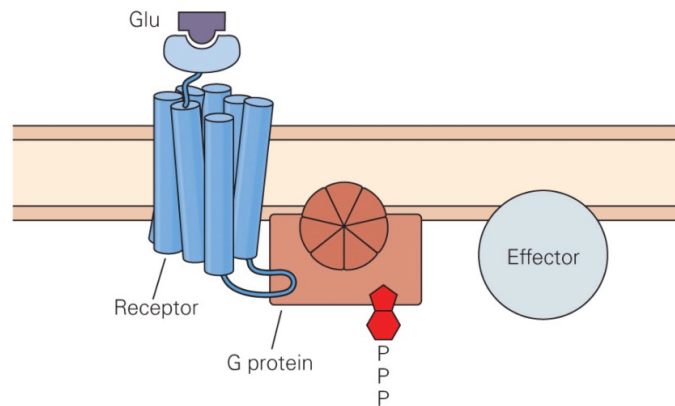
Figure 2. Diagram of the glutamatergic receptors. A) iGluRs and B) mGluRs responsible for propagating Glu signaling in the central nervous system. Image modified form Kandel et al. Principles of Neural Science. 5th Edition, 2012.

and insertion into the membrane, and thereby effect receptor signaling and responsiveness to future Glu activation.[21, 22] The mGluRs receive Glu activation from synaptic spillover from vesicular released Glu, or from tonal, extracellular levels of Glu maintained by mechanisms of glial-mediated Glu extrusion.[23]

Over-activation of Glu receptors can lead to pathological consequences such as disruptions in modulatory signaling or neuronal cell death by excitotoxicity.[17] In order to prevent these effects, astrocytes, and, to a lesser extent, neurons, express Glu transporters that remove Glu from the synapse to maintain low levels of extracellular Glu. Although whole brain concentrations of Glu are in the millimolar range, the extracellular levels are kept to the nano- or micromolar range.[24] The formation of the tripartite synapse (pre- and post-synaptic neurons and the astrocyte) facilitates the spatial and temporal control needed for extracellular Glu levels (Figure 3). The entire excitatory amino acid transporter (EAAT) family helps maintain these consistently low and tightly regulated extracellular levels. There are five transporter members (EAAT 1-5) in this family, all with distinct roles and expression patterns.[25] The most abundant of these transporters is EAAT1 or GLAST (glutamate/aspartate transporter). GLAST is expressed throughout the nervous system, mainly on astrocytes, and is more of a general low-affinity regulator of extracellular Glu.[26] The other highly abundant Glu transporter is EAAT2 or GLT-1, and its primary role is maintaining the clearance of synaptic Glu. This transporter is also expressed primarily on astrocytes and the high density and ability for rapid Glu binding and transport make it crucial for proper neuronal communication.[27, 28] Expression studies show that while GLAST is expressed throughout the astrocyte, GLT-1 protein is densely expressed in the processes that extend into synaptic connections.[29] GLT-1 is also
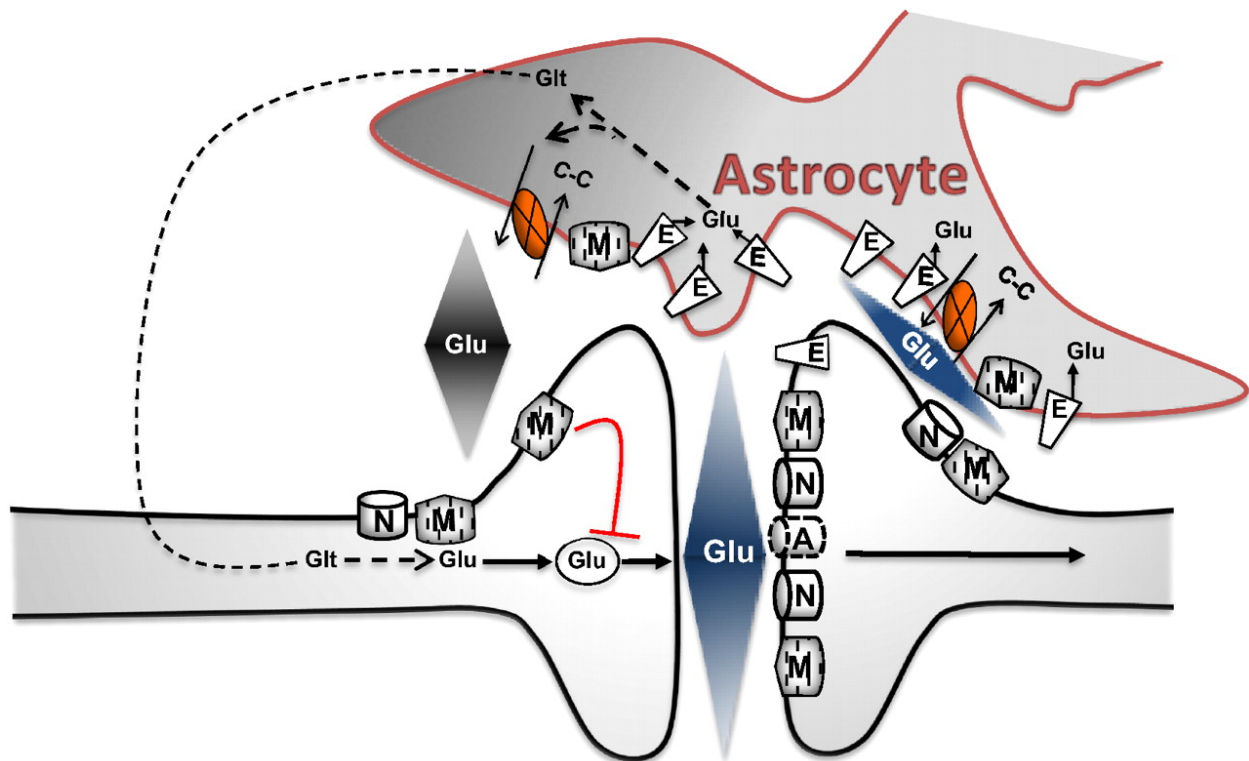
Figure 3. Tripartite glutamatergic synapse. Image more clearly depicts the relative amounts of Glu at the synapse compared to extracellular levels. Also shows the importance of location of GLT-1 and XC- transporters and their contributions to effecting Glu concentrations. Modified from Bridges et al. Pharmacol Rev. 2012 Jul;64(3):780-802.

expressed by neurons at lower levels, but cell type specific knock-out (KO) models indicate that the neuronally-expressed transporters are not critical for proper brain development or mature brain function. Conversely, the KO of the astrocytically expressed GLT-1 results in death of over 50% of the animals after one month of birth, highlighting the importance of proper clearance of synaptic Glu from the synapse.[30, 31] Once Glu is cleared from the synapse it is mainly converted to Gln for transport back to the neurons to maintain the Glu necessary for neurotransmission. A fraction of transported Glu is also used for the synthesis of glutathione (GSH), or as a carbon source for cellular metabolism pathways that are necessary for a functioning nervous system.[32]

In conjunction with Glu from GLT-1 used for GSH synthesis, another transporter, system X_c^- (X_c^-), supplies the other critical element for GSH, cysteine Cys). This Glu/cystine antiporter is responsible for a 1:1 exchange of Glu export to Cys import.[33, 34] The expression and of X_c^- are tightly regulated by cellular redox systems and signaling pathways.[33, 35] X_c^- localizes to astrocytic membranes, but contrary to GLT-1, the physical locationof X_c^- is thought to exist farther from the synapse where the transporter exerts control on extrasynaptic Glu and cystine/Cys levels (refer again to Figure 3). There are few antibodies or *in situ* methods that have been successful in describing the exact localization of this transporter, but it is known to be expressed widely throughout the brain and less so in the periphery, being restricted to few organs (i.e. spleen).[36] This transporter is part of the heterodimeric amino acid transporters (HATs), and is defined by heavy and light chain components. The light chain, known as xCT, is the functional, catalytic antiporter subunit. The heavy chain subunit, 4F2h, is a secondary transporter subunit common to many transporters, that aids in membrane localization and is bridged to the

light chain unit through a disulfide bond.[35, 37, 38] As hinted above, the action of xCT is important for two reasons: it brings cystine into the cell, where it is rapidly reduced to Cys and used for GSH production, and at the same time transports Glu out into the extracellular space. Brain tissue levels of Glu are around 10mM, but because of the many Glu transporters the extracellular concentrations are comparatively low and tightly controlled to the low micromolar range (0.2-9uM).[39] X_c^- is the primary contributor, or modulator, of extra synaptic Glu levels and thereby an important player in the regulation of synaptic transmission. The Glu exported by X_c^- can activate the mGluRs on the pre- or postsynapse (mGLUR2/3 and mGLUR5, respectively), as well as extrasynaptic NMDA receptors.[40, 41] Aberrant signaling or function of this transporter can lead to disruptions in the Glu homeostasis and thereby result in changes to cell signaling, cell death, and maladaptive behaviors.[33, 35]

Given the pervasive and extensive nature of Glu signaling in the brain, it is not surprising that there are many diseases and disorders associated with Glu dysfunction, ranging from depression to amyotrophic lateral sclerosis (ALS), to addiction and Huntington's disease.[42-44] Some of these are rooted in known genetic causes, as in the case with ALS and Huntington's. Familial ALS is associated with a superoxide dismutase 1 (SOD1) point mutation resulting in specific degeneration of the motor neurons of the spinal cord due to dysregulation in redox states, specifically within astrocytes. This mutation, and resultant astrocytic dysfunction, makes the neurons more susceptible to excitotoxicity due to excess Glu in the extracellular space.[45] In this regard, changes in the level and activity of GLT-1 are thought to contribute to the pathophysiology of ALS.[45, 46] Huntington's is a genetic, heritable disease where a trinucleotide (cytosine-adenine-

guanine, CAG) stretch gets repeated in excess. Huntingtin protein with more CAG repeats than normal results in neuronal degeneration that is, again, due in part to excitotoxic mechanisms, and unbalanced signaling between dopamine (DA) and Glu.[47] Other types of Glu related brain injury and degeneration are more acute, but have the same result of neuronal cell death due to over excitation. These include traumatic brain injury (TBI) and ischemic stroke.[48, 49] In both cases, the trauma to the brain causes a significant and rapid elevation of Glu to the site of injury, which then causes a whole host of issues, one of which is cell death.[50] The long term behavioral effects after cell death are dependent on the region of the nervous system that the trauma effects. In particular, cognitive and motor coordination deficits are common symptoms (Figure 4).

Other Glu related disorders are due to changes in glutamate signaling and circuits, and do not necessarily result in cell death or degeneration. These alternations, whether attained over time due to the environment or because of genetic etiologies, have a broad symptomology. From addiction to schizophrenia to depression, there are dysregulations in Glu signaling. Glu signaling, with details of Glu involvement becoming increasingly clear over the past decade.[4, 41, 51, 52] Schizophrenia has long been thought to be due to alterations in DA signaling, but recent evidence supports a dysregulation of NMDA receptors as a contributing factor.[52, 53] Depression, typically treated with a variety of tricyclic antidepressants or SSRIs (selective serotonin reuptake inhibitors) has recently been effectively treated with ketamine, a NMDA antagonist.[54] For over 20 years, there has been evidence that glutamatergic synaptic plasticity could play a role in depression, but because of the efficacy of SSRIs, the role of Glu in depression has not been thoroughly understood or researched. It is not necessarily surprising to find that altered
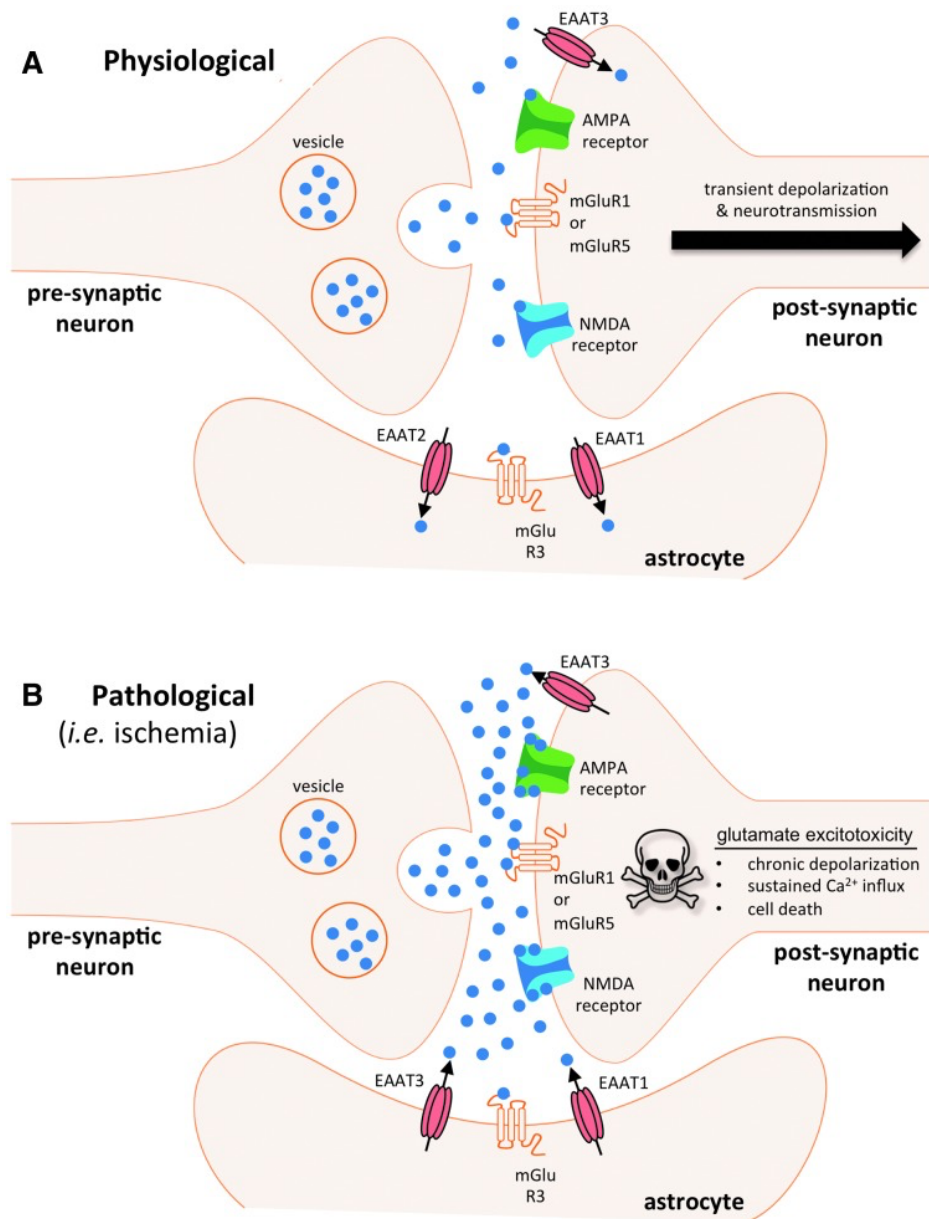
Figure 4. Diagram of neuronal cell death due to excitotoxicity. Glu is released from the presynaptic terminal but not cleared efficiently, resulting in over excitation of the postsynaptic receptors. In the instance depicted above ischemic stroke also induces reverse function of EAATs increasing synaptic Glu. Modified form Khanna et al. Antioxid Redox Signal. 2015 Jan 10;22(2):175-86.

Glu signaling could be a factor in depression onset and progression, as Glu controlled or modulated circuits are intimately connected to cognitive and emotional processing, the two main components that are effected in major depressive disorder.[55] Importantly, a large population with treatment resistant depression still need effective therapies.[56] Targeting glutamatergic systems may be the next avenue in developing pharmacotherapies for depression. In the process of addiction, from acquisition to withdrawal to relapse, there are neuronal plasticities continually adapting and changing, and eventually these changes become a permanent rewiring of natural reward circuits.[57] These of learning and memory plasticity mechanisms are well documented to be glutamatergic processes. In the progression of addictive behaviors, expression changes to proteins that also directly interact with Glu, like GLT-1 and X_c^- play a role in modulating this maladaptive synaptic plasticity (Figure 5).[41]

The two main types of Glu dysfunction described above have few currently available drugs to relieve symptoms or reverse behavioral maladaptation. There are many drugable targets of the Glu signaling system, but with Glu affecting all of the most basic functions of the brain, designing effective drugs can be difficult and targeting many would likely produce a variety of undesirable side effects. Regardless, further research and compound development could be quite useful to a huge population of people suffering from the diseases described above, along with others.

The discovery of β-lactam antibiotics as neuroprotective agents

Jeff Rothstein's group, well known for efforts to explore mechanisms associated with ALS, sought to identify compounds that targeted the Glu system. One of their studies
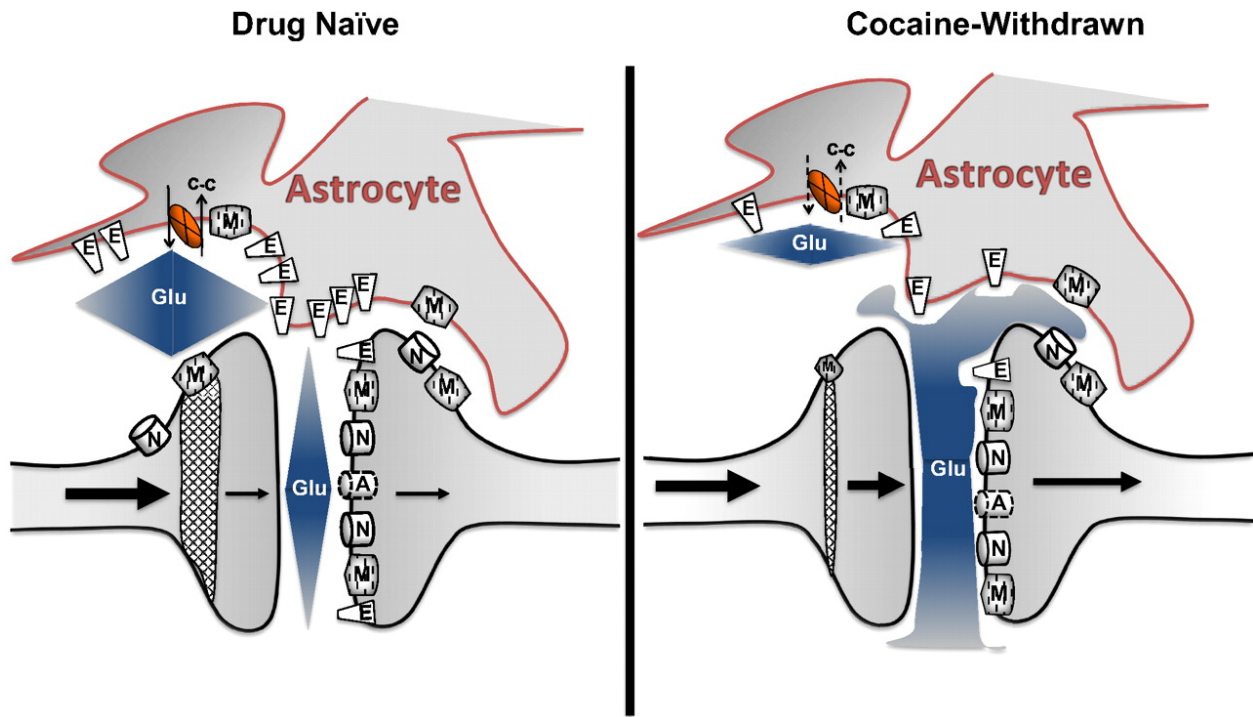
Figure 5. Model of glutamatergic synaptic changes after drug exposure. Reduction in transporter function leads to changes in extrasynaptic Glu signaling, both on the pre- and post-synapse. These changes correlate to the behavioral maladaptation seen in animal models of addiction. Modified from Bridges et al. Pharmacol Rev. 2012 Jul;64(3):780-802.

aimed to look for compounds that could offer neuroprotection by increasing the expression of GLT-1 to combat the excitotoxicity based neurodegeneration. Over ten years ago, his group focused on testing FDA approved pharmaceuticals for off target effects that could alter GLT-1 expression and easily translate to the clinic.[43] Through this screen of possible neuroprotectors, it was discovered that one class of compounds, the β–lactam antibiotics, was particularly effective at increasing the expression of GLT-1. β–lactam antibiotics are used in the clinic for the treatment of bacterial infections. As a whole, most of the antibiotics tested were able to induce GLT-1 expression, and through luciferase based assays, they determined this was probably due to transcriptional activation. In this initial study, both *in vitro* and *in vivo* models were used to show that β–lactam antibiotics could prevent cell death, slowing disease progression in an animal model (Figure 6).[43] The antibiotic ceftriaxone (Cef) was focused on in this study, and in future work, because of its high potency and its ability to cross the blood brain barrier (BBB).[58]

Rothstein's initial findings drove other research groups to explore the effects of Cef in different animals models with underlying Glu dysfunction. Similar to the effects seen in Cef action with models of ALS, models of brain trauma by modeling ischemic stroke have shown that pretreatment with Cef can reduce the amount of cell death and improve recovery from such an event.[49] In addition to excitotoxic events, Cef has demonstrated to be effective in reestablishing Glu homeostasis and reverse maladaptive circuit changes, specifically and most studied, in rodent models of addiction.[59] It is in this field that the bulk of Cef effects have been studied with Peter Kalivas' group pioneering these efforts. Primarily, their findings have shown that Cef treatment during the abstinence period can
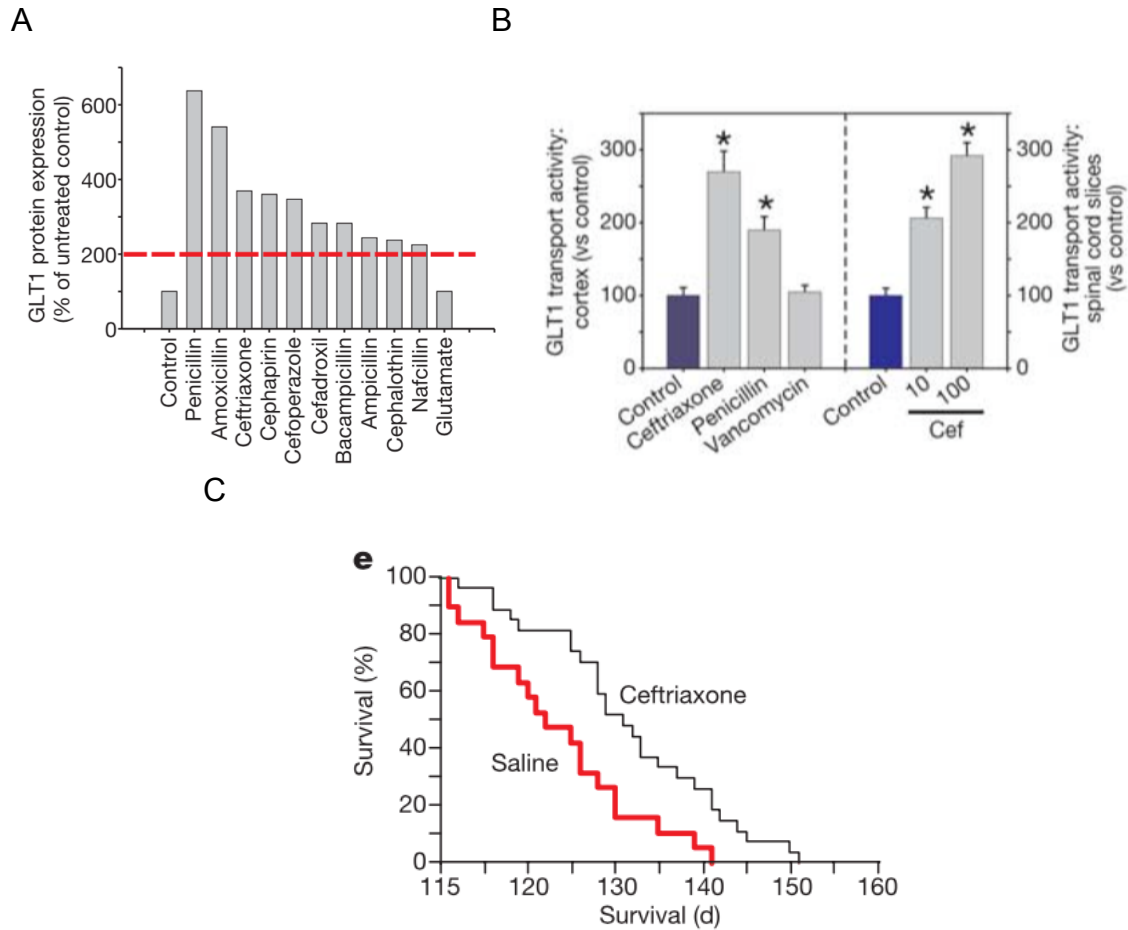
Figure 6. β-lactam compounds found to be a novel class of compounds to be neuroprotective agents. A) Bar graph depicting efficacy of different β-lactam antibiotics to increase the expression of GLT-1 *in vitro*. B) Ability for β-lactams to increase GLT-1 activity in the brain and in spinal cord slices. C) *In vivo* data showing ability for Cef to increase the life span of animals models of ALS. Data panel is taken from figures in Rothstein et al. Nature. 2005 Jan 6;433(7021):73-7.

blunt the reinforcing effects of cue, context, and drug exposure.[42, 59] These investigators were the first to report that X_c^- contributes to the mechanism of action of Cef administration.[59] Subsequently, many other groups have studied the effects of Cef on reinstatement with other drugs, reward preference, locomotor behavior, and have begun to look at the molecular changes that occur in these different conditions.[60-62] Cef administration has been shown to be effective at blunting effects of all drugs of abuse tested, but interestingly does not have effects on natural rewards.[63] While this is indicative of Cef being a viable candidate for treatment of all forms of addiction, it also points to a common mechanism of Glu dysregulation that is hijacked during the process of developing addiction.

The *in vivo* evidence for neuroprotective effects of Cef are convincing and much more expansive than the overview presented here, but all of this is indicative that β-lactam antibiotics may be effective treatments for diseases with underlying glutamatergic dysfunction. However, a lack of understanding of the mechanism of how Cef works on a molecular level makes its use less desirable. Having already a particular use as an effective antibiotic, it is hard to prescribe Cef for off-label use when it can increase risk of bacterial resistance. Additionally, the high dose of Cef that is needed to be administered is not efficient for large scale studies.

To get at a more complete understanding of the molecular changes that take place during Cef administration, several groups have turned to reduced cell preparations and *in vitro* studies to provide evidence of the proposed downstream effects of Cef treatment. A handful of studies have indicated that the observed expression changes to both GLT-1 and X_c^- transporters are due to transcriptional regulation. GLT-1 and X_c^- are known to be

transcriptionally controlled by NFκB and Nrf2, respectively.[64, 65] Data using primary cultured astrocytes demonstrates that Cef treatment on cultured cells increases expression and nuclear localization of both transcription factors (NFkB and Nrf2). These changes are paralleled by concordant changes in transporter expression, indicating transcription activation is needed for Cef action.[64-66] These studies have also pointed out that, in contrast to known transcriptional activators (i.e. tBHQ), Cef treatment requires more time to activate these transcriptional mechanisms and could contribute to the reason why in every study of *in vivo* treatments of Cef need at least five days of administration to see neurological effects.[65] The *in vitro* work characterizing Cef action points to mechanisms upstream of the transporters that drive the neuroprotective effects. However, though this previous work is convincing, there are caveats to using *in vitro* systems. It is well understood that the expression of certain proteins is not necessarily recapitulated *in vitro* as it is *in vivo*. To this point, it was recently reported by Lori Knackstedt's group that there are no changes in mRNA levels of either GLT-1 or X_c^- with Cef treatment *in vivo*.[67]

As demonstrated by these opposing findings, research in this area is still necessary, ongoing, and lacks a molecular target of Cef to activate the transporter expression changes, whether via transcriptional regulation or other mechanisms. Few groups have tried to isolate a binding partner for Cef within the cell, but as with the above results, there is still a debate on the validity of the methods utilized. The two brain proteins that have been implicated in Cef binding are glial fibrillary acid protein (GFAP) and α−synuclein.[68, 69] Both proteins were shown to have the ability to interact with Cef through methods that require the use of purified protein. These methods also required an extended incubation period, on the order of days, to see the effects of Cef. Molecular

computer modeling suggested the capability of binding, even though neither of these proteins have the canonical binding domains known to interact with Cef and other β–lactam antibiotics.[68, 69]

Identifying potential targets for Cef may benefit from an understanding of the known mechanisms of Cef. Similar to all β–lactams, Cef, is a four-membered ring structure that inhibits bacterial growth via blockade of cell wall synthesis.[70, 71] Over time, bacteria have evolved to produce mechanisms against β–lactam compounds in order to resist their deathly effects. Through efflux mechanisms and expression of β-lactamase enzymes, bacteria can ward off antibiotic action.[72] β–lactamase enzymes can catalytically inactivate these molecules through cleavage of the C-N bond of the β–lactam ring structure.[70, 73] These enzymes, first described in the mid 1960s, were found to be a threat to bacterial infection treatment, and are still seen that way today. Much more is known about their mechanism of action, and thousands of types and different β-lactamase enzymes have since been found.[73] Species outside of bacterial world also express β-lactamase-like proteins. However, bacterial enzymes have been the most widely studied and understood.

There are four main groups of β-lactamases based on structure. Groups A, C, and D are the serine lactamases, meaning a serine in the catalytic site is required for action. Group B is comprised of the metallo-β-lactamases (MBL), which require the presence of divalent metal ions, typically zinc.[73, 74] The serine enzymes were the first discovered in a variety of bacterial species and posed the most prominent threat to clinical populations. Whereas the serine lactamases are the most widely expressed type of β-lactamase enzymes, the MBLs, originally not thought to be threatening, are just as worrisome for

bacterial resistance.[70] Their reliance on divalent ions for activity allows them to be more effective at hydrolyzing some of the less classical β-lactam subtypes (i.e. carbenapems, or cephalosporins).[75] The ability for these inducible, and mobile bacterial genes to easily transfer from species to species make them dangerous as a resistance mechanism for bacteria.[76]

For catalytic action, MBLs in bacteria require the presence of four to five His residues, and an Asp residue that will coordinate the catalytic site and Zn^{2+} ions. These diverse enzymes have distinct structural and sequence divergence from the serine lactamases.[77] Crystallographic studies of a zinc MBL from *Bacillus cereus* allowed for a more detailed understanding of the mechanism and necessity for metal ions in its function (Figure 7A). These studies, detailing the crystal structure from Bacillus cereus, gave rise to the understanding of a novel protein fold of the MBL proteins, the αββα fold (Figure 7B).[78] As mentioned previously, there are many species and organisms that also express β-lactamase proteins, and these include the MBL family. However, many of these proteins are not traditional β–lactamase enzymes with traditional substrates, but the catalytic mechanisms are typically conserved.[79]

The identification of a metallo-β-lactamase containing protein, MBLAC1

In 2015, Hardaway and colleagues from the Blakely lab reported the identification of a novel metallo-β-lactamase domain containing protein, designated as SWIP-10 in the nematode *C. elegans.* Using the mutagenic compound ethyl methanesulfanate, our lab created multiple *C. elegans* lines with disruptions in genes functionally linked to

A
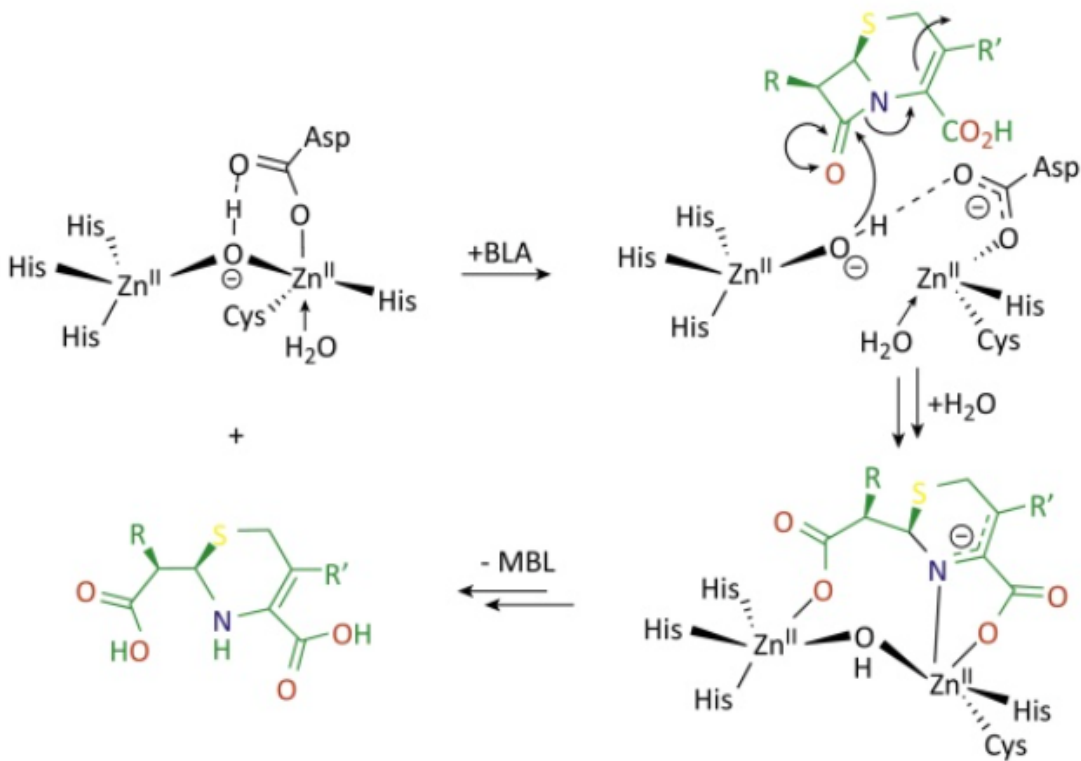
B
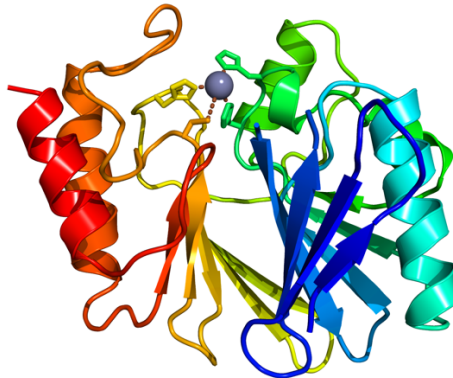
Figure 7. Metallo-β-lactamase enzyme mechanism and fold. A) Catalytic mechanism requires coordination of Zn^{2+} ions and water molecule to break open the β-lactam ring, rendering them inactive. Image taken from Pentanatti et al Trends Biochem Sci. 2016 Apr;41(4):338-55. Structure taken from online PDB files (http://www.rcsb.org/pdb/home/home.do File ID:1BMC)

dopamine signaling.[80] Because *C. elegans* have a simplified nervous system, studying proteins that regulate neural signaling is easier than in the more complex mammalian brain. Additionally, there are many phenotypic screens one can do in *C. elegans*, that are more efficient than mammalian experimentation. DA in the worm, as well as in humans, can control movement, allowing our lab to isolate mutagenized worms that effected DA signaling in worms based on the tractable phenotypic screen called SWIP (Swimming Induced Paralysis).[80] Using this screen, two mutations within the same gene led to a hyperdopaminergic phenotype which caused the SWIP phenotype. These mutations were traced to the gene now annotated as *swip-10*. The two mutations within the *swip-10* gene were single nucleotide changes that resulted in either a missense or a nonsense mutation. The missense mutation (vt33 per our lab's notation) changes a Glu to a Gly residue, whereas the nonsense mutation (vt29) changes a Trp to a stop codon, and results in an early truncation of the protein.[81] Using a fluorescent reporter, under control by the endogenous promoter of the *swip-10* gene, expression was observed outside of the DA neurons and in particular, high expression was present in the glial cells of the worm.

Further experiments with Ca^{2+} imaging revealed that glial loss of *swip-10* resulted in hyperexcitability of DA neurons, indicating that SWIP-10 normally prevents overexcitation of DA neurons that can cause excess release of DA and leading to the SWIP phenotype.[81] Genetic manipulations showed that deletion of certain Glu receptors resulted a suppression of the SWIP phenotype, indicating that Glu signaling is, in part, causing the changes seen in the *swip-10* mutants (Figure 8).[81] This intersection of DA and Glu signaling is of interest, not only on a basic signaling level, but also because much
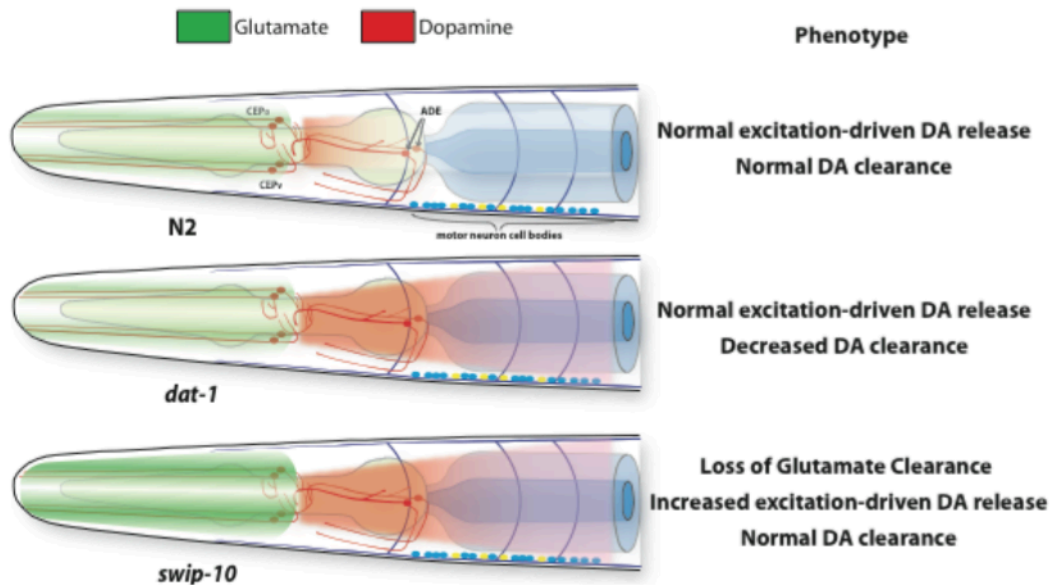
Figure 8. Model of loss of *swip-10* in *C.elegans*. Absence of *swip-10* results in increased dopaminergic tone on the cholinergic motor neurons causing paralysis in water. This is thought to be driven by excess Glu over activating the DA neurons. Image from Hardaway et al. J Neurosci. 2015 Jun 24;35(25):9409-23

evidence indicates that certain disease from schizophrenia to addiction, to Huntington's Disease have etiologies in the dysregulation of both DA and Glu.[47, 82, 83] Due to this connection to human health and disease, the SWIP-10 amino acid sequence was examined using the NCBI protein BLAST tool to look for other homologous protein that exist in other species. Here it was found that a MBL domain containing protein (MBLAC1) was the closest relative to SWIP-10 in mammals.[81] There is about 35% sequence homology between the two proteins (Figure 9A). Other proteins across phylogeny also share a metallo-β-lactamase domain (MBD) that comprises the majority of the coding sequence like MBLAC1, whereas SWIP-10 and nematode orthologues (see *C. briggsae* in Figure 9B) possess a much longer N-terminus with no identified functional domains. The main part of the homology between MBLAC1 and SWIP-10 is derived at the C-terminal end of the proteins where SWIP-10 houses its MBD. MBLAC1 has about half as many amino acids as SWIP-10, and most of those comprise the MBD. The MBDs of each protein illustrated share His and Asp residues characteristic of metal binding and catalysis, respectively. Both MBLAC1 and SWIP-10 have the defining residues of the MBL domain; HxHxDHnHnH, where x stands for any one amino acid and n for any amino acid but more than one. Site-directed mutagenesis experiments with SWIP-10 in the worm showed that previous successful rescue of the SWIP phenotype with cDNA was lost after the His residues of SWIP-10 were mutated to Ala. As with the mutations originally found in the mutagenesis screen, the His residues seem necessary for function or proper folding of the protein.[81] MBLAC1 contains this same defining motif within its protein sequence, which suggests that the protein has enzyme activity. When MBLAC1 was originally found to be a putative orthologue for SWIP-10 there were no published
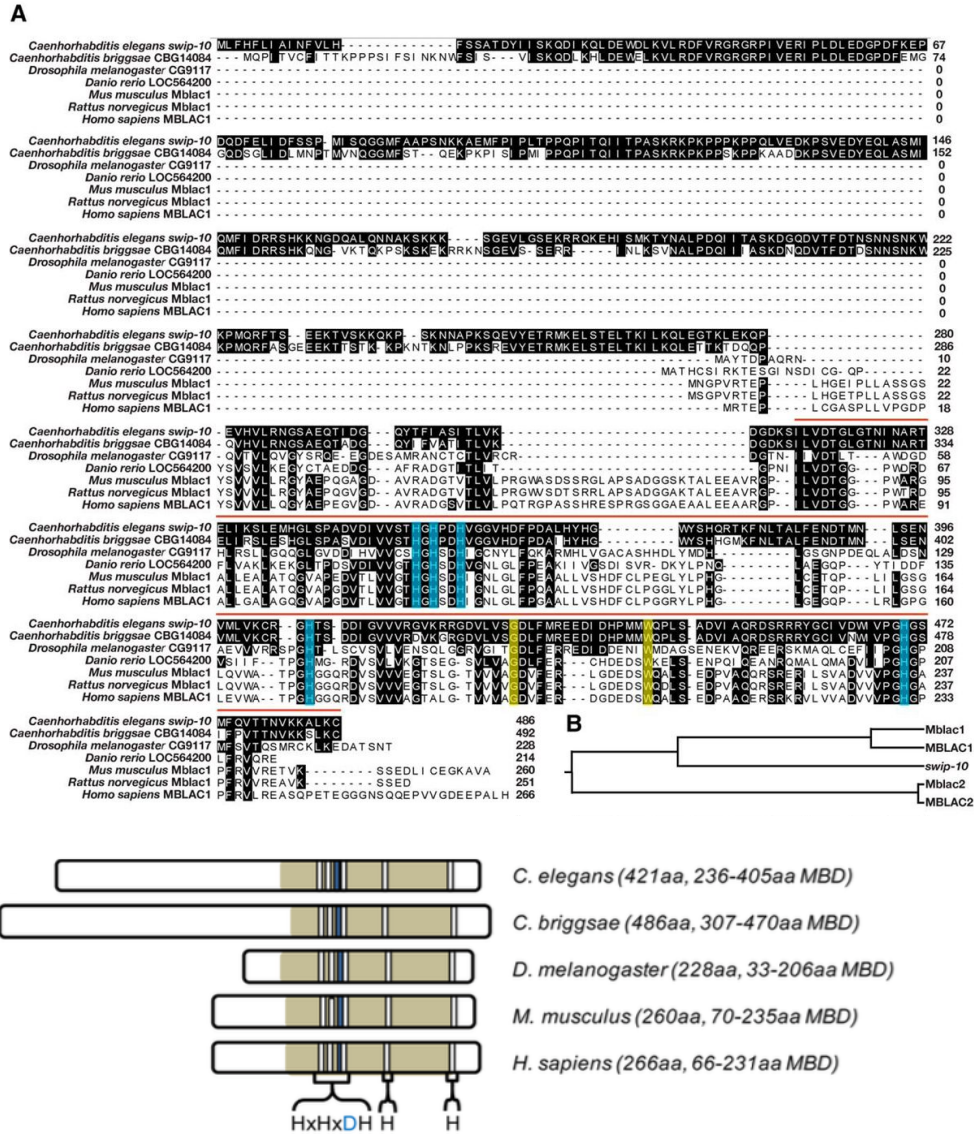
Figure 9. MBLAC1 across phylogeny. A) Amino acid sequence homology across phylogeny from *C. elegans swip-10* to mammalian MBLAC1. Highlighted in black are residues that are exactly conserved from SWIP-10. Blue highlighted residues are the His that are critical for forming the catalytic core of the molecule. Yellow residues highlighted are where original siwp10 mutations. Image from Hardaway et al. J Neurosci. 2015 Jun 24;35(25):9409-23.B) Alignment of putative MBLAC1 orthologues across phylogeny. Except for nematodes, the MBD is the primary component of these proteins. Bars represent critical residues for metal binding and catalytic activity (His in white, Asp in blue, "x" indicates any other amino acid). MBD positioning within each protein (aa=amino acids) was established with the SMArt database online tool (acquisition number SM00849). Figure modified form Retzlaff et al. ACS Chem Neurosci. 2017 Oct 18;8(10):2132-2138.

studies looking at what role MBLAC1 plays within the cell, or how it fits within the larger framework of brain and behavioral function. Initial studies into MBLAC1 expression in mammalian systems discovered mRNA expression within the brain and peripheral tissues like the heart, lung, and liver (Figure 10). Our interest lies in what function MBLAC1 has within the brain, which it is highly expressed per the mRNA.

Before the work presented below, there were only data describing the location and existence of the MBLAC1 gene that encodes a protein with a single MBL domain. MBLAC1 is not the only MBL containing protein expressed in mammals. There are 18 known human MBL fold proteins that are divided into three groups based on function and substrate recognition. The first of these subgroups includes MBLAC1 part of the glyoxalase II family. The enzymes of this family have catalytic mechanisms that are most closely related to those of the bacterial enzymes.[79] This being said, the substrates hydrolyzed vary widely within the family and are quite different from bacteria. Only three of the seven enzymes in the subgroup have been identified with a known role in the cell, whereas the others remain to be studied, including MBLAC1. The enzyme namesake of this glyoxalase group, GLOII or HAGH (hydroxyacylglutathione hydrolase) is responsible for converting toxic aldehyde molecules into cell stable compounds that can signal on their own, such as GSH and lactate.[79, 84] Another characterized MBL in this group is ETHE1, which is a mitochondrial expressed protein that detoxifies persulfide molecules into GSH and persulfite. This enzyme is correlated with encephalopathy and is shown to interact with NFκB and HDAC proteins. The last defined protein in the group is PNKD, which is also associated with brain disorders, specifically Dystonia 8.[79] The proteins within the group that MBLAC1 aligns, all seem to play important roles in either brain cell
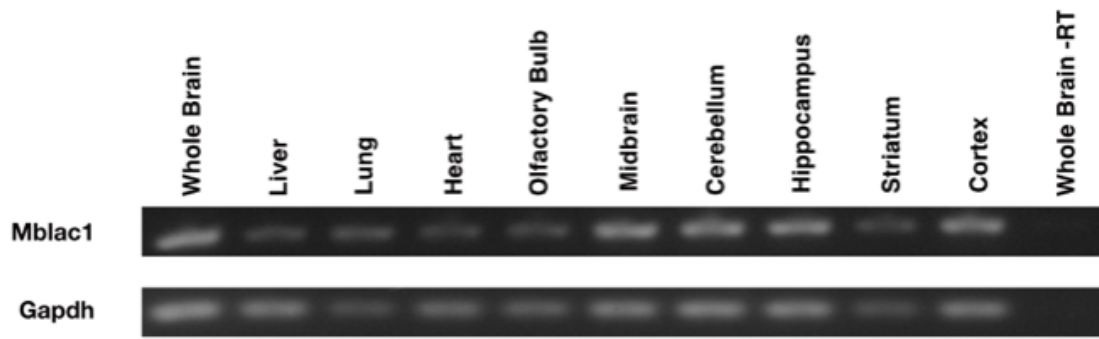
Figure 10. RT-PCR of Mblac1 in mouse tissue. Peripheral and brain tissue were analyzed for mRNA expression of Mblac1. Image modified from Hardaway et al. J Neurosci. 2015 Jun 24;35(25):9409-23.

metabolism or cell signaling mechanisms. Though we have yet to uncover what role MBLAC1 is playing within the cell, we can hypothesize that it may be participating in the overlapping webs of cellular metabolism and might point to novel pathways that further detail the complexities of cellular signaling. Other mammalian MBL enzymes are known to participate in cellular detoxifying pathways and this could be another pathway in which MBLAC1 participates.

Given the expression of MBLAC1 in the brain and the MBD it contains we hypothesize:

1. MBLAC1 could interact with Cef and be a molecular target of Cef in the brain.

2. The interaction of Cef and MBLAC1 is necessary for *in vivo* action of Cef and its neuroprotective actions. Using MLBAC1 KO mice I can examine the sufficiency or necessity of MBLAC1 expression in the brain.

3. MBLAC1's endogenous role may be to participate in cellular redox pathways within the cell. To gain insight into the potential role of MBLAC1 I will determine the possible overlap of Glu transporter regulation and MBLAC1 expression using *in vitro* methods.

CHAPTER 2

MBLAC1 AS A SPECIFIC, HIGH AFFINITY TARGET FOR CEFTRIAXONE

Introduction

Molecules bearing a four membered β-lactam ring, typified by penicillin, are widely prescribed antibiotics.[85] Within this family of compounds exist many other more diverse 'R' groups off the β-lactam ring. These compounds include penicillin derivatives, cephalosporins, and carbapenems, among others.[86] All of these compounds work similarly to interfere with cell wall synthesis and to halt bacterial cell division.[70, 87] This will lead to bacterial cell death unless β-lactams are inactivated by bacterial mechanisms that result in compound export or compound inactivation, of which the latter is by far the most common and effective. This process is largely achieved by the expression of β-lactamase proteins.[72] As touched on in the introduction, these molecules pose the greatest threat to the use of antibiotics in the clinic because of the resistance they provide for infectious bacteria.[88] Interestingly, studies over the past decade have revealed that a number of these β–lactam compounds exhibit CNS actions independent of their antimicrobial actions.[43, 89, 90] Rothstein and colleagues, seeking opportunities to repurpose FDA-approved medications for the treatment of ALS, identified β-lactam antibiotics as candidate compounds based on their ability to elevate expression of the Glu transporter, GLT-1. In particular, Cef, a CNS penetrant, cephalosporin-type, β-lactam antibiotic, showed high-potency (EC_{50}=3.5 μM) in *ex vivo* studies.[43] Subsequently, multiple groups have demonstrated Cef action in a range of neurological and neurobehavioral disease models, including those for stroke, epilepsy, Parkinson's Disease, and addiction,

paralleled by normalization of pathological elevations in synaptic Glu levels.[49, 59, 64, 90-95] Cef has also been reported to elevate expression of the glial expressed X_c^-, thereby also normalizing extrasynaptic Glu levels.[59, 65, 96, 97]

At present, the CNS target responsible for Cef action is unknown, although studies have proposed possible interactors,[68, 69] and NFκB and ARE-1 transcriptional programs appear to contribute to Cef induction of GLT-1 and X_c^-, respectively.[64-66] Studies using circular dichroism and modeling have pointed to small cytosolic proteins expressed in either neurons or glia as having the ability to interact with Cef. One protein insinuated to interact with Cef is α–syneuclein.[68] Additionally, GFAP, a glial expressed protein, has also been implicated in binding with Cef, using similar tools as those employed in the α–synuclein study. The Cef-GFAP interaction affinity could not be directly assessed, but using molecular modeling it is suggested that these two can interact outside the presence of a canonical binding motif.[69] Additionally, the methods used require high quantities of purified protein which makes these data hard to interpret since there is no cellular context from which to extrapolate functional consequence.

Understanding Cef's mechanism of action could provide opportunities to develop new therapeutics for the many disorders attributed to Glu dysfunction. As discussed in the Introduction, identified mutations in the *C. elegans* gene *swip-10* result in Glu-dependent, DA neuron hyperexcitability. Rescue studies indicate that loss of SWIP-10 function in glia accounts for these effects, suggesting that the protein participates in glial regulation of extracellular Glu homeostasis, such as those impacted by Cef.[81] To date, no studies have explored the ability of MBLAC1 to interact with Cef.

In this study, we pursued the hypothesis that MBLAC1 is an endogenous, CNS-expressed binding partner for Cef using affinity chromatography and backscattering interferometry (BSI). Though affinity chromatography is an effective method the non-isotopic nature of BSI allowed us to more quantitatively asses the interaction between Cef and MBLAC1. As shown below, these complementary approaches demonstrate specific, high-affinity, temperature-sensitive binding between MBLAC1 and Cef, both in cell and brain lysates. Moreover, immunodepletion studies support MBLAC1 as a major, if not exclusive, CNS target for the antibiotic.

Methods

Materials and Animals

All biochemical reagents, salts and buffers were obtained from Sigma-Aldrich (St. Louis, MO) unless otherwise specified and were of the highest quality available. All experiments with animals were performed under a protocol approved by the Vanderbilt Institutional Animal Care and Use Committee (IACUC). Studies with mice utilized animals of the C57BL/6J strain obtained from Jackson Laboratories (Bar Harbor, ME).

Polyclonal Antibody Generation

Mouse brain mRNA was isolated as described[81] and then *Mblac1* cDNA was amplified by PCR prior to cloning in frame with glutathione S-transferase (GST) in pGEX2T (GE Healthcare Life Sciences, Chicago, IL), followed by transformation into BL21 cells (New England Biolabs, Ipswitch, MA). Expression of GST-mouse MBLAC1 fusion protein was induced using 0.3 mM isopropyl β-D-1-thiogalactopyranoside (IPTG)

and purified from bacterial cells via affinity chromatography using glutathione-coupled Sepharose® (GE Healthcare, Chicago, IL), following manufacturer's protocol. Purified GST-mouse MBLAC1 with adjuvant was injected into two rabbits (#4979 (#79) and #4980 (#80), Thermo Fisher, Waltham, MA) and boosted monthly to produce antiserum. To purify antisera, we cloned mouse *Mblac1* cDNA in frame with maltose binding protein (MBP) coding sequences in pMal-cRI (New England Biolabs, Ipswich, MA). Full length MBP-mouse MBLAC1 protein was generated as described for GST-mouse MBLAC1. MBP-mouse MBLAC1 fusion protein was purified via affinity chromatography over amylose resin (New England Biolabs, Ipswich, MA USA) and concentrated by spin filtration. To remove GST-directed antibodies, we incubated antisera with MBP-mouse MBLAC1-conjugated Affi-gel 10 (BioRad Clarity ECL, Hecules, CA), followed by three washes in wash buffer (20 mM Tris-HCl, 200 mM NaCl, 1mM EDTA, pH 7.4). Bound antibodies were eluted with 150 mM glycine pH 2.0, collecting 1mL fractions into 200 μL 2M Tris-HCl pH 8.0 for neutralization. Samples were pooled and dialyzed in 1X PBS (290mM NaCl, 3mM KCl, 10mM NaHPO$_4$, 1.8mM KH$_2$PO$_4$) at 4 °C overnight. Dialysate was then concentrated by spin filtration and assayed for protein content (Bradford, Bio-Rad, Hercules, CA). Antibodies were used at 1μg/mL for Western blots unless otherwise specified.

HEK Inducible Cell Line Generation

HEK Flp-In T-REx-293 cells (T-REx) expressing mouse or human MBLAC1 proteins were generated per manufacturer's (ThermoFisher, Waltham, MA, USA) instructions. Briefly, mouse and human *Mblac1* cDNAs were subcloned into

pcDNA5/Frt/TO vector and then co-transfected with pOG44 plasmid (encoding Flp recombinase) by lipid based transfection into Flp-In T-REx-293 cells using TransIT-LT1 (Mirus, Madison, WI). Stable integrants were isolated following selection with 100 µg/ml hygromycin. Expression of MBLAC1 protein was induced by addition of 1 µg/mL tetracycline (TET) to the media. Maintenance media contained 15 µg/mL blasticidin (Life Technologies/ThermoFisher, Waltham, MA), 100 µg/mL hygromycin B (Life Technologies/ThermoFisher, Waltham, MA) as selection agents, in addition to 10% fetal bovine serum (Gibco/ThermoFisher, Waltham, MA), 2 mM L-glutamine, and 100 Units/mL penicillin-100 µg/mL streptomycin. See figure 11 for diagram of T-Rex cells.

Western Blotting

Protein samples for Western blot analysis were quantified for total protein (BCA Pierce/ThermoFisher, Waltham, MA) and heated to 95 ^{o}C for 5 min with 1X Laemmli buffer before separation via SDS-PAGE using 10% polyacrylamide gels and transfer to Immobilon PVDF membranes (Millipore, Billerica, MA). Membranes were blocked for 1 hr at 25 ^{o}C (room temperature) with 5% milk in TBS/0.1% TWEEN (TBST). Primary antibody, diluted 1:1000 in 5% milk/TBST, was incubated with membranes overnight at 4 °C. After washing 4x for 5 min with TBST, secondary antibody (peroxidase-conjugated mouse-anti-rabbit, Jackson ImmunoResearch, West Grove, PA) in 5% milk/TBST was incubated for 1 hr at rt. Blots were washed again before band visualization and quantitation by enhanced chemiluminescence (BioRad Clarity ECL, Hercules, CA) using an ImageQuant LAS 4000 imager (GE Heathcare Life Sciences, Chicago, IL).
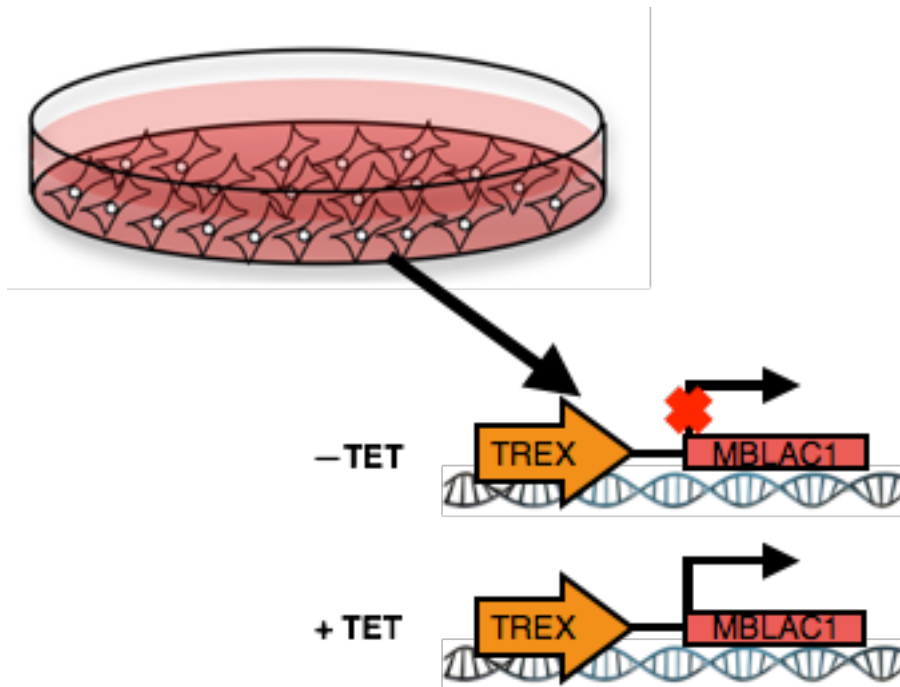
Figure 11. HEK T-REx cell gene induction. Diagram of TET activated gene transcription is mediated within the HEK T-REx cells used for Cef and MBLAC1 bindning assays.

Subcellular Fractionation

Plated 3T3 cells were washed in PBS and pelleted for resuspension in a digitonin buffer (150 mM NaCl, 50mM HEPES, 200 µg/mL digitonin, pH 7.4) for 10 min while rotating. Lysate was then spun at 2000xg and resultant supernatant was kept (cytosolic fraction). The remaining pellet was resuspended in NP40 buffer (150 mM NaCl, 50 mM HEPES, 1% NP40, pH 7.4) and lysate was left on ice in NP40 buffer for 30 min and then centrifuged at 7000xg. Resultant supernatant was kept for membrane and organelle fraction, whereas the pellet was resuspended in RIPA buffer (150 mM NaCl, 50 mM HEPES, 0.5% Na-deoxycholate, 0.1% SDS, 1 U/ml Benzonase, pH 7.4) and rotated for 1 hr at 4°C then centrifuged for 10 min at 7000xg. Supernatant was kept for nuclear protein fraction. Each fraction was then subjected to Western blot analysis as described above.

Immunodepletion Studies

Wild type C57BL/6J mice (Jackson Labs, Bar Harbor, ME) were rapidly decapitated and frontal cortex was dissected. Tissue was homogenized in ice cold 20 mM HEPES and protease inhibitors (pH 7.4) using a Dounce homogenizer (Wheaton, Millville, NJ), and then sonicated (F60 sonic dismembrator, Fisher Scientific, Waltham, MA) using 5, 1 sec pulses. Lysates were then centrifuged at 100,000xg for 30 min. Supernatants were collected, diluted with 2X lysis buffer (40 mM HEPES, 220 mM KCl, 20 mM NaCl, 4 mM MgCl$_2$, 10 mM KH$_2$PO$_4$, 500 µM ZnSO$_4$) and protein concentration determined (BCA Protein Assay, ThermoFisher, Waltham, MA). Lysates were incubated at 4 ^{o}C overnight with 5 µg of either normal rabbit IgG (Antibodies Inc., Davis, CA) or affinity-purified

MBLAC1 antibody #80. Samples were then incubated with Magnetic Protein G beads (Dynabeads, ThermoFisher, Waltham, MA) for 2 hr at 4 ^{o}C. Supernatants were removed for BSI and Western blot analysis. A portion of supernatants were heat inactivated at 95 ^{o}C for 5 min prior to BSI experiments (see below). Beads were washed 3x with 1X lysis buffer and MBLAC1 protein was eluted with 4X Laemmli buffer and diluted prior to SDS PAGE and Western blot analysis.

Affinity Capture of MBLAC1 with Cef-Conjugated Sepharose®

Cyanogen bromide (CN-Br) activated Sepharose® 4B beads were prepared and conjugated to Cef following manufacturer's recommendations (GE Healthcare Life Sciences, Pittsburgh, PA). Briefly, lyophilized beads were suspended and washed 3x in 1 mM HCl, pH 3.0. Beads were then equilibrated in coupling buffer (500 mM NaCl, 0.1 mM NaCHO$_3$, pH 8.3), and divided into conjugated and unconjugated samples. Conjugated beads (250 μL) were left to rotate for 1 hr at 25 ^{o}C with 2.5 μmoles of Cef in coupling buffer. The unconjugated beads were treated the same except no Cef was added. After coupling, remaining reactive CN-Br groups were inactivated by incubation (3 hr) with 0.1 M Tris-HCl (pH 8.0). Following inactivation, beads were subjected to alternating acid/base washes with 0.1M Na-acetate (pH 4.0) and 0.1 M Tris-HCl (pH 8.0). Beads were then equilibrated in lysis buffer (above) prior to lysate addition. Final protein concentrations (100 μg protein at 0.1 mg/mL) were incubated for 1 hr at 25 ^{o}C with 100 μL beads (50% slurry). In competition experiments, excess β-lactam compound (50 μM, final concentration) was mixed with lysates 10 min prior to addition of beads at 25 ^{o}C.

Beads were washed 5x in lysis buffer prior to elution of bound MBLAC1 in 2X Laemmli buffer, followed by SDS-PAGE and Western blot analysis.

Site-Directed Mutagenesis

Creation of the SWIP-10 mutations within the *MBLAC1* sequence utilized the NEB Q5 mutagenesis kit. Primers made (listed below) were to the specifications recommended by this kit. For each mutation, one antisense and one sense primer were made with blunt ends that abut each other. For the PCR reaction, primers were mixed with 10 ng of template DNA (pcDNA3 MBLAC1), and hot start mix provided with 1 Unit of Q5 taq enzyme. Then the PCR product was incubated with a mix of kinases and ligases before being transformed into chemically competent bacterial cells, provided with the kit. Cells were set on ice with 5µL of the KLD reaction/PCR product mix for 30 min, after which the bacteria were heat shocked at 42 ^{o}C for 45 sec before being placed back on ice for 5 min. The cells were then left to recover for 1 hr in nutrient rich SOC media with shaking at 37°C. 100 µL of the SOC media with cells were plated on LB ampicillin agar and left to grow overnight at 37 ^{o}C. Colonies were picked the following day (six of each mutant) for growth in 5mL cultures for DNA isolation (Qiagen Miniprep Kit) and eventual sequencing for confirmation of successful mutations.

Primers:

vt33

Forward (RB5449): GGTGGTGGCTGGTGATGTGTTCG

Reverse (RB5427): ACGGTGCCCAGGCTGGTGC

vt29

Forward (RB5450): GGACTCCTGACAGGCCCTGA

Reverse (RB5429): TCGTCACCAAGTCGCTCGAACACAT

Backscattering Interferometry Binding Assays

A BSI instrument was assembled and employed as previously described.[98, 99] Briefly, the instrument was comprised of a helium-neon (He-Ne) laser (Melles Griot), a microfluidic chip (Micronit), and a charge-coupled device (CCD) camera acting as a linear array detector (Ames Photonics). The chip contained flow channels with a 100 μm by 210 μm semicircular cross-section that, upon illumination with parallel rays from a laser (λ632.8), creates an optical resonance phenomenon. As a result of the beam-channel interaction, BSI has a long effective optical path-length leading to high sensitivity refractive index (RI) sensing. The RI signal was transduced by measuring shifts in the backscattered fringes, by a camera, which in works in concert with a Fourier analysis program.

For the screening studies, samples were prepared that contained Cef at concentrations of 0 µM, 5 µM, and 50 µM and cell or tissue lysate concentrations of either 300 µg/mL (mouse cell lysates) or 100 µg/mL (human cell lysates and mouse brain lysates). A set of samples was also prepared with Cef at the same concentrations with the lysate buffer. The samples were incubated on ice for 1 hr to allow for binding and to ensure that equilibrium has been reached.

Upon the samples reaching equilibrium, BSI measurements were taken. To measure the screening signal, the sample with 0 µM Cef was injected into the channel in a stop-flow manner using a vacuum and allowed to reach temperature and pressure

equilibrium (~10 sec), at which point the phase value (BSI signal) was measured for 20 sec. The channel was then evacuated with the vacuum and rinsed with buffer. Then the sample with 5μM Cef was injected into the channel and the BSI signal measured in the same manner. The channel was again rinsed with buffer and the sample with 50 μM Cef was introduced into the channel and the BSI signal measured in the same manner. The channel was thoroughly rinsed with buffer and the measurements for the entire concentration series were repeated for three complete trials. The screening signal was calculated as the difference between the samples with Cef and the samples without Cef. To determine the specific signal representing the amount of binding that occurred within the sample and remove any signal due to change in Cef concentration, the screening signal of Cef in lysate buffer alone was subtracted from the screening signals of the lysate samples.

For the Cef affinity determination, a dilution series of Cef was prepared in water over a concentration range of 1.56 μM to 100 μM. A solution of human cell lysates treated to express MBLAC1 were diluted to a concentration of 200 μg/mL total protein. A solution of human cell lysates that did not express MBLAC1 were also prepared at a concentration of 200 μg/mL total protein. For the binding samples, the 200 μg/mL MBLAC1 lysate was mixed 1:1 with the Cef dilution series to result in a set of samples with 100 μg/mL MBLAC1 lysate and a range of Cef from 0.78 μM to 50 μM. For the reference samples, the Cef dilution series was mixed 1:1 with the 100 μg/mL wild type lysates to result in a set of samples with the same range of Cef (from 0.78 μM to 50 μM), but with 100 μg/mL cell lysate without MBLAC1. The samples were incubated on ice for 1 hr to allow for binding and to ensure that equilibrium has been reached.

Upon the samples reaching equilibrium, BSI measurements were taken. To measure the binding signal, the reference sample was injected into the channel in a stop-flow manner using a vacuum and allowed to reach temperature and pressure equilibrium (~10 sec), at which point the phase value (BSI signal) was measured for 20 sec. The channel was then evacuated with the vacuum and the binding sample with the same Cef` concentration was injected into the channel and the BSI signal measured in the same manner. The channel was rinsed with buffer. This procedure was repeated for increasing concentrations of Cef. After the highest concentration of Cef (50 µM), the channel was thoroughly rinsed with buffer and the measurements for the entire concentration series were repeated for five complete trials. The binding signal was calculated as the difference between the sample and reference signals for the same Ab concentration. This signal, representing the amount of binding that occurred within the sample, was plotted versus concentration and fitted with a single-site saturation binding curve to determine the affinity using GraphPad Prism software.

BSI assays are relative measurements,[100] therefore RI changes are quantified by comparing the signal for a test and reference sample. The fringe shift is measured as a phase value (in milliradians) and is directly proportional to changes in the RI between a reference sample and a test sample. Recently, Bornhop and colleagues have shown that these values are highly correlated with the conformation and hydration changes resulting from a molecular interaction,[99] in this case Cef binding to the MBLAC1 protein.

Results

To study the putative SWIP-10 mouse and human ortholog, MBLAC1, we raised and purified rabbit polyclonal antisera against MBLAC1 fusion proteins, and generated stably transfected cell lines that, in the presence of TET, express mouse or human MBLAC1 (Figure 12A). Both antibody #79 and #80 detected mouse MBLAC1 in extracts of TET-induced HEK-cells, whereas only #79 detected human MBLAC1. Antibody #80 also detects MBLAC1 in rat brain lysates (Figure 12B). In the non-induced cells, neither antibody detected a protein of the equivalent mass as MBLAC1.

To determine the subcellular localization of endogenous MBLAC1 protein, we implemented a subcellular fractionation protocol using extracts of mouse NIH 3T3 cells (Figure 12C). Identity of cytosolic, organelle (e.g. ER), and nuclear fractions were confirmed by immunoblotting with antibodies targeted to compartment-specific proteins. MBLAC1 protein was found to localize to cytosolic fractions characterized by glyceraldehyde 3-phosphate dehydrogenase (GAPDH) enrichment (Figure 12C). Owing to the CNS being the likely site of action for the behavioral actions of Cef, we blotted mouse brain extracts for the presence of MBLAC1 protein. Consistent with a relatively even pattern of Mblac1 mRNA expression detected across mouse brain regions in our prior study,[81] we detected statistically equivalent levels of anti-MBLAC1 immunoreactive protein in extracts of hippocampus, striatum, cortex, cerebellum, and midbrain (Figure 12D).

To determine if MBLAC1 and Cef interact, we developed an MBLAC1 pulldown assay using Cef-conjugated CN-Br activated Sepharose beads (Figure 13). Conjugated
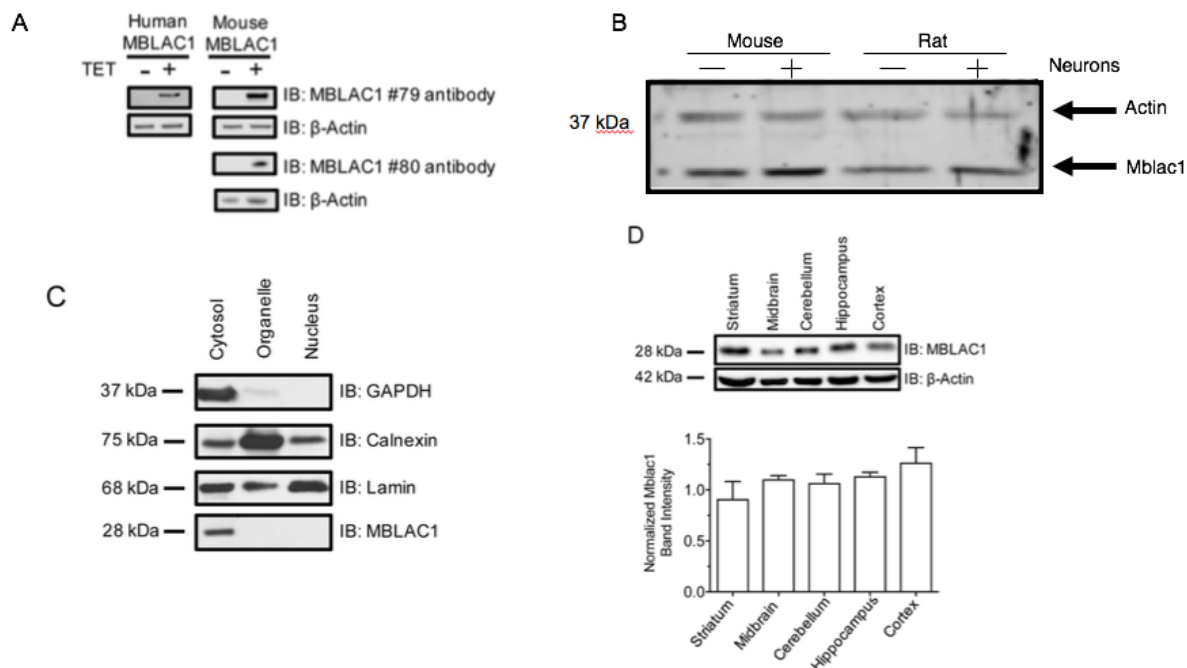
Figure 12. Expression and Detection of MBLAC1. A) Detection of mouse and human MBLAC1 from stably-transfected T-REx cells. Cells were induced with TET prior to SDS-PAGE and Western blotting of cell lysates. Antibody #79 detects human and mouse MBLAC1 (top immunoblot (IB)), whereas antibody #80 can only detect the mouse isoform. β-Actin blots below verify that though loaded with equivalent protein, the non-TET cells do not express MBLAC1. B) Primary glial cultures from mouse and rat showing MBLAC1 expression in both, and this expression increases with the addition of neurons C) Subcellular fractionation of NIH 3T3 mouse fibroblast cell lysates reveal MBLAC1 expression is relegated to the cytosolic fractions, based on co-fractionation with GAPDH. D) Presence of MBLAC1 protein in various regions of the mouse brain. Bar graph shows normalized densitometries of bands over multiple experiments (n=6, one-way ANOVA shows no significant main effect of brain region ($P>0.05$). Figure modified form Retzlaff et al. ACS Chem Neurosci. 2017 Oct 18;8(10):2132-2138.
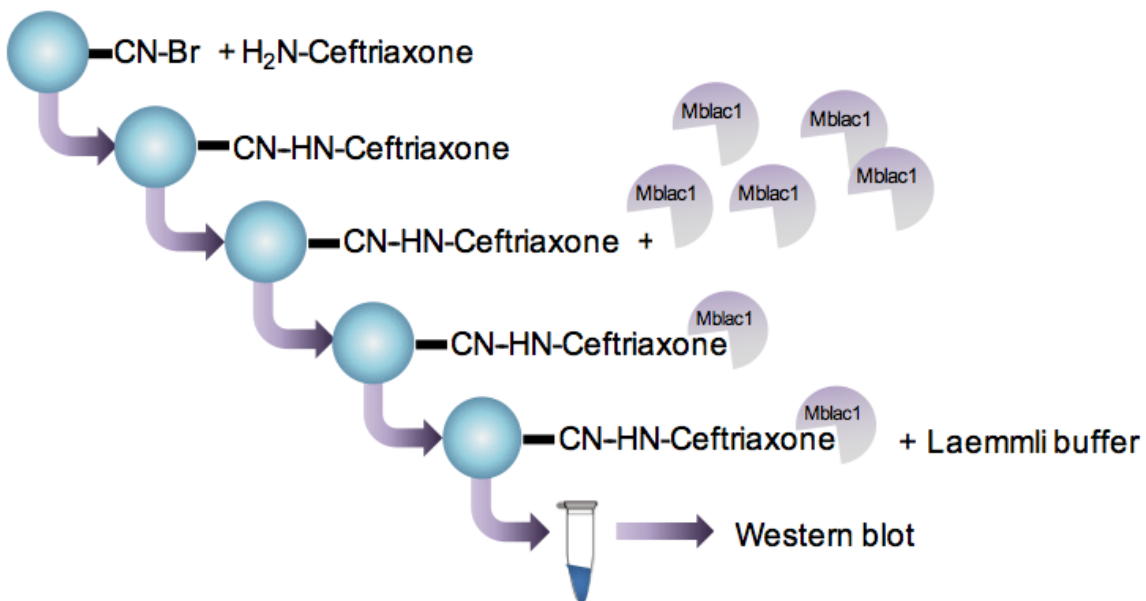
Figure 13. Method for MBLAC1 binding to Cef-conjugated Sepharose beads. Schematic depicting Cef conjugation to CN-Br Sepharose beads via coupling to free amine group. Figure modified form Retzlaff et al. ACS Chem Neurosci. 2017 Oct 18;8(10):2132-2138.

and unconjugated beads were incubated with lysates from TET or non-TET induced T-REx cells (Figure 14A). Cef-conjugated beads extracted significantly more MBLAC1 from lysates than unconjugated beads, with no evidence of MBLAC1-immunoreactive species detected when Cef-conjugated beads were incubated with uninduced cell extracts. To further assess specificity and affinity between these two molecules, we incubated MBLAC1 expressing cell lysates with Cef (50 µM) prior to incubation with Cef-conjugated beads, which significantly diminished MBLAC1 capture (Figure 14B).

To explore the specificity of this interaction we wanted to look at other β–lactam compounds. In Rothstein's original screen, they found that many β–lactam antibiotics were capable of inducing GLT-1, or activating its 3' UTR promoter, as shown via luciferase assay. We tested four other β–lactam containing compounds, cephalosporin C (CephC), dicloxicilin (Diclox), ampicillin (Amp), amoxicillin (Amox), and clavulanic acid (CA). Both Amp and Amox were compounds that showed the ability to increase GLT-1 expression with treatment on *ex vivo* spinal cord preparations; however, CephC did not. In luciferase based assays CephC, a β–lactam that is part of the same class as Cef, did not show promoter activation and indicates there is some preference for certain β–lactam antibiotics to confer neuroprotection. As shown in Figure 15, use of other antibiotics using the same chromatography method shows Amp can drastically decrease the ability for Cef to capture MBLAC1 on beads, reducing binding to about 20% that of basal. CephC and CA show modest ability to interfering with Cef pulldown at 50 µM, not to a statically significant level. Amox and Diclox show a slight trend to be able to inhibit this interaction, but not to the same extent, and with much more variability.

43
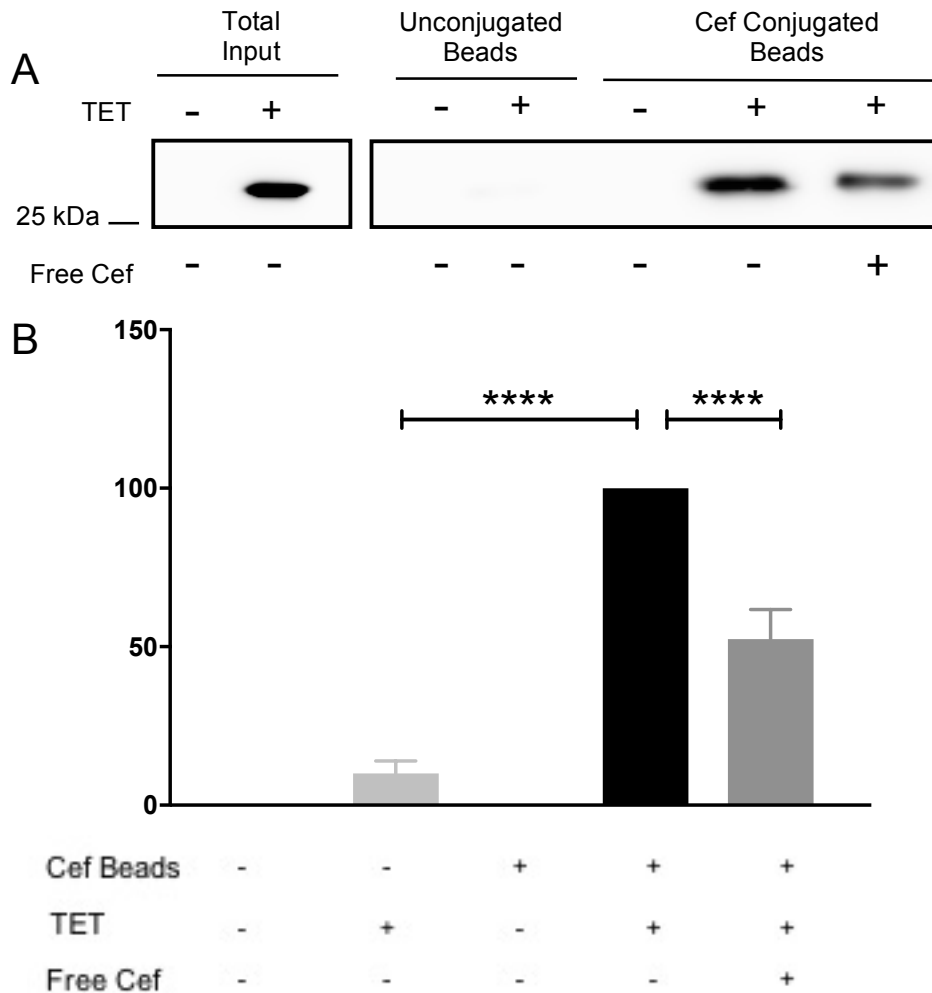
Figure 14. MBLAC1 binding to Cef-conjugated Sepharose beads. A) Evidence of MBLAC1 binding to bead-conjugated Cef. Left panel shows immunoblot detection of total MBLAC1 input of T-REx cells ± TET induction. Right panel shows immunoblot detection of MBLAC1 in SDS eluate from Cef-conjugated beads ± preincubation of Cef (50µM) with MBLAC1 containing extract. B) Quantitation of free Cef competition for binding of MBLAC1 to immobilized Cef (n=6, one-way ANOVA, Dunnett's multiple comparison test, **** (P<0.001)). Mean reduction in MBLAC1 binding in the presence of 50µM free Cef is 52.4 ± 9.3%. Figure modified form Retzlaff et al. ACS Chem Neurosci. 2017 Oct 18;8(10):2132-2138.
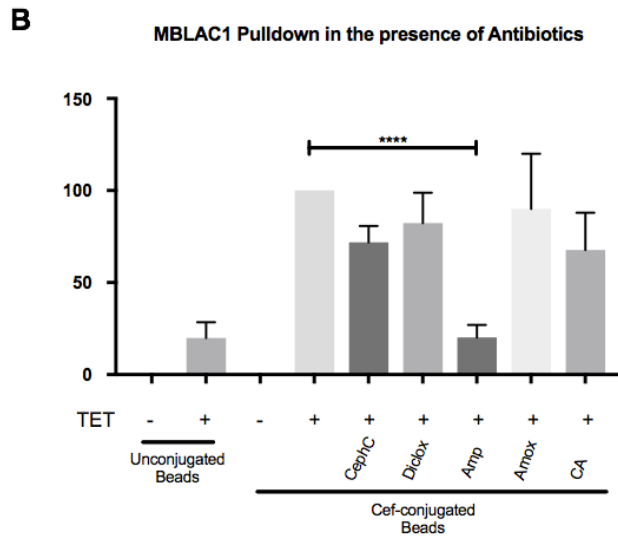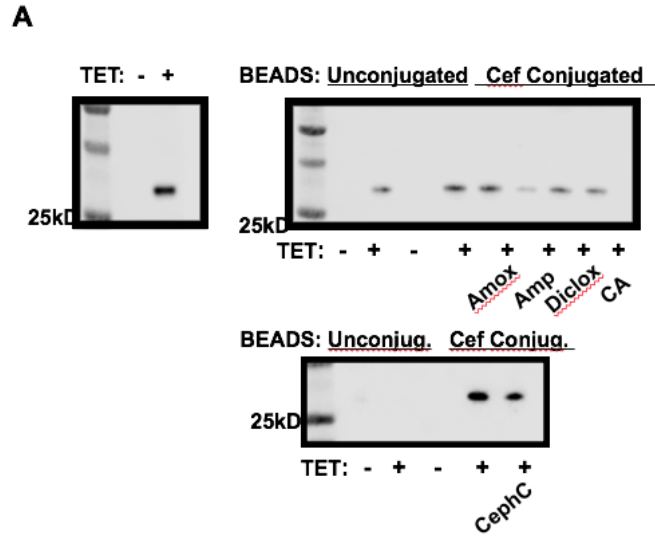
Figure 15. Competition of affinity captured MBLAC1 with β-lactam compounds. A) immunoblot detection of MBLAC1 after Cef conjugated bead pulldown. Pre-incubation was performed with various β-lactam compounds at 50uM. B) Quantification of MBLAC1 binding. Significant reduction in binding with Amp present (**** P=0.0001). (n=5 for all β-lactam antibiotics, and n=3 for CA, one-way ANOVA, with Dunnett's multiple comparison's test.)

To gain insight in to the mechanism of the Cef-MBLAC1 binding interaction, mutations within MBALC1 were made to determine whether the evolutionarily conserved residues. The mutations made in *MBLAC1* were the same as found in the *C. elegans* screen that uncovered *swip-10*. The first mutation was a missense mutation that mutates a Gly to a Glu (MBLAC1 G190D), and the second was a nonsense mutation that inserts a premature stop codon (MBLAC1 W202STOP). Both of these mutations in the worm resulted in a hyperdopaminergic phenotype. We assessed if these mutations affect the binding of MBLAC1 with Cef. From these experiments we observed no statistical difference for MBLAC1 G190D to bind Cef comparably to MBLAC1 (Figure 16B, C). This was not the case for MBLAC1 W202STOP, as there was so little protein produced from this transfection that binding was not observed much above background. Total protein level for this mutant was only about 10% to that of wild type (WT) or MBLAC1 G190D, suggesting protein instability (Figure 16A).

Although our pulldown approach provided initial evidence of Cef interactions with MBLAC1, the efficiency of competition was lower than expected, based on prior studies reporting the *in vitro* potency of Cef for GLT-1 induction. We reasoned that steric hindrance could limit high-affinity interactions of MBLAC1 with Cef-conjugated beads. As radiolabeled Cef was unavailable, we sought a non-isotopic approach that could examine Cef/MBLAC1 interactions without ligand immobilization. Backscattering interferometry (BSI) is a sensitive approach that can detect both kinetic and equilibrium associations of unlabeled, small molecule interactions with unmodified target proteins. Using lysates from uninduced and induced T-REx cells expressing mouse or human MBLAC1, we implemented BSI as described in Methods and detected significant, dose-dependent BSI

Figure 16. Affinity capture of MBLAC1 and mutants. A) Immunoblot showing totals (left) and pulldown (right) of MBLAC1 with WT, G190D, and W202STOP. No significant reduction in binding with G190D mutation, but drastic reduction with W202STOP, most likely due to decreased protein production of this mutant. B) Quantification of pulldown assays (n=4, One-way ANOVA, Dunnett's multiple comparison's test.)

signals only in induced cell lysates (Figure 17A, B). BSI signals were eliminated by heat denaturation of extracts prior to analysis, consistent with Cef binding as arising from a proteinaceous species versus TET used to induce MBLAC1 expression. The BSI results both confirmed the Cef/MBLAC1 interactions detected in Cef-conjugated bead assays and established a quantitative approach that could be used to estimate the affinity of unconjugated Cef for MBLAC1. Indeed, binding data collected in BSI assays conducted across a range of Cef concentrations were well fit (r^2=0.96) to a single site binding equation with a K_D of 2.2 ± 0.56 µM (Figure 17C).

To explore the promiscuity of MBLAC1 interaction with other β-lactam antibiotics, we compared BSI signals with CephC to those obtained with Cef. In our studies, we again detected significant dose-dependent BSI signals with Cef, but were unable to see a significant CephC BSI signal (Figure 17D). To detect endogenous Cef binding and to determine whether MBLAC1 is likely to be responsible for observed interactions, we repeated our BSI experiments using mouse frontal cortex lysates, with and without prior heat denaturation. To determine whether, and to what degree, Cef binding signals derive from MBLAC1, we performed BSI studies on lysates that had been immunodepleted of MBLAC1 protein by anti-MBLAC1 antibody (#80). Clearance of frontal cortex lysate using MBLAC1 antibody, but not control antiserum, resulted in the elimination of MBLAC1 protein from cortical extracts (Figure 17E). When BSI binding assays were conducted with immunodepleted extracts, the Cef binding signal was abolished (Figure 17F).
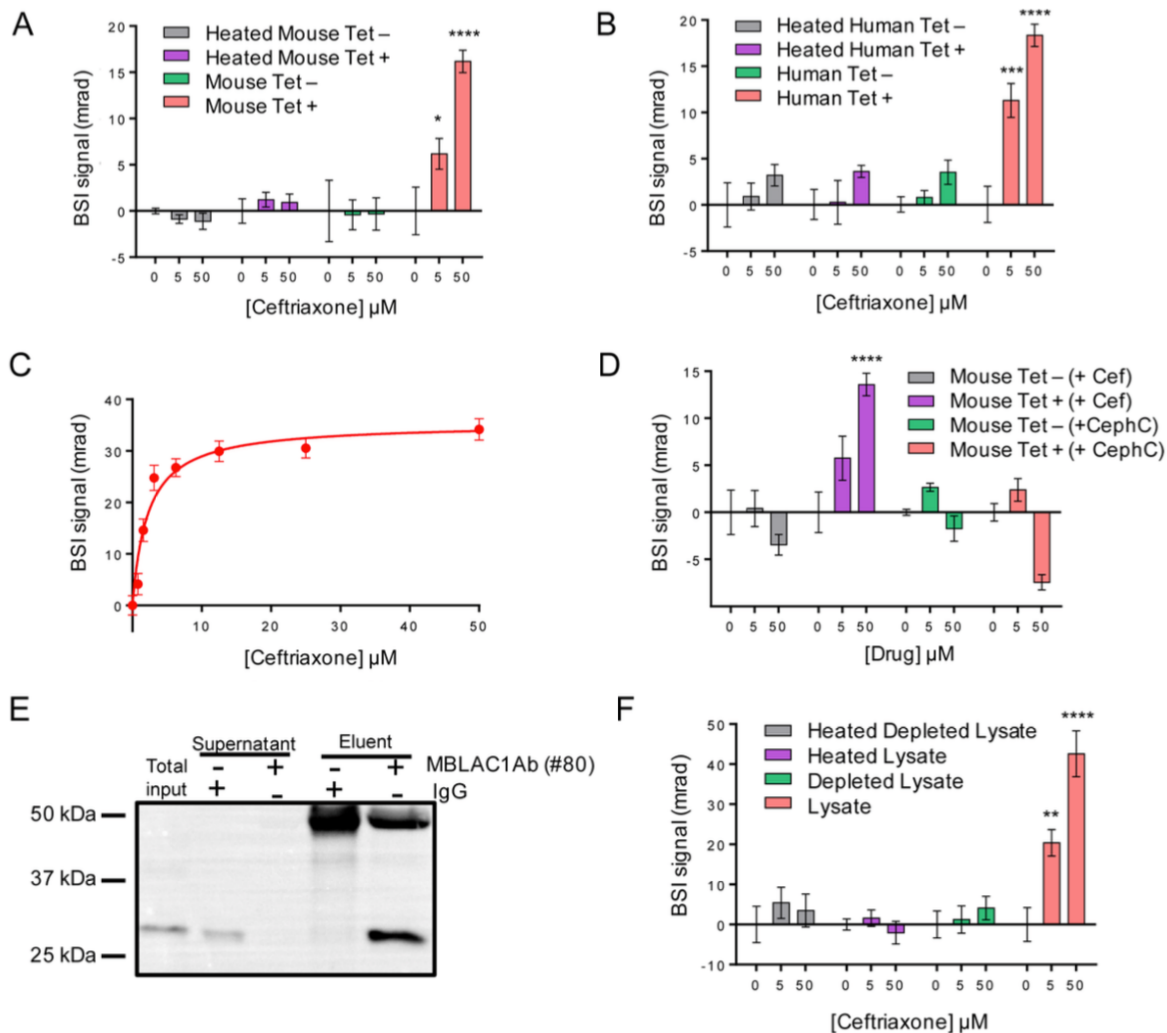
Figure 17: BSI analysis of MBLAC1 binding to unconjugated Cef. A) Lysates from TET induced T-REx cells expressing mouse MBLAC1 demonstrate concentration-dependent, heat-sensitive BSI binding signals that are absent from cells lacking TET induction. (TET− vs TET+ at 5µM and 50µM, * ($P<0.05$) and **** ($P<0.0001$), respectively) B) Lysates from TET induced T-REx cells expressing human MBLAC1 demonstrate concentration-dependent, heat-sensitive BSI binding signals that are absent from cells lacking TET induction. (TET− vs TET+ at 5µM and 50µM, *** ($P<0.001$) and **** ($P<0.0001$), respectively). C) Estimation of Cef binding affinity to lysates from mouse MBLAC1 TET cell using BSI. Single site binding equation fit to BSI binding data ($r^2=0.96$) yields a K_D for binding of 2.2µM ± 0.56. D) Multiple concentrations of CephC result in a non-significant reduction in BSI signal using mouse MBLAC1 expressing cells (TET− vs TET+ at 50µM Cef **** ($P<0.0001$), TET− vs TET+ at 5µM or 50µM CephC, $P>0.05$). E) Immunoblot of mouse frontal cortex extracts subjected to immunodepletion with MBLAC1 Ab #80 compared to IgG control immunodepleted extracts. F) Lysate of mouse frontal cortex shows binding signal with Cef that was abolished when MBLAC1 was immunodepleted using MBLAC1 antibody #80, or when the samples were heat inactivated prior to BSI analysis (Lysate vs depleted lysate at 5µM and 50µM, ** ($P<0.01$) and **** ($P<0.0001$), respectively). All experiments were analyzed using a two-way ANOVA and Tukey multiple comparisons tests. Figure modified form Retzlaff et al. ACS Chem Neurosci. 2017 Oct 18;8(10):2132-2138.

Discussion

Through the use of purified antibodies, expression levels of MBLAC1 have been assessed in major brain regions with no significant differences identified as predicted by mRNA analyses.[81] Though this is the first time MBLAC1 has been verified on a protein level, details of compartmental expression (i.e. synaptic processes vs. cell bodies) still need to be performed. The current set of antibodies are suitable for detection of MBLAC1 protein in tissue extracts, but other bands are evident on tissue western blots making this a difficult to use for histological studies of regional distribution. Efforts are underway to generate more MBLAC1 antibodies suitable for these neuroanatomical studies (see these efforts in Appendix I).

The studies to determine the ability for MBLAC1 and Cef to interact were made possible by the utilization of two methods. Affinity chromatography experiments were utilized to demonstrate direct binding between the two molecules. Evidence from these studies indicate MBLAC1 and Cef can interact in a specific manner, as excess Cef is able to compete off this interaction. Furthermore, this interaction is prohibited by the excess of some, but not all β–lactam compounds. As shown, additional compounds like Amp were particularly effective in competing with the Cef:MBLAC1 interaction, showing a 80% reduction in binding, greater than that of Cef.[43] Amp is a lot smaller compound, with fewer ring structures, and might easily intercalate into the binding site of MBLAC1. Comparing the structures of the β-lactams that had efficacy in this assay could pin point chemical structures that are important for occupying the antibiotic binding site, which is presumably the active site of this enzyme. Recent interest and use of CA in the literature as a neuroprotective agent lead us to explore the interaction between these two molecules.

CA has proven effective like Cef in models of addiction and Parkinson's disease.[101, 102] Fewer studies have explored the mechanism of this compound, but as it also houses a β–lactam ring, the assumption is that it would work similarly to Cef. This compound is typically used in conjunction with Amox as a two-hit strategy to combat bacterial infection in the clinic, as CA is a β–lactamase inhibitor and not an antibiotic. CA is able to be given at a lower dose than Cef in studies for neuroprotection (10 mg/kg vs 200 mg/kg, respectively), which is desirable for translation to human studies. In our studies, we did not see that CA was as effective as Cef for competing with this interaction, but dosing *in vitro* vs *in vivo* might require more troubleshooting to find *in vitro* concentrations at which CA are most potent and are comparable to the pharmacokinetics of the compound. These results could also indicate that CA might be working via a different mechanism than Cef.

Manipulating the MBLAC1 protein sequence allowed for examination of evolutionarily conserved residues and their contribution to Cef binding. Our results suggest that the missense mutation (G190D) does not significantly effect binding, while the truncation mutation robustly limits the amount of protein produced, and thereby shows little to no Cef binding. In relation to the *C. elegans* data, these data suggest the robust SWIP phenotype seen with protein truncation could be caused by low protein expression. However, since protein expression is normal with the missense mutation, SWIP may be caused by altered interaction with endogenous substrates that cannot be assessed by current strategies.

Though the affinity chromatography experiments were effective at showing binding a second, non-isotopic method was necessary to more quantitatively examine the Cef:MBLAC1 interaction. BSI analysis results with cell lysates provided strong evidence

for specific, high-affinity binding between Cef and MBLAC1. This approach provided a binding affinity for this interaction, paralleling Rothstein's data indicating a 3.5 μM EC_{50} for Cef's induction of GLT-1 expression. BSI analysis of CephC interaction with MBLAC1 were not statistically significant. The negative BSI signal observed in the presence of CephC indicates that there may be an interaction between MBLAC1 and CephC at high concentrations, though the nature of this interaction would appear to be molecularly different from the interaction we observe between Cef and MBLAC1. Furthermore, there is not significant reduction in binding with CephC at the same high concentration. TET induced cell experiments alone do not rule out the possibility that other high-affinity targets of Cef exist. Other groups have shown Cef binding with purified GFAP, though estimates of affinity for this interaction were unattainable.[69] This same group also reported binding of Cef to purified α-synuclein, a neuronal protein, with a propensity to aggregate in Alzheimer's Disease patients.[68] These previous binding studies required purified protein out of physiological buffers and required extended incubation times to see binding. Cef has been used in mouse models of Alzheimer's to alleviate or slow the progression of the disease process.[103] This comes after a study showing decreased GLT-1 function exacerbates the Alzheimer's learning deficits in mice.[104] The affinity for this interaction was observed to be in the micromolar range. Modeling studies in these two reports suggest residues that could facilitate binding of Cef, these sites have yet to be evaluated (e.g. through mutagenesis studies), and do not conform to binding sites typical of those interacting with β-lactam antibiotics, like those present in MBLAC1. Additionally, interaction with α-synuclein would not explain the full range of efficacy that Cef has been reported on. Recently, Lee et al. reported a high affinity interaction (2-4 μM) between

cephalosporin β-lactam type antibiotics and the exonucleases SNM1A/SNM1B, proteins that contain a MBD.[105] We know of no studies describing CNS expression of SNM1 proteins and brain expression is not evident in the Allen Brain Atlas (http://www.brain-map.org). Several brain-expressed proteins contain MBDs that could also conceivably bind Cef with high-affinity, including MBLAC2, an unstudied orphan protein expressed in brain with modest similarity to MBLAC1, and Glyoxalase II. To rule out other *in vivo* binding partners, BSI experiments using tissue lysates allowed us to analyze the contributions of MBLAC1 to Cef binding signals. Immunodepletion of MBLAC1 abolished the BSI binding signal. These findings support the contention that, under our binding conditions, MBLAC1 is likely the primary species in brain lysates capable of interacting with Cef at high-affinity.

Our data above provide strong support for the assertion that the well-replicated actions of Cef in the CNS arise through MBLAC1 interactions, but we recognize that these binding studies reflect short-term interactions whereas chronic administration of Cef is required in most, though not all, studies.[106] Thus, it remains possible that lower affinity interactions, maintained for a longer period of time, could support the biochemical, behavioral, and neuroprotective actions of Cef described to date. Additionally, our studies were pursued in cytosolic lysates and cannot rule out the possibility of interactions occurring in nuclear, organelle, or membrane fractions. Just as likely, however, the interactions of Cef with MBLAC1 may induce cellular adaptations that take weeks to materialize. Future studies should examine the impact of manipulation of MBLAC1 expression on published *in vivo* Cef effects, such as reduction of excitotoxic cell death and prevention of psychostimulant reinstatement. Our studies also encourage

investigation as to the endogenous substrate for MBLAC1, which is presently unknown. Identification of this molecule, and the pathways through which it works, may provide important information related to how Cef modulates Glu homeostasis, and perhaps, new leads to the mechanisms by which disorders rooted in perturbed Glu signaling arise.

CHAPTER 3

CREATION AND CHARACTERIZATION OF MBLAC1 KNOCK-OUT MOUSE

Introduction

Behavioral and biochemical characterization of Cef action in the brain has been explored *in vivo* across a broad range of neurological and neuropsychiatric diseases.[42, 44, 49, 107-110] Animal models of disorders and diseases like stroke, ALS, and addiction were some of the first forays exploring the effects of Cef action.[42, 43, 49, 111] However, many other models of diseases have also been studied, such as seizure, Huntington's disease, Parkinson's disease, and traumatic brain injury (TBI).[48, 109, 112, 113] Behaviors associated with these diseases such as survival rates of ALS models, neuronal cell survival rates as in the case with TBI and Parkinson's, or disease progression and symptomology have all shown improvement with chronic Cef treatment.[43, 48, 114] Much of the work associated with Cef's action *in vivo* has also centered around Cef's powerful effects in the addiction field.[42, 59, 62, 115, 116] The many phases of addiction (acquisition, chronic use, withdrawal/abstinence, and relapse/reinstatement) call upon different molecular and circuit mechanisms.[117] Years of previous work has led to the idea that glutamatergic changes within the mesolimbic system and reward circuits contribute to the long lasting, more permanent changes of disease progression.[82, 118] It is these changes and maladaptation in glutamatergic signaling in animal models that are sensitive to Cef administration, and provide the basis for the behavioral changes observed.[118-120]

Effects of Cef administration have been studied across many different contexts related to drug abuse and addition ranging from changes in locomotor behavior, to blunting reinstatement, to alleviating drug induced side effects.[60-62, 121] Peter Kalivas and his group have been pioneers in utilizing Cef to understand its role in reinstatement after cocaine exposure.[42, 59, 67] Particularly, they have focused on the use of Cef during the withdrawal period, when administration is most effective. Locomotor sensitization is a common effect to many psychostimulants and is defined by a progressive increase in activity over the course of repeated injection, followed by a period of drug abstinence. After this set period of time a last injection of the drug is given producing an even greater, or sensitized, response in activity. This sensitized response is due to the long-term plasticity changes that occur in the glutamatergic system after chronic drug use.[122, 123] The known changes in transporter expression (i.e. GLT-1 and X_c^-) that occur after drug exposure alter extracellular levels of Glu, which changes receptor sensitivities, distribution, and Glu release probabilities.[40, 124] These changes in Glu signaling modulate the drive on the DA neurons and motor systems that are directly responsible for the locomotor changes.[41] Interestingly, administering Cef during the period of psychostimulant withdrawal, blunts these sensitizing effects on locomotor activity.[61, 92] This is thought to be due to the normalization in transporter expression by Cef, rectifying the maladaptive changes that have occurred.[59] With the extensive literature supporting profound behavioral effects of Cef, and our recently published binding data that provides evidence that MBLAC1 could be the exclusive binding partner of Cef, we were prompted to the create a MBLAC1 knock-out (KO) mouse.[125] This KO animal model can provide insight into the mechanism of Cef action and its effects on Glu homeostasis. The following

data are our initial studies regarding the characterization of this novel KO mouse line, and our preliminary work to examine the effect of psychostimulants in the absence of MBLAC1.

<div align="center">**Methods**</div>

CRISPR/Cas9 transgenic lines

All animal experiments were performed according to the approved IACUC protocols active at Vanderbilt and Florida Atlantic University. Targeting CRISPR/Cas9 system to the *MBLAC1* gene provided the opportunity for insertion or deletion mutations within the DNA sequence that would alter the transcription and translation of this protein resulting in a total KO of MBLAC1 protein. Oligonucleotides targeting *MBLAC1* were designed using software developed by the Zhang lab at MIT (Massachusetts Institute of Technology, http://crispr.mit.edu). Two constructs containing CRISPR elements, Cas9 enzymes, and our *MBLAC1* gene targeting oligonucleotide probes were injected into C57/Bl6 pronucleus of embryos. These constructs were targeted to a region 46bp past the ATG start and were sense and antisense to the sequence below. Mice that were viable were grown, and their DNA was sequenced for insertions or deletions in *MBLAC1*. All founder animals with KO mutations were initially heterozygous for the mutation. Mice were further bred with other C57BL/6J mice to make sure mutations were in the germline. Animals from subsequent generations were also sequenced for evidence of the mutation. Two lines of KO mice were kept for future experiments and mice were continued to be backcrossed against C57 WT mice for four generations to limit the retention of any non-specific mutations that might have occurred as a result of the CRISPR/Cas9 system.

Genotyping was originally determined by PCR using primers that crossed over the deletion areas. We used a third party contracted sequencing based company to determine genotypes of our mice. Transnetyx creates qPCR oligonucleotide primers against the genomic DNA to identify and quantify the presence of WT and MBLAC1 KO alleles. Sequences used for genotyping by Transnetyx are below.

Sequence targeted for CRISPR: CTTTGCTGGCGT<u>CCA</u>GCGGC (PAM site underlined)

Primers for 5bp mutation (Transnetyx): Forward- GACAGCGATAGTTTAGTTTC

                                    Reverse- TCCCTGGCGTCCAGCGGC

Primers for 14bp mutation (Transnetyx): Forward- CGAGCCCCTGCATCCT

                                    Reverse- GCCGCGCAGCAGAAC

Western blots

Protein samples for Western blot analysis were quantified for total protein (BCA Pierce/ThermoFisher, Waltham, MA) and heated to 95 ^{o}C for 5 min with 1X Laemmli, separated via SDS-PAGE using 10% Bis-Tris Novex pre-cast gels (Invitrogen), and transferred to Immobilon PVDF membranes (Millipore, Billerica, MA). Membranes were blocked for 1 hr at 25 ^{o}C with 5% milk in TBS/0.1% TWEEN (TBST). Primary antibody, diluted 1:1000 in 5% milk/TBST (typically 5 ug of Ab), was incubated with membranes overnight at 4 °C. After washing 4x for 5 min with TBST, secondary antibody 1:10000 (peroxidase-conjugated mouse-anti-rabbit, Jackson ImmunoResearch, West Grove, PA) in 5% milk/TBST was incubated for 1 hr at rt. Blots were washed again before band visualization and quantitation by enhanced chemiluminescence (BioRad Clarity ECL, Hecules, CA) using a LiCor FC digital imager (LiCor Omaha, NE).

Synaptosomes

Mice were rapidly decapitated and brains regions were dissected on ice before being placed in 3 mL of 0.32M sucrose. The brain regions were then homogenized using a Dounce homogenizer, and then spun at 800xg for 10 min. The supernatant was divided into two equal halves, and then spun at 13000rpm for 15 min. This pellet was then resuspended in either Na-free KRH buffer (replace NaCl with N-methyl-D-glucamine (NMDG)) or regular KRH buffer (120 mM NaCl, 1 mM KH2PO4, 5 mM KCl, 1.3 mM CaCl$_2$, 1.4 mM MgSO$_4$, 10 mM Glucose, pH 7.4). Protein assays were performed to determine total protein concentrations. The total volume for each tube was 250 µL, containing 25 µg of protein. Tritiated Glu ([^{3}H]Glu) was made up in stocks at 10x concentrations and concentrations of Glu higher than 50 µM were made at a 1:1000 ratio [^{3}H]Glu: Glu. [^{3}H]Glu was added right before tubes were submerged in a 37 ^{o}C shaking water bath for 10 min. The uptake was terminated by running the samples through a 48 tube Brandel Cell harvester where radioactivity was captured on glass filter paper that had been pre-soaked in 0.3% PEI. These filters were allowed to dry and then placed in scintillation vials with 7 mLs of Ecoscint H (National Diagnostics). Samples were left to incubate overnight and then quantified on TriCarb scintillation reader where CPMs were recorded. These CPMs were then converted into rates of Glu uptake.

Amino acid analysis using UPLC tandem mass spectrometry

For analysis of tissue samples, the tissue sections were homogenized, using a tissue dismembrator, in 100 µl of 0.1 M TCA, which contains 10^{-2} M NaCH$_3$COO, 10^{-4}M EDTA, 5 ng/ml isoproterenol (as internal standard) and 10.5 % methanol (pH 3.8). Twenty

microliters of homogenate were used for protein assay. Then samples were spun in a microcentrifuge at 10,000xg for 20 minutes.

To prepare tissue or media samples for mass spectrometric analysis, 5 μl of the tissue sample supernatant was diluted with 20 µl ice-cold acetonitrile. The mixture was then derivatized by sequential addition of 10 µl of 500 mM sodium carbonate and 10 µl benzoyl chloride (2% (v/v) in acetonitrile). The reaction was terminated after one minute with 20 µl of 20% acetonitrile in water with 3% sulfuric acid containing $^{13}C_6$-benzoyl chloride derivatized internal standards. 40 µl of water was added to reduce the organic content of the samples.

Calibration standards are prepared in the tissue homogenate buffer. 5 µl of each standard solution was diluted with 20 µl ice-cold acetonitrile and then derivatized in the same manner as the samples.

Derivatized samples were analyzed by UPLC–MS using a Waters Acquity UPLC (Milford, MA, USA) coupled to a SCIEX 6500+ QTrap mass spectrometer (Framingham, MA, USA) operating in multiple reaction monitoring (MRM) mode. 10 µl was injected onto an Acquity BEH C18 column (1 mm × 100 mm, 1.8 µm, 100 Å pore size) in partial loop injection mode. Mobile phase A was 10 mM ammonium formate with 0.15% formic acid, and mobile phase B was acetonitrile. The flow rate was 125 µl/min and the elution gradient was as follows: initial, 2% B; 0.01 min, 15% B; 0.5 min, 17% B; 3 min, 55% B; 4 min, 100% B; 4.5 min, 100% B; 4.8 min, 2% B; and 6 min, 2% B. The autosampler was kept at ambient temperature and the column was kept at 27 °C. Electrospray ionization was used in positive mode.

Quantification of tissue protein levels. Protein concentration was determined by BCA Protein Assay Kit (ThermoScientific). Ten microliters of the tissue homogenate was distributed into 96-well plate (in duplicate) and 200µl of mixed BCA reagent (25 ml of Protein Reagent A is mixed with 500 µl of Protein Reagent B) was added. The plate was incubated at 25 ^{o}C for two hours for color development. A bovine serum albumin (BSA) standard curve was run at the same time. Absorbance was measured by the plate reader (POLARstar Omega, BMG LABTECH Company).

HPLC Analysis of Monoamine Tissue Content

Mice were sacrificed and brains were removed, dissected for dorsal striatum, snap-frozen, and stored at -80 ^{o}C. Samples were sonicated in 250 mL of 0.2 M $HClO_4$ and 10 ng isoproterenol as an internal standard was added, the protein was denatured, samples centrifuged at 20,000xg for 15 min at 4 °C, and 1 M sodium acetate was added to modify the pH of the supernatant to pH3.0. The supernatant was filtered with a spin column and analyzed by HPLC. The HPLC system consisted of an Eicom Insight Autosampler (AS-700) and an Eicom Stand-Alone HPLC-Electrochemical Detection System (HTEC-510), Eicompak SC-30DS (ID 3.0 x 100 mm) reverse-phase column (Eicom), a working electrode graphite (WE-3G) using an applied potential of +750 mV vs. Ag/AgCl. A mobile phase consisting of 85% 0.1 M citrate-acetate buffer (pH 3.5) 15% methanol, 220 mg/l sodium octane sulfonate and 5 mg/l EDTA was used to separate NE, DA, 5-HT, and their metabolites. The signals produced by the oxidation of monoamines and metabolites were measured and compared with those of known concentrations of standards using Envision Data System software. The final oxidation current values were converted to ng and

adjusted to mg protein amounts determined by BCA protein assay. Values are expressed as ng per mg protein.

Irwin Screen

Animals were assessed for the different tests as presented in Table 2. This was a modified Irwin Screen as preformed previously in our lab. [126]Animals were cared for and kept to the specifications of the IACUC protocol in place at Florida Atlantic University. Male and female mice, age matched and littermate controls were used for these assessments (n=4 each group).

Locomotor sensitization

Wildtype and MBLAC1 KO mice between 8-12 weeks of age were habituated to activity chambers (MedAssociates) for 60 min for 2 days. On day 3, mice were acclimated to the chambers for 30 min and then given a saline injection, and monitored for basal locomotor activity for 60 min post-injection. Days 4-8, mice were given injections of 10 mg/kg cocaine after 30 min habituation to activity chambers, and their total locomotor activity was recorded for 60 min post injection. These cocaine injections were followed by a final saline injection with activity monitoring as before. Mice were left in home cages for 14 days without drug or saline injections. On day 28 of the experiment (2 weeks after the last saline injection) the mice were given a final cocaine injection, and their activity was recorded as before.

Results

BIOCHEMICAL CHARACTERIZATION

Initial biochemical characterization of the MBLAC1 KO mice sought ot verify loss of protein. Western blot analysis confirmed the lack of the 27 kDa protein that is MBLAC1. Although other non-specific bands exist with our antibody, there is a clear lack of a band at the molecular weight we expect MBLAC1 (Figure 18). The lack of MBLAC1 protein is apparent with both of the created lines, and throughout the whole animals as peripheral tissue also does not express MBLAC1 protein in the KO mouse, confirming these mice are constitutive KOs (Figure 18C).

Eliminating the expression of MBLAC1 protein in the whole animal can lead to many changes to basal and systemic cellular metabolism. Therefore, we examined if there were any broad changes to amino acids, or other metabolites. In collaboration with the Vanderbilt Neurochemistry Core, we analyzed whole tissue levels of a panel of amino acids. The included molecules analyzed were: GABA, Glu, Gln, arganine, proline, lysine, taurine, Cys, cystathionine, and homocysteine. Tissue samples taken from heart, liver, lung, and four main brain regions (striatum, cortex, cerebellum, hippocampus), as well as serum from 3 WT animals and 4 KO animals were sent for analysis. The data in Figure 19A shows that no discernable differences in any of these metabolites or amino acids in any of the brain regions. Interestingly, there is a statistically significant decrease in taurine levels in the serum of KO animals (Figure 19B).

In addition to the changes in amino acids, we also wanted to examine at the possible effect of loss of MBLAC1 on the other neurotransmitters of the brain, namely the

63
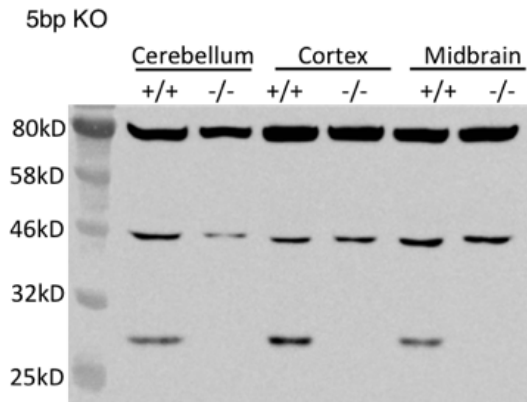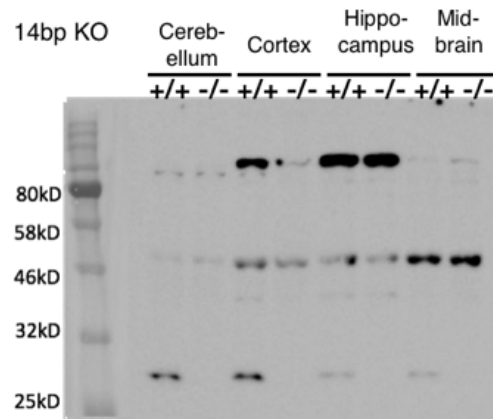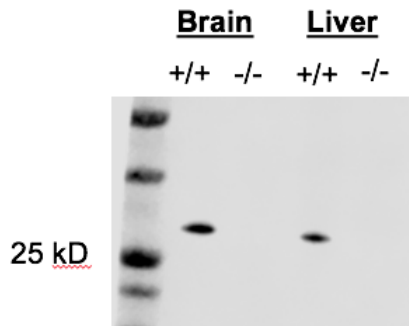
Figure 18. Verification of KO animals via Western blot analysis. A) Brain tissue from animals with 5bp KO line, showing no immunoreactivity at 27kDa, the predicted location of MBLAC1. B) Brain tissue from animals with 14bp MBLAC1 KO line. Also showing no immunoreactivity at 27kDa, as with the other KO line. C) Whole brain tissue lysates compared to liver homogenate to see that in peripheral tissues MBLAC1 expression is also gone. All blots were probed with #80 primary MBLAC1 polyclonal antibody.
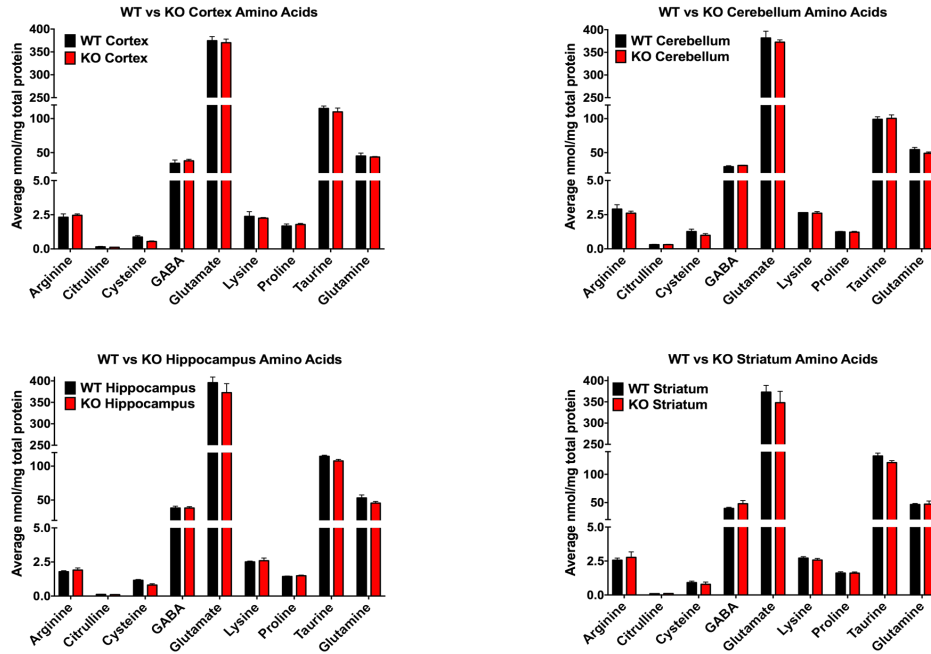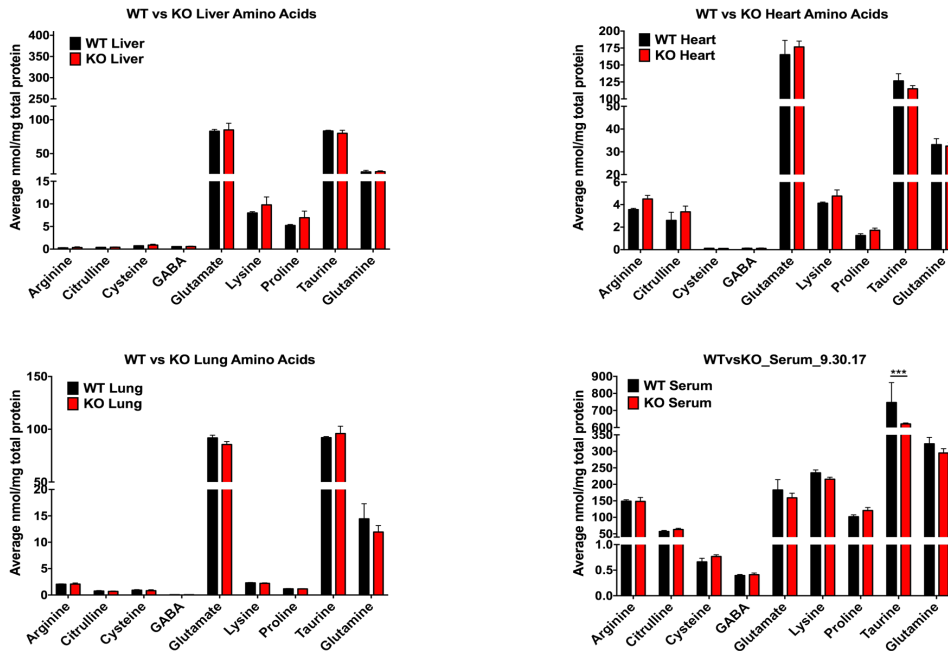
Figure 19. Amino acid analysis between WT and KO animals. A) Major regions of the brain (Ctx, Hipp, Str, and Cere) show no statistical differences in the amino acids tested here. B) Peripheral tissue and serum analysis of amino acid panel show significant reduction (P<0.001) in taurine levels only.

monoamines and their metabolites. For the cortex (Ctx) there were no statistically significant changes between WT and KO animals. These results are preliminary and need to be of a higher N to be fully confident in the data (Table 1, Figure 20).

Next, we wanted to determine if KO of MBLAC1 effects the expression of other proteins. We were particularly interested if the Glu transporters GLT-1 and X_c^- show any differences because of their relevance to the Cef literature. Western analysis of whole cell Ctx lysate shows that there is no difference in GLT-1 expression between the KO and WT animals. However, there is a small but significant reduction in the total expression of X_c^-. As shown in Figure 21, the 37 kDa band, a main proteolytic fragment of the transporter unit, shows less immunoreactivity in the KO as compared to the WT.

Although there are no differences in protein expression of GLT-1, we wanted to test if the lack of MBLAC1 effects GLT-1 function.[127] Crude synaptosomes were used for the assessment of GLT-1 mediated uptake. Although this Na^+ dependent [^{3}H] Glu uptake could reflect all EAAT family transporters, based on expression patterns, and affinities, only those near synaptic sites would be isolated in this preparation and be able to contribute significantly to uptake (i.e. GLT-1). We do not observe any differences in Na^+ dependent [^{3}H] Glu uptake in the KO animals as compared to WT littermate controls at high or low concentrations of Glu (Figure 22).

BEHAVIORAL CHARACTERIZATION

Initial behavioral tests were performed to assess any gross abnormalities that may have acquired from a global MBLAC1 KO. General observations suggest the KO animals are grossly normal with respect to basic sensorimotor functions and there are no issues with mothering in the KO or heterozygous (HET) animals.

	NE	DOPAC	DA	5-HIAA	HVA	5-HT
Front Ctx WT 1	3.84	7.01	4.53	4.68	6.81	2.96
Front Ctx WT 2	3.72	22.52	28.43	6.13	16.74	3.15
Front Ctx WT 3	3.24	1.94	0.42	3.77	5.04	2.09
Average	3.60	10.49	11.12	4.86	9.53	2.73

	NE	DOPAC	DA	5-HIAA	HVA	5-HT
Front Ctx KO 1	3.46	2.96	2.50	2.90	4.10	2.22
Front Ctx KO 2	2.61	2.10	1.18	2.54	2.90	1.58
Front Ctx KO 3	4.50	2.84	1.69	4.61	5.04	2.57
Front Ctx KO 4	3.10	4.63	6.11	3.83	6.70	2.20
Average	3.42	3.13	2.87	3.47	4.68	2.15

Monoamine Analysis
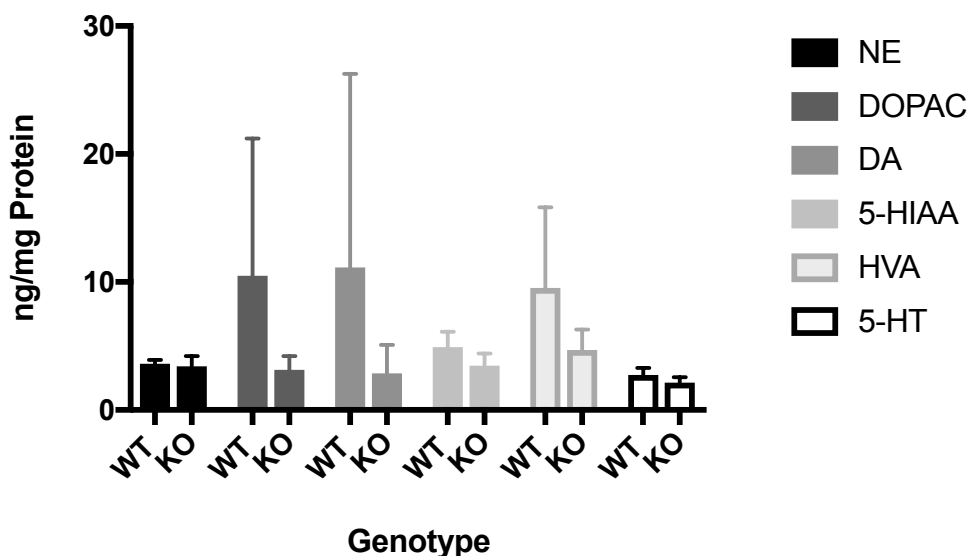
Table 1 and Figure 20. Monoamine analysis between WT and KO animals. A) Table of results looking at monamines and their major metabolites. (NE, norepinephrine; DOPAC, 3,4-Dihydroxyphenylacetic acid; DA, dopamine; 5-HIAA, 5-Hydroxyindoleacetic acid; HVA, Homovanillic acid; 5-HT, serotonin) B) Bar graph representing the tabular data in A. Shows little differences in levels of monoamines. DA and its metabolites show high variablitiy possibly due to contamination of striatum within the cortex samples.
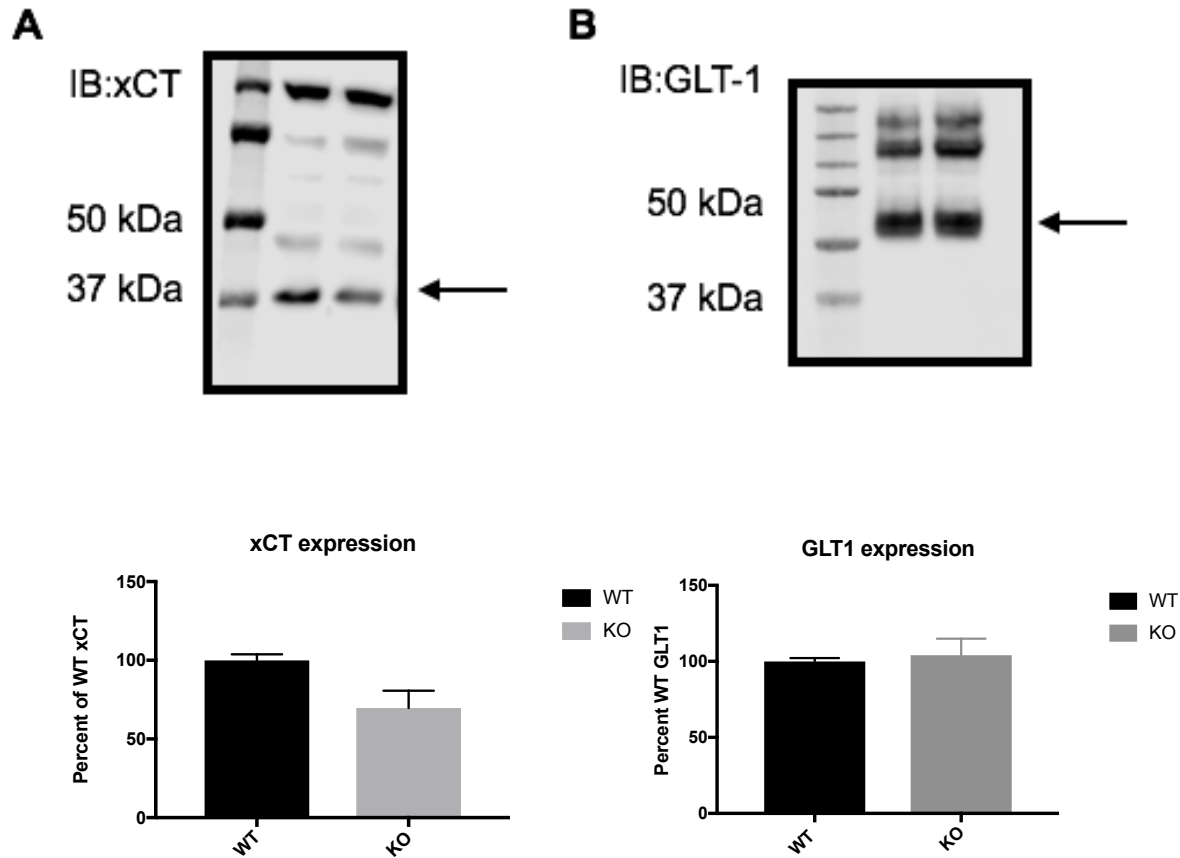
Figure 21. Glutamate transporter expression in MBLAC1 KO animals. A) Western blot and quantification of transporter expression between WT and KO animals show lower, trending levels of xCT expression in the KO animals. (n=4, Welch's T-test P=0.06, analysis of all blots were done by comparing densitometries of the 37kD band in WT and KO animals). B) Western blot and quantification of GLT-1 transporter expression between KO and WT animals. (n=2, preliminary results).

A

Na⁺ dependent Glu Uptake (50 μM)

B

Na⁺ dependent Glu Uptake (10 nM)
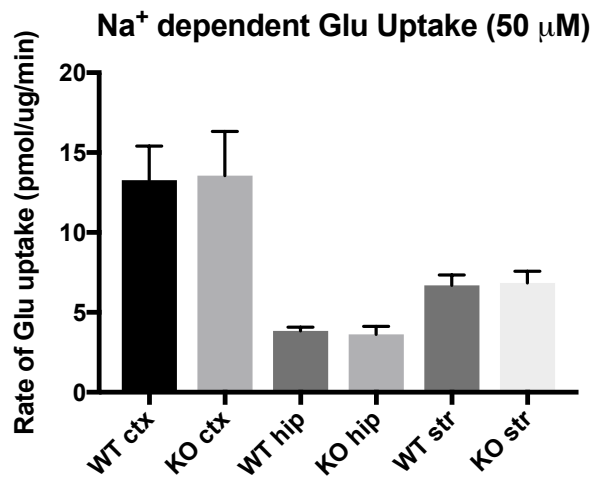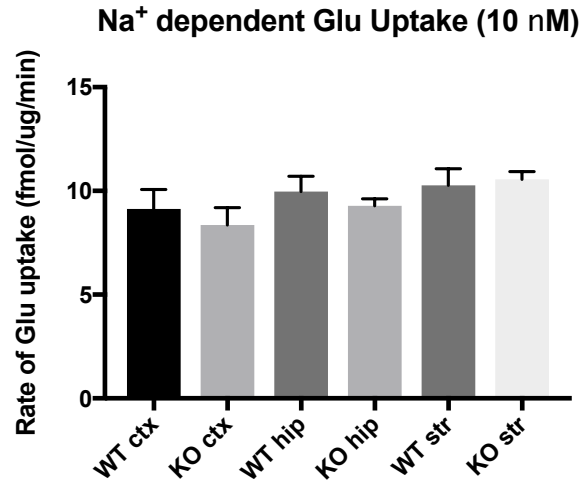
Figure 22. Synaptosomal [³H]Glu uptakes in WT and KO animals. A) High concentration of Glu (10 μM) uptake results from ctx, hipp, and str of WT and KOs. B) Low Glu concentration uptakes (10 nM) in ctx, hipp, and str. Both conditions show no significant difference in the capacity for Na+ dependent uptake (Unpaired T-test comparing WT and KO of each region, P>0.5).

The MBLAC1 KO mice breed at normal ratios and the Chi square test shows that there are no abnormalities in the Mendelian genetics of the KO and WT animals based on HETxHET breeding (Table 2).

Animals, both male and female, were subjected to modified Irwin screens, which look at basic physicality and motor function of the animals.[126] These tests included reporting on coat and grooming, as well as things like grip strength and stamina. All of these results are comparable between the two genotypes and do not indicate any overt phenotypes. This complete list of tasks and observations are shown in Table 3.

Our next studies were focused on how KO of MBLAC1 can affect Cef related behaviors. The data provided in Chapter 2, indicating that Cef and MBLAC1 directly interact, leads to the hypothesis that MBLAC1 is necessary for Cef mediated neuroprotection. In the future, we will test if Cef efficacy is lost in the MBLAC1 KO mouse, but we must first assess basal phenotypes of the KO animals as compared to WT. Since Cef literature is dominated by the effects of cocaine, we decided to pursue studies with cocaine in the KO mouse to directly compare our results with those already published. Our results of WT animals repeatedly injected with cocaine showed a robust sensitizing response, as predicted. This data also showed that the KO animals have a significantly larger response to this final injection of cocaine (Figure 23A). First exposures to cocaine also are significantly different between KO and WT animals, with the KOs having a higher locomotor response to cocaine injection. This trend was not maintained over repeated injections, and points to a mechanism related to cocaine-induced locomotor sensititzation that differs between WT and KO animals (Figure 23B).

	Male	Female	Total
Expected			
WT	34.25 (25%)	32.25 (25%)	66.5 (25%)
Het	68.5 (50%)	64.5 (50%)	133 (50%)
Homo	34.25 (25%)	32.25 (25%)	66.5 (25%)
	Male	**Female**	**Total**
Observed			
WT	29 (21.17%)	25 (19.38%)	54 (20.30%)
Het	69 (50.36%)	63 (48.84%)	132 (49.62%)
Homo	39 (28.47%)	41 (31.78%)	80 (30.08%)
Chi Squared	1.467	4.039	5.098
P-value	0.48	0.133	0.078

Table 2. Chi Square test of HETxHET breading of MBLAC1 KO animals. Table shows that these animals breed normally, and have litters as expected from Mendelian genetics. (Modified from Gibson et al. 2017, under review).

General	WT Female	HOM Female	WT Male	HOM Male
Missing whiskers	0/4	0/4	0/4	0/4
Poor coat condition	0/4	0/4	0/4	0/4
Piloerection	0/4	0/4	0/4	0/4
Bald patches	0/4	0/4	0/4	0/4
Respiration rate	0/4	0/4	0/4	0/4
Tremor	0/4	0/4	0/4	0/4
Gait	0/4	0/4	0/4	0/4
Heart rate	0/4	0/4	0/4	0/4
Body tone	0/4	0/4	0/4	0/4
Limb tone	0/4	0/4	0/4	0/4
Motor ability				
Trunk curl	0/4	0/4	0/4	0/4
Forepaw reaching	0/4	0/4	0/4	0/4
Inverted screen (latency to fall, sec)	60.0 ± 0.0	60.0 ± 0.0	54.5 ± 5.5	59.0 ± 1.0
Pole climb	0/4	3/4	2/4	2/4
Positional passivity	0/4	0/4	0/4	0/4
Rotorod (latency to fall, sec)	206.6 ± 26.2	232.6 ± 20.4	144.1 ± 14.7	207.3 ± 25.0
Grip Strength (N)	0.76 ± 0.05	0.75 ± 0.08	0.98 ± 0.05	0.98 ± 0.13
Reflexes				
Righting reflex	0/4	0/4	0/4	0/4
Air righting reflex	0/4	0/4	0/4	0/4
Ear twitch	0/4	0/4	0/4	0/4
Petting escape	0/4	0/4	0/4	0/4

Table 3. Irwin screen of WT and KO male and female mice. Littermate control animals were put through a modified Irwin screen and the results are presented above. No distinct differences in any of the tests performed.
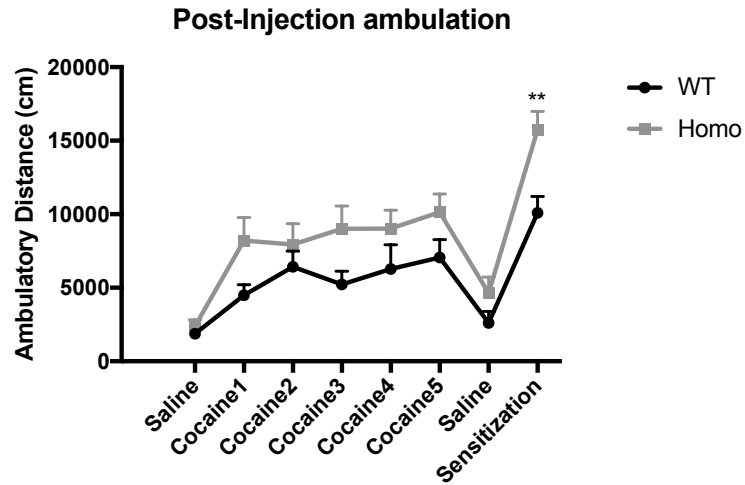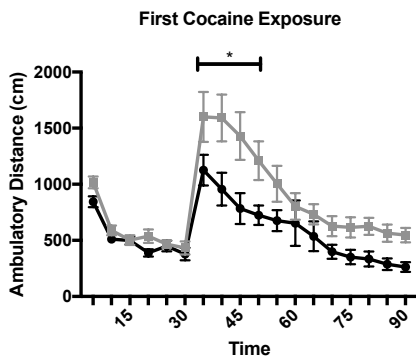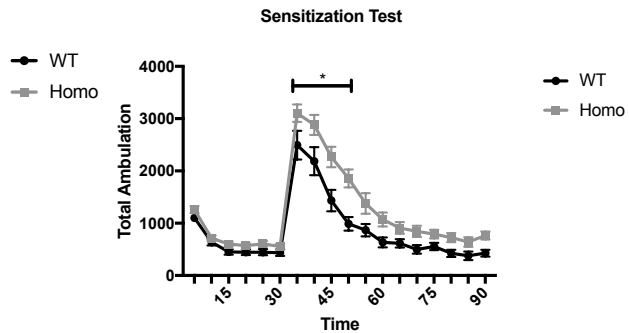
Figure 23. Cocaine locomotor sensitization. A) Values represented are ambulatory movements after cocaine injection, and do not include habituation time in the chamber. Analysis of all time points at the same time result in significant increase in KO response to reinstatement (sensitization test day) injection of cocaine. (Two-way ANOVA, multiple comparisons test, P= 0.0081, **) B) Plot of locomotor activity between WT and KO animals after first exposure to cocaine (left). KO have statically increased activity 5-15 min post-injection (Two-way ANOVA, multiple comparisons; 35 min P<0.037, 40 min P<0.0008, 45 min P<0.0005, 50 min P<0.0293). Plot of locomotor activity after final injection of cocaine to test for sensitized response (right). KO animals have significant increased locomotor activity in response to this injection of cocaine, similar to the first expose to cocaine. (Two-way ANOVA, multiple comparisons; 35 min P<0.0084, 40 min P<0.0013, 45 min P<0.0001, 50 min P<0.0001)

Discussion

We opted to use a different strategy for creating our MBLAC1 KO mice that has shown to be a quicker alternative than traditional KO strategies hat rely on homologous recombination in embryonic stem cells. CRISPR (clustered regularly interspersed short palindromic repeat) was originally discovered as part of the adaptive immune system in bacteria.[128] This technology exploits the CRISPR associated enzyme complexes (Cas) that exist in bacteria to ward off foreign invaders.[128, 129] By utilizing the same CRISPR machinery and RNA or DNA oligonucleotides, distinct DNA regions can be isolated and then targeted for cleavage by the Cas enzymes. These enzymes nick or cleave the DNA, requiring the need for repair mechanisms. A few different DNA repair mechanisms can be employed for repair such as non-homologous end joining (NHEJ). The goal of CRISPR/Cas9 for creating KO animals is to anticipate that some of the repair will be via NHEJ, a notoriously low fidelity process resulting in mismatching DNA. This will create incorrect DNA strands and leads to insertions or deletions within the original DNA sequence, thereby interfering with proper translation and transcription.

Using this CRIPSR/Cas9 gene editing technology, we successfully produced two viable mouse lines with deletions within MBLAC1 that confer the absence of MBLAC1 protein throughout the whole animal. Western blot analysis confirm loss of MBLAC1 protein expression. Interestingly, looking at preliminary basal tissue levels of amino acids, and monoamines within the peripheral tissues and the brain, indicate there no significant differences between the WT and KO animals. The monoamine data indicates high variability and requires further investigation. The one exception is with decreased taurine levels within serum of KO animals. These data are quite relevant for an ongoing project

in the lab, using metabolomic mass spectrometry approach to uncover pathways or substrates that are related to MBLAC1. In an initial attempt to analyze distinct pathway differences between WT and KO animals, serum was taken from age matched female mice and analyzed via LC/MS/MS where one of the handful of metabolic pathways different between WT and KO mice were taurine and hypotuarine (Gibson et al. 2017, *under review*). These amino acid analyses thereby validate the changes that were observed using the metabolomics approach. Though there are no differences in the brain this could point to a general metabolic process that MBLAC1 might participate in that more directly effects serum concentrations of circulating metabolites. Taurine is a byproduct of cysteine metabolism and is implicated in many biological processes from bile acid production to antioxidant properties.[130] Even levels of extracellular Glu have been shown to affect the circulating levels of taurine in the brain.[131]

Other efforts to explore the molecular changes that occurred in the KO of MBLAC1 include assaying the function and expression of Glu transporters GLT-1 and X_c^-. Though we do not see any differences related to function of GLT-1 within the brain of KO animals, we do see a slight reduction in X_c^- protein levels. Functional deficits remain to be evaluated, as we have not yet determined if the Na^+ independent uptake is different in these animals, an experiment that is a necessary future experiment. Interestingly, studies looking at the effects of X_c^- on basal Glu levels only have to reduce the amount of X_c^- by about 20-30%, similar to what we see in our MBLAC1 KO, to see effects in microdialysis measurements of extracellular Glu levels.[67] Attaining these types of measurements would be important and interesting for our KO line, as changes in expression do not necessarily confer changes in function. Changes in X_c^- expression indicate a potential for MBLAC1 to

participate in a pathway to effect the regulation of that transporter. Two basic mechanisms could account for this change in expression. First, the substrate for MBLAC1 accumulates within the cell and is a signal for downstream changes that result in a down regulation of protein X_c^-, or the lack of MBLAC1 product is signaling for a down regulation of X_c^- expression. As there is no evidence that direct interaction exists between X_c^- and MBLAC1. This is another avenue to be explored through co-immunoprecipitations. These results show total protein levels of these transporters, but attaining information on the cellular distribution of these transporters would be even more enlightening.

Irwin screens and basic locomotor activity data determined no significant differences between WT and KO animals. Though there were no stark differences between genotypes, the lack of severe phenotypes provides a much larger dynamic range and breadth of behaviors to explore with this new KO model than if the deletion left the animals completely debilitated. We drew from the Cef literature to guide our first behavioral experiments with these mice. Cef has been used many times in models of addiction as there is an observed blunting of reinstatement of drug seeking behaviors and locomotor sensitization.[92] Behavioral test of sensitization has been linked to a propensity to relapse.[123] Though the first injection of cocaine shows an increased response in locomotor activity, the WT and KO animals normalize over repeated cocaine injections. However, after two weeks of abstinence, the KO animals show a robust and higher locomotor activity response to a reinstating, one-time injection to cocaine. The mechanisms that underlie the plasticity changes are typically attributed to alterations in Glu signaling.[82, 118] The mechanisms of acquiring vs expression of sensitization are distinct, which could point to why we observe nominal changes between WT and KO

initially, but after a period of abstinence we see more exaggerated differences. While the acquisition phase of sensitization during the repeated injections, occurs in the VTA, and thought to be a heavily dopaminergic process, the nucleus accumbens is the effected site of the expression of a sensitized response. This region, heavily influenced by DA, is modulated by Glu innervation from the prefrontal cortex that can control and extent of release of DA. Our results, indicating higher sensitization to cocaine in the KO mouse, could be explained by the glutamatergic signaling changes that occur during this abstinence period. These adaptations result in Glu having a higher release rate to cocaine after a period of abstinence, because of low basal Glu levels.[132] This lowers the inhibitory tone on the mGluR 2/3 that control presynaptic release, which allows for excess of Glu to be released upon a stimulus. The known reductions that occur to the Glu transporters allow this Glu signaling to go on longer than typical, prolonging the signaling of Glu on the postsynaptic neurons.[133] Given that X_c^- is down regulated after repeated administration of cocaine and with the likelihood that there is already a deficit of X_c^- expression in our mice, this potential altered expression could explain part of the mechanism of these behavioral differences. The KO mice might already be operating in a partial withdrawal state, leading to potential reduced basal Glu levels, that are seen with animals that have been given cocaine multiple times. Future experiments will need to explore these results further with alternative behavior experiments. Importantly, the next experiments will need to include a Cef treated group to test the necessity of MBLAC1 in Cef action.

CHAPTER 4

MBLAC1 AND GLUTAMATE TRANSPORT INTERACTIONS

Introduction

Interaction or co-regulation of GLT-1 and X_c^- transporters remains a regularly studied topic within the field. Though it makes sense that these two transporters' activity and regulation would affect each other, there are few studies directly linking the activities of the two transporters. What is known is how they can be transcriptionally and translationally controlled under the same cellular conditions, but not necessarily in the same direction or to the same extent.[45, 134, 135] It is understood that X_c^- antiporter activity relies on intracellular Glu levels to drive the export mechanism.[136] Intracellular levels of Glu are heavily influenced by GLT-1 (Figure 24).[137] The Glu taken into astrocytes by GLT-1 is converted to Gln as part of the Glu/Gln cycle described in Chapter 1, but can also be used for GSH synthesis.[32] Indeed, GSH production appears to rely on the cooperative action these two transporters.[137] Furthermore, GSH depletion is part of the pathophysiology of many diseases in which Cef has been an effective treatment and it does so by increasing the levels of both of these transporters.[103, 109, 138, 139] GSH is a tripeptide made up of Cys, glycine (Gly), and Glu. These three amino acids are linked together through a two-step enzymatic process where the Cys and Glu are combined by the enzyme γ-glutamylcysteine ligase (γ-GCL), which is made up of two subunits, a catalytic unit (γ-GCLC) and a modifier unit (γ-GCLM).[140] The γ-GCLC enzyme carries out
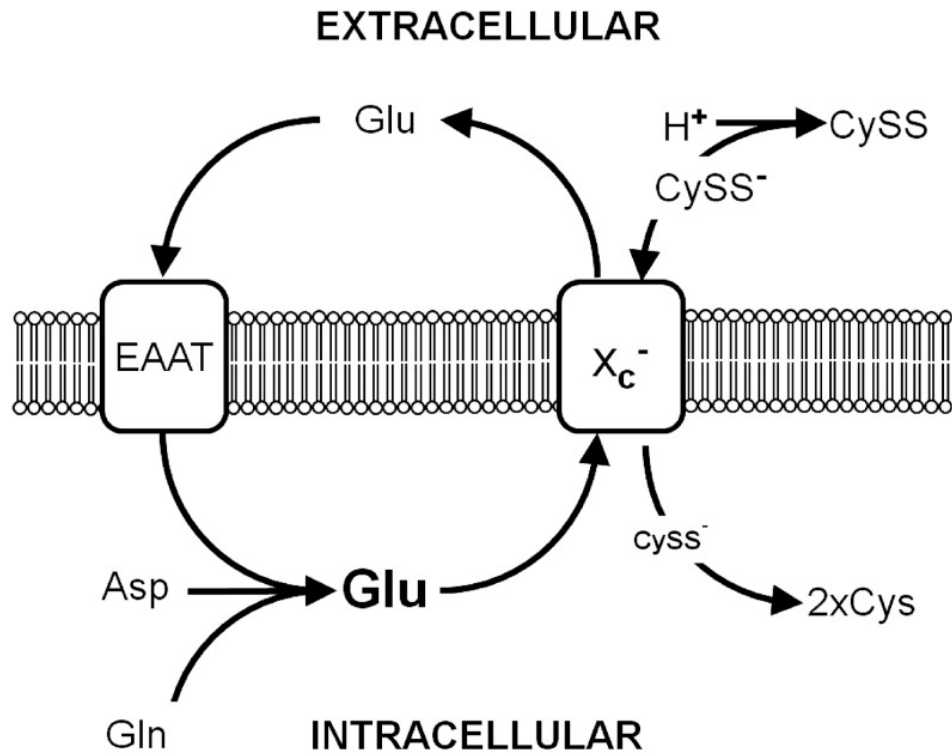
Figure 24. Diagram of EAAT/X_c^- cooperation. Adapted from Lewerenz et al. The Cystine/Glutamate Antiporter System x_c^- in Health and Disease: From Molecular Mechanisms to Novel Therapeutic Opportunities. Antioxid Redox Signal, 2013.

the rate limiting step of GSH synthesis, which is followed by the second amino acid linking step where Gly gets added to the Glu-Cys dipeptide via GSH synthase enzymes. It is of note that GSH is a negative feedback signaling molecule of itself through interaction with the γ-GCLM subunit.[140] [32] Levels of GSH within the cell are typically quite high, ranging from 1-10 mM, signifying the importance of this non-protein thiol.[32] Compounds that deplete stores of GSH have been used for decades to examine the role GSH, and the supporting proteins, play within the cell.[141-143] Many of these compounds are sulfur containing molecules that inhibit the enzymes within the GSH synthesis pathway. One such molecule used for *in vivo* and *in vitro* studies is buthionine sulfoximine (BSO), an inhibitor of γ-GCL activity. By enzyme inactivation, GSH levels are reduced over time, which induces cell activation of compensatory measures to make up for this deficit.[144] Transcriptional programs are activated in this altered redox state and there is an upregulation in the production of antioxidant enzymes and proteins that can combat this change in GSH homeostasis. In instances where GSH is low, one of the proteins induced is X_c^-.[144] Studies suggest that Cef administration can increase levels of GSH, likely through the increase of X_c^- expression.[65] Pharmacological interventions like N-acetylcysteine (NAC) have also been shown to combat low GSH levels through increases in activity of X_c^-. Increasing GSH levels can reduce protein oxidation, which has been shown to effect GLT-1 mediated Glu transporter activity.[145, 146] These studies further support cooperativity between these two transporters. Given that MBLAC1 can bind to Cef and *in vivo* could be the sole cytosolic interactor, it can by hypothesized that MBLAC1 is participating in upstream pathways that can effect both GLT-1 and X_c^-.[125] Since the GSH pathway shows overlap in these two transporters, BSO was used in the studies

below to antagonize the GSH system. Changes were assessed both in MBLAC1 expression, as well as transport activity.

Methods

Western Blots

For these cell experiments, NIH 3T3 mouse fibroblast cells were used. NIH 3T3 cells are known detect endogenous expression of MBLAC1.[125] For BSO or co-BSO/NAC treatments, cells were plated at 450,000 cells/well in 6-well plates, and allowed to settle overnight. On the following day, BSO (500 μm) or NAC (1 mM) treatments were intiated. To obtain cell lysates, cells were rinsed (3x) with 1X PBS, before the addition of 250 μL of RIPA+ protease inhibitor. Cells were shaken for 1 hr at 4 ^{o}C, then centrifuged for 30 min at 13,000 rpm. Protein samples for Western blot analysis were quantified for total protein (BCA Pierce/ThermoFisher, Waltham, MA) and heated to 95 ^{o}C for 5 min with 1X Laemmli buffer before separation via SDS-PAGE using 10% polyacrylamide gels and transfer to Immobilon PVDF membranes (Millipore, Billerica, MA). Membranes were blocked for 1 hr at 25 ^{o}C with 5% milk in TBS/0.1% TWEEN (TBST). Primary antibody, diluted to 1μg/mL in 5% milk/TBST, was incubated with membranes overnight at 4 $^{\circ}$C. After washing 4x for 5 min with TBST, secondary antibody (peroxidase-conjugated mouse-anti-rabbit, Jackson ImmunoResearch, West Grove, PA) in 5% milk/TBST was incubated for 1 hr at rt. Blots were washed again before band visualization and quantitation by enhanced chemiluminescence (BioRad Clarity ECL, Hecules, CA) using an ImageQuant LAS 4000 imager (GE Heathcare Life Sciences, Chicago, IL).

Cell Transport Assays

NIH 3T3 cells were plated at 100,000 cells/well in a 24 well plate and subsequtnely assayed the following day. BSO treatments were administered the same day as plating to assess for 24 hour treatments or same day as the uptake in the case of 1 hour treatments. If cells were transfected to overexpress MBLAC1, they were transfected the day of plating and assessed for transport the next day. For uptake, cells were washed 3x in warm Na^+ free KRH buffer (120 mM NMDG, 1 mM KH_2PO_4, 5 mM KCl,1.3 mM $CaCl_2$, 1.4 mM $MgSO_4$, 10 mM Glucose, pH 7.4) and then 200 μL of KRH+/- sulfasalazine (1 mM) were incubated with the cells for 10 min at 37^oC. $[^3H]$ Glu (200 nM final concentration; 1:4 $^{[3]}$H-Glu: Glu (Perkin Elmer)) was then added to each well and left to incubate for 10 min at 37 ^oC. Cells and uptake were then quenched with ice cold KRH buffer 3x, and followed by the addition of 400 μL of EcoScint in each well. The plate was then left to shake overnight at 25 ^oC before read on TopCount machine. CPM recordings were converted to rates of uptake.

Glutathione levels

To assess the levels of GSH in 3T3 cells we utilized the BioAssay Systems Glutathione kit. This allows for the detection of total GSH in a sample. Protocols provided in the kit were followed. Briefly, cells were sonicated in cold PBS and 1 mM EDTA, followed by centrifugation at 10,000x*g.* Samples were then diluted 20-fold and the used for GSH level detection. Equal volume of Reagent A (provided) and cell lysate samples were mixed, and then spun for 5 min at 14,000x*g.* The resultant supernatant of Reagent

A/sample solution was added to 96 well plate (200 μL). Reagent B was then added to the wells (100 μL) to produce a colormetric detectable response. Plate was then incubated at 25 ^{o}C and then read at 412 nm.

Results

To probe the connection between MBLAC1 and the glial expressed antiporter X_c^-, we explored the acute of effects of BSO treatment on MBLAC1 expression. NIH 3T3 cells were used for all of the following experiments, as they endogenously express MBLAC1 and X_c^-. Seib and colleagues showed that BSO can upregulate the X_c^- transporter after 24-72 hours of treatment.[144] After shorter incubations with BSO, GSH levels can also drop significantly, but these reductions occur only with much high concentrations of BSO than in my current study.[147] Acute (1-24 hour) treatment of BSO on 3T3 cells induced a temporary increase in MBLAC1 expression (Figure 25). At 1, 4 and 8 hours there are significant increases in the immunoreactivity of MBLAC1. However, after 24 hr of BSO the expression of MBLAC1 diminishes, on average, to 49% of basal expression. Interestingly, this is when the expression of X_c^- starts to increase, based on previous published work.[144] Because of poor antibodies to X_c^- we opted to assay activity of the transporter. After 1 hr BSO there was a slight, but significant, decrease in uptake, correlating to when we saw a rise in MBLAC1 expression (Figure 26). Furthermore, when MBLAC1 was overexpressed in 3T3 cells I also observed a significant decrease in X_c^-
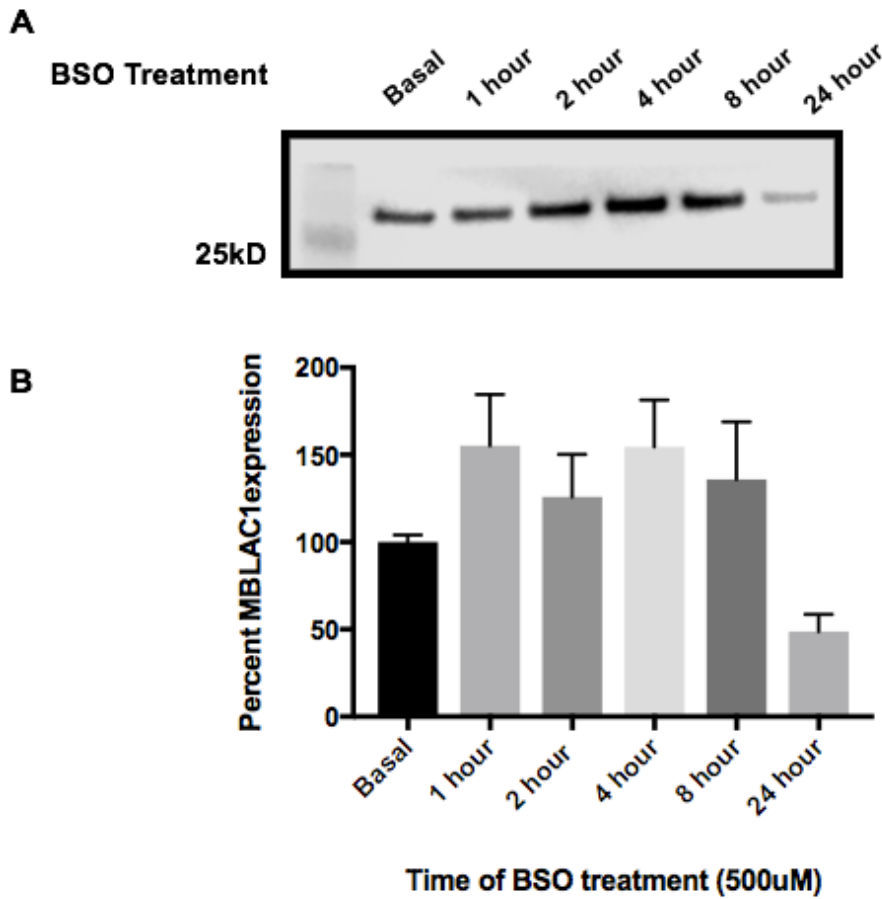
Figure 25. Time course of MBLAC1 expression with BSO. A) Blot of MBLAC1 expression in 3T3 cells after BSO treatment. B) Over the course of 24 hr BSO increases, then significantly decreases the expression on MBLAC1 in 3T3 cells. Nearly significant increase of MBLAC1 occurs at 1 hr (P=0.0529, unpaired t test) and 4 hours (P=0.0384, unpaired t test) of BSO treatment. At 24 hr MBLAC1 drops below basal levels (Mean difference is 51.2% ± 9.8, P<0.001, unpaired t test). Conditions were normalized to actin control. Ordinary One-way ANOVA, with Dunnett's multiple comparisons tests do not show significance at any of the acute time points.

uptake (Figure 26B, C). Together, the reductions I observed in X_c^- mediated uptake indicates that inducing expression, either genetically or pharmacologically, of MBLAC1 can effect X_c^- transport activity. The changes in activity of X_c^- in the presence of BSO for times longer than 24 hours indicate that it is the reduction in GSH that is the catalyst to increasing X_c^- expression and activity. We also see as significant increase in X_c^- activity, as shown in Figure 27A, correlating with a significant drop in total GSH levels in NIH 3T3 cells after BSO treatment (Figure 27B). Over the whole time course of BSO treatment (1-24 hr), GSH levels do not significantly change until BSO has been present for 24 hr. The lack of correlation between GSH levels and MBLAC1 expression suggests that the MBLAC1 expression changes and the reduction in X_c^- activity observed after 1 hr of BSO treatment do not correlate to a change in GSH levels.

Discussion

By probing the cellular context with a known GSH depletion drug, I wanted to provide evidence that X_c^- and MBLAC1 are supported by common pathways. Through pharmacological interruption of GSH synthesis via BSO treatment, known to effect X_c^- expression and activity, we examined changes in MBLAC1 expression. Largely, the studies that involve BSO take place over an extended period of time. [144, 148, 149] Initial efforts were to determine if acute, *in vitro* treatments effected the expression of MBLAC1. Interestingly, only a few hours or less of BSO treatment was enough to induce significant, but temporary increases in MBLAC1 expression. However, this did not necessarily
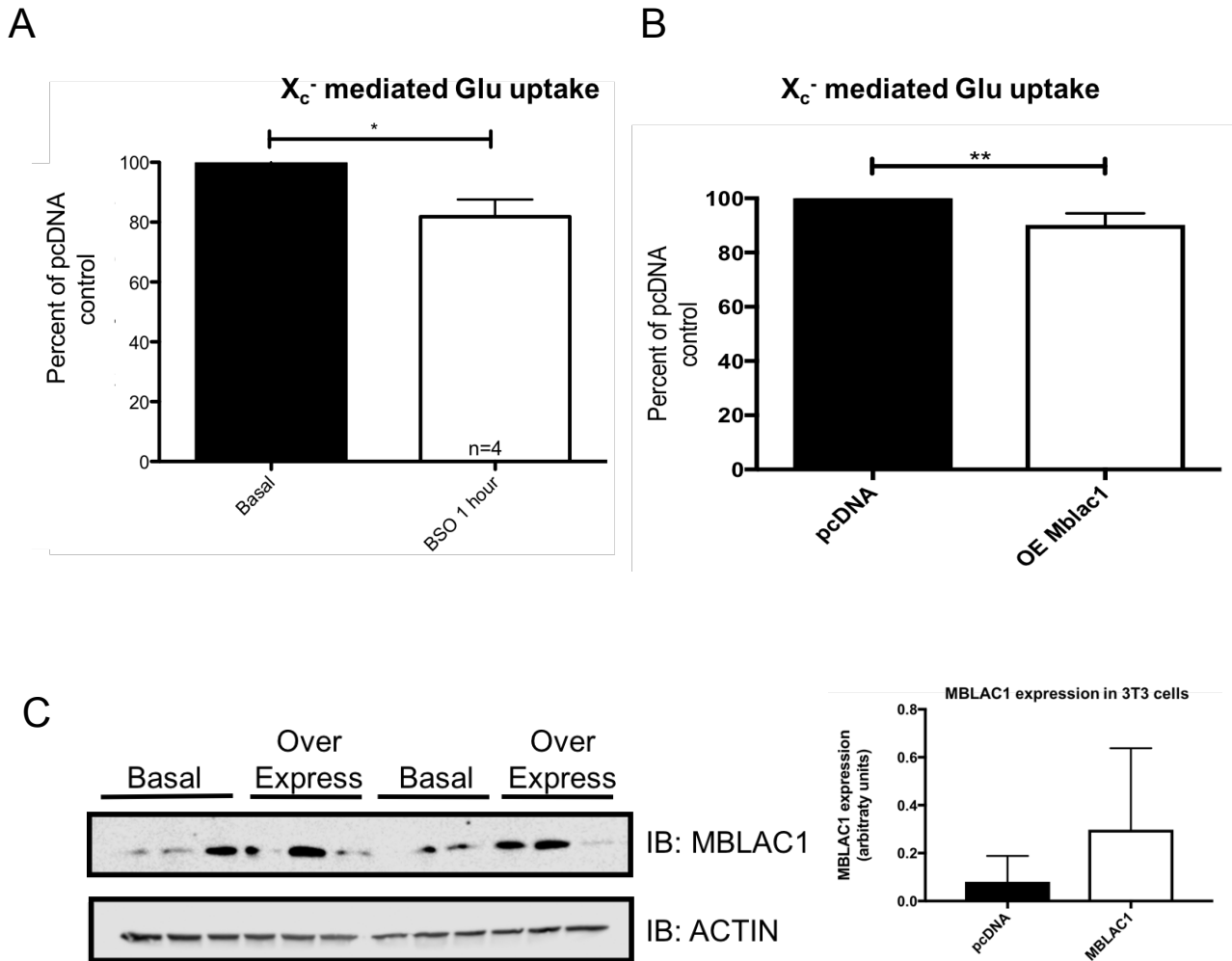
Figure 26. Analysis of MBLAC1 overexpression and its effect on X_c^- transport activity. A) Bar graph of X_c^- mediated Glu uptake between cells treated for 1 hr with BSO (500 μM) and those not. (n=3, Mean difference 17.4% +/-6.9, two-tailed paired t test P<0.02) B) X_c^- mediated Glu uptake between cells that were transfected to over express MBLAC1 and those not. Slight but significant reduction in uptake is apparent when MBLAC1 in both instances (n=6, Mean difference 9.8% +/-1.7, two-tailed paired t test P<0.0024).C) Western blot and quantification verifying overexpression of MBLAC1 (not statistically significant, P=0.16, unpaired t test).
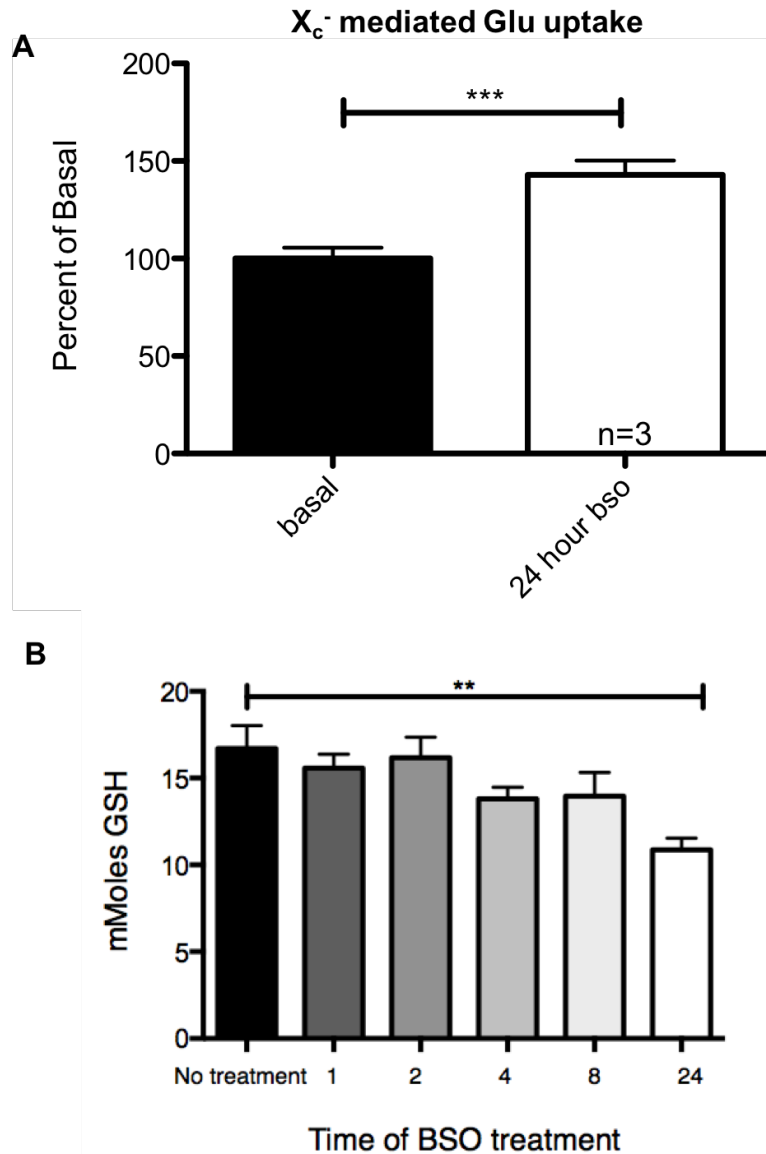
Figure 27. Analysis of BSO treatment effect on X_c^- transport activity and GSH levels. A) Bar graph of X_c^- mediated Glu uptake between cells treated with BSO (500 uM) for 24 hr and those treated with vehicle (H_2O). Significant increase in uptake is apparent when BSO is present for 24 hr (n=3, Mean increase is 42.97% ± 9.3, Two-tailed pair t test P=0.0218). B) Glutathione analysis after time course of BSO treatment. Graph representing mMoles of GSH present in 3T3 cell after different times with BSO in the media. Only at 24 hours of BSO treatment is there a significant reduction in detectable GSH levels. (n=6, One-way ANOVA, P=0.0059).

correlate to changes in total GSH within the cell. This quick accumulation of MBLAC1 immunoreactivity could result from several mechanisms. BSO treatment could be changing the post-translational modifications of MLBAC1 protein though S-glutathionylation or other adducts that are common due to changes in cellular redox. Additionally, there could be mechanisms of rapid translation of the protein, if there are mRNA stores of MBLAC1 in reserve. Transcriptional activation, though possible, is less likely to be the mechanism by which MBLAC1 expression is changing given the time scale. The presence of BSO could also be activating mechanisms of MBLAC1 stabilization that are only temporary while the cell finds a new homeostatic set point in the presence of BSO. Understanding what the cycle of MBLAC1 protein turnover would illuminate what of the above processes could be at play.

It is known that BSO treatment typically decreases GSH levels and activates the Nrf2 pathway to initiate transcription of proteins that are important to overcome elevated ROS levels.[150] Many studies show that these effects are most dramatically seen with exposure to BSO over the course of 1-3 days.[144] Since the experiments described above were performed for an acute time course, the changes that were happening are less well understood. Given that the total levels of GSH do not change over the same time course of MBLAC1 protein increase, I cannot say definitively if MBLAC1 expression and GSH levels are linked. However, changes between the ratio of GSH to GSSH (a reduced form) could be altered with BSO treatment, leading to the effects I observed. This particularly assay did not allow for the detection of both forms of GSH.

Because of the established link between BSO and X_c^-, I wanted to explore how MBLAC1 and X_c^- could be co-regulated. Using transporter activity as a proxy for change

in transporter modulation, we assessed X_c^- activity in three conditions; the first being under 1 hr BSO, another after with overexpression of MBLAC1, and lastly after 24-hour BSO treatment. The acute 1 hr treatment of BSO and the overexpression of MBLAC1 conditions both examine X_c^- activity in the presence of excess MBLAC1 protein. Both pharmacological and genetic manipulations produced reductions in X_c^- activity. Though the time scales of treatment between BSO and MBLAC1 overexpression were different, these changes in MBLAC1 result in the same effect on transporter activity. These data suggest that MBLAC1 expression can alter the normal function of X_c^- but doesn't identify a mechanism. Future work will explore the mechanism behind these data. One possibility could be that the substrate(s) or product(s) of MBLAC1 may indirectly effect X_c^- activity by acting as blockers, or change the interacting proteins connections of X_c^-. Alternatively, MBLAC1 could directly interact with the transporter itself, but there is no evidence of this as of now, and we have not seen any MBLAC1 in membrane fractions of 3T3 cells before. The data showing an increase in X_c^- activity of transport was acquired at the same time points where I observed decreases in MBLAC1 expression. The opposing responses to 24 hr BSO treatment of MBLAC1 and X_c^- imply that MBLAC1 may negatively regulate X_c^- during basal cellular conditions. The exposure to BSO may override this regulation and induce expression of X_c^- to increase activity to compensate for the reduced GSH levels. This work opens many questions regarding MBLAC1 protein regulation and future experiments to examine the transcription and degradation path of this enzyme will better position future experimenters to know which other pharmacological treatments to use or avenues to explore.

CHAPTER 5

FINAL DISCUSSION AND FUTURE DIRECTIONS

The work described in this thesis opens many new avenues for future experiments and explorations into the previously unstudied MBLAC1. With strong expression throughout the brain, MBLAC1 was shown to interact in both cells and tissue with the neuroprotective agent Cef. This β–lactam antibiotic has been used for over a decade to provide a therapeutic intervention for many animal models of neurological disorders and diseases that are caused by, or are in part due to, dysregulated Glu signaling.[42, 43, 92, 95, 110] By increasing the expression of GLT-1 and X_c^-, astrocytically expressed Glu transporters, Cef allows for a resetting of extracellular and intracellular Glu levels, reestablishing Glu homeostasis.[42, 59] Additionally, in cases where cell death progression is due to neuronal excitotoxicity, Cef provides an increase in GLT-1 that can help prevent hyperactivity of the Glu receptors.[90, 91, 95, 151] Prior studies have sought to understand the mechanism by which Cef activates the transporters and although some work points to transcriptional regulation, few studies have proposed a molecular target of Cef to enact the cellular changes observed.[64, 65] The Blakely lab previously discovered a *C. elegans* protein containing a MBL domain that was shown to regulate DA neurons through a glutamatergic mechanism of hyperexcitability. This protein, known as SWIP-10, has a putative mammalian ortholog, MBLAC1.[81] With the structural motif and catalytic domain known to interact with β–lactam antibiotics in bacteria, we chose to explore the possibility that MBLAC1 could bind to Cef. Using a two pronged approach with affinity chromatography and BSI methods, we observed that MBLAC1 was capable of interacting

90

with Cef with low μM affinity consistent with effective *ex vivo* concentrations.[43] This work provides the first evidence for a protein to interact with Cef at physiologically relevant concentrations, and with canonical interacting domains.[125] Other groups have shown Cef can potentially interact with proteins like α–synuclein and GFAP, but the experimental method relies on purified proteins not whole cell extracts, and though Cef can fit within the tertiary structure of the proteins based on modeling, a canonical binding domain would provide a more stable and high affinity interaction.[68, 69] As a target of Cef action, MBLAC1 could operate as a modulator of astrocytic Glu signaling and could be a new drugable target for rational drug design. The assays employed for our Cef binding studies are effective, but lack a high throughput aspect that would be necessary for the testing of more compounds. We have sought other methods to facilitate a more high-throughput system, but these strategies have not yet worked. The OctetRED system, a plate based platform for monitoring binding kinetics between proteins and small molecules, was tried to create a higher throughput system for MBLAC1 and Cef interaction. This method requires purified protein, and our initial efforts in isolating MBLAC1 from bacterial preparations resulted in high levels of aggregation. Even in collaboration with Dr. Tina Iverson of Vanderbilt University, an expert in protein purification, we were unable to gather enough functional pure product for these studies. Chris Schofield's group at Oxford has purified many MBD containing proteins using different bacterial cells or Sf9 cells for expressing enzyme.[105] Bacterial preparations may not be suitable for this protein growth due to lack of proper chaperone proteins or cofactors. Growth of MBLAC1 protein using large cultures of human based cell lines might be an alternative method to try in the future.

Ongoing efforts are currently assessing the viability of transforming the bead-based assay into a plate-based one. Initial attempts suggest increased steric hindrance with Cef attachment or loss of efficient coupling reaction. The Sepharose beads currently used rely on a CNBr coupling reaction, but the available plates use a maleic acid coupling mechanism. Previous attempts at Cef coupling to other non-CNBr moieties were not successful, suggesting the plates may not be an effective method either. The CNBr coupling reaction might be more stable and provide a stronger bond to Cef than other available free amine reactors. A way to circumvent this issue would be to add a linker on to Cef that would be be able to be conjugated to the plates offering more free chemical space for MBLAC1 interaction. This is something we are currently exploring with collaborators at Florida Atlantic University.

The binding site of the Cef: MBLAC1 interaction also needs further investigation. The nature of this interaction remains a question of inhibition or activation. Many compounds interact with their targets as inhibitors, and this is most likely how Cef is working. However, even though less likely, it could be an activator of activity or bind to MBLAC1 in a way to promote endogenous substrate binding through binding site cooperativity. Preliminary investigation to assess requirements for binding included mutating distinct, highly conserved residues and observing if they were still able to interact with Cef. Whereas the missense mutation, G190D, is expressed equally to that of WT, and seems to bind to Cef just as well, a truncation mutant, W202STOP, is barely detectable in Western Blots. Although this inability to detect protein could be due to antibody epitope loss, it could also point to an important regulatory part of the protein that is necessary for proper folding, function, or protein-protein interaction. Exploring other

sites of mutagenesis could determine critical sites of interaction between Cef and MBLAC1 and further our knowledge of MBLAC1 function. Additionally, understanding the state at which MBLAC1 sits in basally (i.e. monomeric or dimeric species) will be critical for being able to design more effective and more potent drugs. Structural information of MBLAC1 will be a valuable asset for future studies. Interestingly, PDB files for human MBLAC1 are available in the Protein Data Bank, but no published studies referencing these files exist to date. Brief examination of this data reveals that MBLAC might exist as a homodimer, though the interactions illustrated may be an artifact of crystalization conditions. Further exploration into these data will be crucial for proper interpretation of future binding experiments.

Another critical step forward with this project would be to uncover the endogenous substrate(s) of this enzyme. Substrate identification will be imperative for designing an activity assay that can be more easily translated to a high throughput assay and used to screen compounds that act similarly to Cef. Although a high throughput binding assay would be beneficial, an activity assay would be more valuable. Efforts have been put forth by a fellow graduate student in the lab to search for endogenous substrates of MBLAC1. To that end, we have used mass spectrometry to determine potential substrates or pathways in which MBLAC1 could participate. Metabolomic software analysis of the data have indicated taurine, glutathione, and linoleic acid pathways are altered in MBLAC1 KO mice (Gibson et al. 2017, *under review*). Though these experiments have not lead to a specific substrate, it has narrowed our thinking about which pathways we can probe for MBLAC1 action.

In conjunction with an *in vitro* based assay for MBLAC1 function, the protein's activity and role in the brain needs to be further characterized *in vivo.* The creation of MBLAC1 KO animals through CRISPR/Cas9 gene targeting and editing allows for *in vivo* testing of these hypotheses. Ascertaining whether MBLAC1 is necessary or sufficient to carry out the effects of Cef action will be a main goal and future direction with this novel KO animal line. Initial efforts in characterizing MBLAC1 KO animals, as tested through Irwin screens, show few basal differences compared to their WT littermates. With no severe basal phenotypes, testing in these animals can be performed in a wide variety of behaviors with a wide dynamic range of testing. With no overt deficits, the animals may only exert differences when placed under stress or under very distinct contexts. As we do not know MBLAC1's endogenous function, it can be difficult to focus on which behaviors to test first. However, we know that this protein can interact with Cef, so our initial efforts focused on behaviors that have exhibited responses to Cef administration.

Initial locomotor sensitization experiments probed the effects of cocaine administration and its effects on MBLAC1 KO animals. First cohorts were assessed for basal effects without the administration of Cef. We see a marked increase in the sensitized response to cocaine in the KO animals, as well as a heightened initial response to the first injection of cocaine. Knowing that acquisition and expression of sensitization is due to glutamatergic plasticities, we can conclude that there is baseline dysregulation of Glu signaling, at least in part, that could be contributing to this phenotype.[82] These mice also have a robust increased sensitized response after a period of withdrawal. Degree of sensitization has been linked to a higher risk of reinstatement or relapse.[152] This could indicate that the MBLAC1 KO mice might be more susceptible to the rewarding effects of

drugs of abuse. Furthermore, an observed reduction in X_c^- total protein could lead to altered Glu homeostasis in MBLAC1 KO animals. In this regard, investigators have shown that X_c^- is responsible for regulating and stabilizing extracellular Glu levels.[40, 67] For these reasons, Glu levels via microdialysis studies are a necessary future direction.

The next step in assessing these animals would be to directly examine if Cef is having an effect in MBLAC1 KO animals. This is a necessary question that needs to be explored, as determining MBLAC1's necessity in Cef's neuroprotective action will validate our *ex vivo* binding data showing MBLAC1 as a sole cytosolic molecular target in the brain. These experiments are vital. Repeating sensitization with a Cef condition would be an obvious next step, but there are also a few experiments that would be more straightforward than retesting sensitization. One such experiment includes recapitulating data out of Scott Rawls' group where a pretreatment of Cef blunts the locomotor response to one acute injection of cocaine.[61] With one injection of cocaine, we could determine if our KO animals are sensitive to Cef administration, determining the necessity of MBLAC1 for Cef mediated neurological effects. However, there are some caveats to this experiment. Typically for Cef treatment to be effective there needs to be an initial insult or stressor. This could mask any behavioral differences between genotypes giving a clouded view of the data.

If we wanted to move away from drugs of abuse to study MBLAC1 in the context of Cef administration, we could explore the many other behaviors that have shown to be modified by Cef treatment. This includes seizure susceptibility, DA neuron sensivity to 6OH-DA toxicity, and ischemic stroke.[91, 114, 153] I was able to show that WT mice treated with Cef for 10 days prior to kainic acid injection delayed the onset of stage 3 seizure

(using the Racine scale) (see Appendix II). This was a straightforward experiment and could easily be replicated in our lab with MBLAC1 KO animals.

Aside from validating Cef targets *in vivo*, this mouse model presents a unique opportunity to study a model of increased propensity to relapse. Many studies rely on pharmacotherapies to reverse a drug induced phenotype, but MBLAC1 KO animals provide a genetic, face valid model for relapse sensitive populations. No known SNPs within the *MBLAC1* gene are known to be a risk factor for addiction, but this could still be a valuable model for testing future compounds and the circuitries involved in these processes. The genetic underpinnings of this model would more readily represent and recapitulate the human condition of those vulnerable to addiction.

Future studies with KO animals could examine Glu circuits and use MBLAC1 KO animals as a model of disrupted Glu to gain further insight into the basic parameters of neuronal signaling. Preliminary data collected in collaboration with Qi Zhang's lab at Vanderbilt University indicates that glial expressed MBLAC1 can affect hippocampal neuron signaling. Astrocyte primary cultures overexpressing MBLAC1 can decrease both amplitude and frequencies of EPSC recordings. These data are interesting and should be kept in mind as future work explores the circuit based differences in KO and WT animals.

We know that SWIP-10 is expressed in glia in worms, but in mammals the orthologue MBLAC1 may also be present in neurons. Glial control over neuronal signaling has been studied in a variety of contexts, and these KO mice could give a unique model to study the effect of glia on neuronal signaling.[154-156] Future studies will also need to delineate MBLAC1 expression in the different cell types of the brain.

In vitro results connecting MBLAC1 and X_c^-, though preliminary, do point to some interesting potential interaction between the two proteins. Though genetic and pharmacological overexpression of MBLAC1 can decrease X_c^- activity, experiments exploring these mechanisms are still needed. Understanding basic principles of MBLAC1 regulation and expression pattern would be essential to further understanding these results and for gaining a more complete picture of MBLAC1's role in the cell. Gaining insights into the mechanistic aspects of how MBLAC1 comes to be upregulated would inform our knowledge on its baseline regulation. This would lead to further understanding of the transcriptional programs that regulate MBLAC1 and which transcription factors activate MBLAC1 expression. This information could further link MBLAC1 to distinct signaling pathways within the cell, illuminating cell networks of note.

Though these data are interesting, we need to compare them to the *in vivo* data we have gathered to gain full insight into the interplay between these two molecules. Although in NIH 3T3 cells we see decrements of X_c^- due to overexpression of MBLAC1, *in vivo* the elimination of MBLAC1 potentially results in the same effect. Though seemingly conflicting ideas, I argue that this could make sense. It is common with many biological molecules, and in particular enzymes, that their activity exists in a U-shaped curve. In both deficits and overabundance, the results can be the same. This has been shown in H_2S signaling where low and high levels of this signaling molecule are predictive of poor clinical outcomes.[157] Applying these ideas to MBLAC1 asserts that it could be acting as a sort of sensor for a cellular state, whether redox state or other, and in times of low or high MBLAC1 the same cellular changes could result. Additionally, it could be the substrates and products of MBLAC1 that facilitate these signaling changes. Comparing

data *in vitro* and *in vivo* can be dangerous as we know the two systems are very different and the actions and regulatory mechanisms are not always the same. This needs to be kept in mind when comparing the experiments and their seemingly opposite results.

Overall, the work and studies presented in this thesis provide novel results on a previously unstudied protein, MBLAC1, and its newly reported interaction with Cef. *In vivo* and *in vitro* work examined potential roles for MBLAC1 in glutamatergic and GSH signaling. There are many exciting and new directions to take these projects. The tools and methods carved out in this work provide a foundation to explore the many facets of MBLAC1 function in future studies.

APPENDIX I

The Creation of More MBLAC1 Antibodies

INTRODUCTION

The antibodies used for the studies in this thesis were satisfactory for western blotting, but with the advent of the KO mouse we found they were insufficient as a specific immunohistochemistry tool. In an effort to design new tools for immunohistochemistry, co-IPs or other antibody recognition work we moved forward to make new antibodies.

In collaboration with ThermoScientific we created six more antibodies for potential use with immuno-studies. The original antibodies (#79 and #80) were made by injecting rabbits with full length GST:MBLAC1 protein fusion protein. These antibodies were purified in the lab (see methods of Chapter 1). For the next round of antibody production, we wanted to use the MBP:MBLAC1 fusion protein, as well as smaller peptides to create more specific antibodies that might be better for immunohistochemical studies. I worked with Thermo to create two distinct peptides that were targeted to the C-terminal end of the protein. ThermoFisher possess software to determine the likelyhood of the antibodies created from these peptides to be effective in certain assays like Western blots, immunostaining, or ELISAs. This software allowed us to choose two peptides (Figure 28) to use as antigen targets. Another method we used to increase our chances of finding effective antibodies was to expand the species of animals to inject. Typically, rabbits are used for the making of polyclonal antibodies, but other animals like chickens and guinea pigs can be used. We opted to use chickens in addition to rabbits for our antibody creation. Using chickens also lessens the chance of cross-

MNGPVRTEPLHGEIPLLASSGSYSVVVLLRGYAEPQGAGDAVRADGT
VTLVLPRGWASDSSRGLAPSADGGSKTALEEAVRGPILVDTGGPWAR
GALLEALATQGVAPEDVTLVVGTHGHSDHIGNLGLFPEAALLVSHDFC
LPEGLYLPHGLCETQPLILGSGLQVWATPGHGGQRDVSVVVEGTSL
GTVVVAGDVFERLGDEDSWQALSEDPVAQQRSRERILSVADVVVPG
HGAPFRVVRETVKSSEDLICEGKAVA

Figure 28. Peptides for antibody production. Amino acid sequence of mouse MBLAC1. Red and green highlight the two peptides we used as antigens for injection into both rabbits and chickens.

reactivity with other mammalian off target antigens. In total we had three different antigens (two peptides and the full length fusion protein) each made in two different animals (rabbit and chicken), and two animals of each species (12 different antibody lots total).

RESULTS and DISCUSSION

Since we have had success in the past with testing antibodies on Western blots, I continued with this method for choosing which antibodies would go forward for boosts or extra bleeds. Using mouse brain tissue, from cortex or whole brain samples of WT and KO animals, and the inducible MBLAC1 cell lines, we tested whether or not the newly created antibodies could detect MBLAC1 in the lysates. In Figure 29 are the initial blots with serum from the first bleed after the full immunization has taken place. From these blots I can see that only a select group of the antibodies could detect the correct MBLAC1 band, verified by no band in the KO or non-expressing cells. Next steps will be to test these antibodies in other assays, specifically on immunohistochemical slices to see if specific MBLAC1 immnoreactivity can be assessed. Antibodies will also need to be purified if they are deemed suitable for Western blotting or immunohistochemistry.
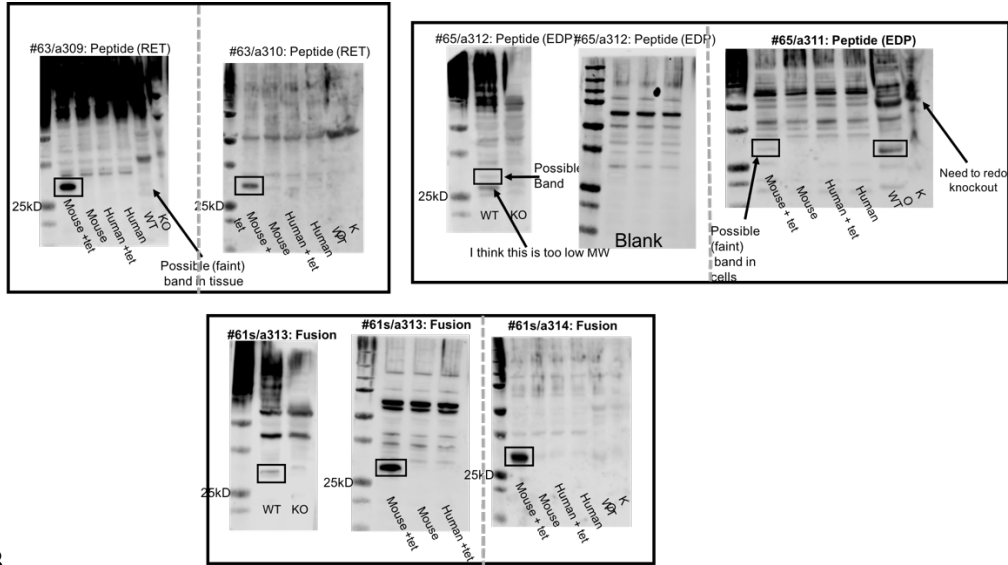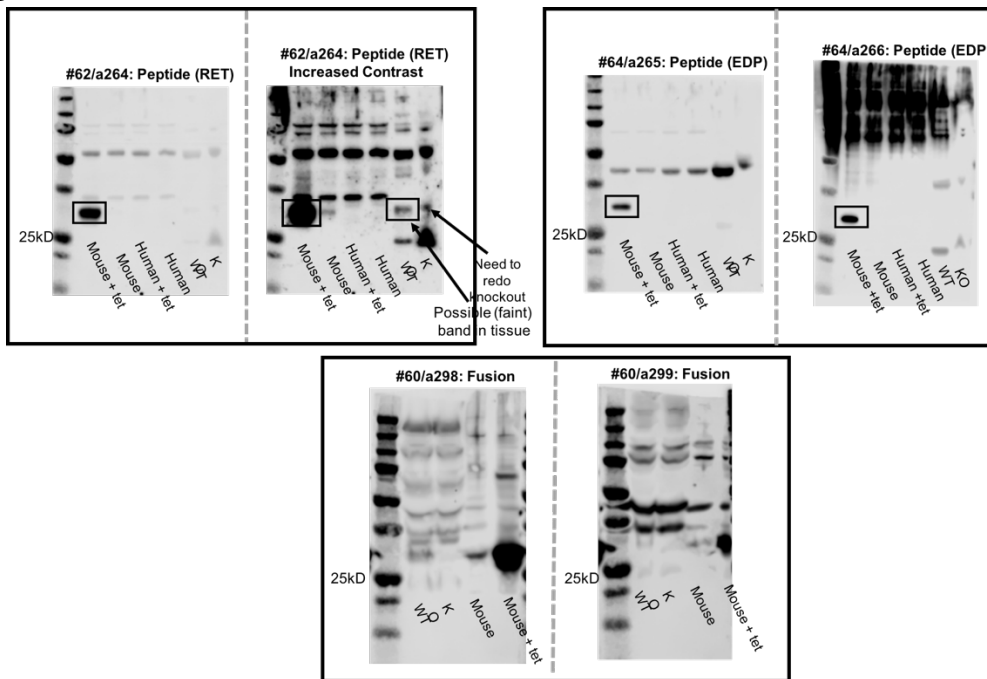
Figure 29. Serum antibody testing. A) Results from antigens injected in to chickens. All serum samples were run against tissue and cells lacking or expressing MBLAC1. B) Results from antigens injected in to rabbits. All serum samples were run against tissue and cells lacking or expressing MBLAC1.

APPENDIX II

Pretreatment of Ceftriaxone Can Delay Onset of Kainic Acid Induced Seizures

INTRODUCTION

Cef has been shown to be neuroprotective and prevent neuronal cell death in models of stroke and TBI.[49, 90, 91, 95, 158] It is well documented that these effects are due to its ability to modulate Glu uptake through induction of Glu transporter expression.[43, 90] Being able to modulate Glu transporters leads to an alteration in Glu homeostasis, something that is acutely altered during seizure activity. Typically, seizures are attributed to dysregulation between the inhibitory and excitatory action. Seizures can be induced by certain drugs, one of which is kainic acid (KA), a glutamate receptor agonist. This will over excite neurons and dysregulate a whole host of other processes. It has been shown that pretreatment with Cef can provide a buffer for this type of induced seizure, by increasing the latency to stage three seizures, using the Racine Scale (unpublished observations from Dr. Fiona Harrison's lab). Wanting to be able to recapitulate some of these findings I sought to test my hand at Cef injection prior to KA induced seizures. I collaborated with Fiona Harrison's lab at Vanderbilt University, as they had preformed these experiments before.

METHODS

WT animals (Jackson Laboratories, Bar Harbor Maine) were handled according the IACUC approved protocols at Vanderbilt University. Animals were pretreated with

200mg/kg Cef for 7 consecutive days, before a 30 mg/kg injection of KA. Animals were then monitored for 60 min and activity was recorded. Signs of the different stages of seizures according to the Racine scale were also documented. If animals reached the last stage of seizure (stage 6) before 60 min, animals were sacrificed as per protocol regulations. After 60 min, animals were sacrificed regardless of seizure stage and brain tissue was collected and froze for future analysis.

RESULTS and DISCUSSION

Pretreatment of Cef for seven days resulted in an increased time to stage 3 seizure (Figure 30). This stage of seizure is defined by involuntary movement of the forelimbs, but before involuntary rearing and falling. The time to stage three with Cef pretreatment was closer to 20 min as compared to 15 min in saline treated animals. This was similar to the results the Harrison lab had seen before in their hands. This allowed for me to gain valuable experience in mouse handling and injection, while validating the Cef work previously performed in this lab. This also prepared me for future behavioral studies working with Cef, mice and injections.

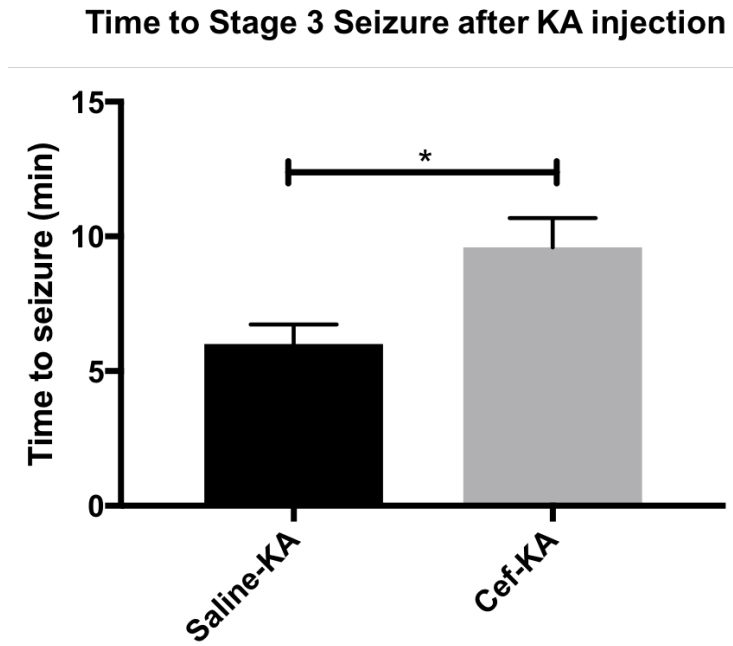**Time to Stage 3 Seizure after KA injection**

Figure 30. Ceftriaxone delays onset of KA induced seizure. Graph represents the average of time for mice to reach stage 3 seizure after injection of KA (30mg/kg). Data shows increased time to this stage if mice were pretreated with Cef (200 mg/kg) for 7 days. (n=10 per group, unpaired t test, P= 0.0132).

REFERENCES

[1] Curtis, D. R., and Watkins, J. C. (1960) The excitation and depression of spinal neurones by structurally related amino acids, *Journal of neurochemistry 6*, 117-141.

[2] Ikonomidou, C., Bosch, F., Miksa, M., Bittigau, P., Vockler, J., Dikranian, K., Tenkova, T. I., Stefovska, V., Turski, L., and Olney, J. W. (1999) Blockade of NMDA receptors and apoptotic neurodegeneration in the developing brain, *Science 283*, 70-74.

[3] Lujan, R., Shigemoto, R., and Lopez-Bendito, G. (2005) Glutamate and GABA receptor signalling in the developing brain, *Neuroscience 130*, 567-580.

[4] Sanacora, G., Treccani, G., and Popoli, M. (2012) Towards a glutamate hypothesis of depression: an emerging frontier of neuropsychopharmacology for mood disorders, *Neuropharmacology 62*, 63-77.

[5] Angulo, M. C., Kozlov, A. S., Charpak, S., and Audinat, E. (2004) Glutamate released from glial cells synchronizes neuronal activity in the hippocampus, *The Journal of neuroscience : the official journal of the Society for Neuroscience 24*, 6920-6927.

[6] Gallo, V., Ciotti, M. T., Coletti, A., Aloisi, F., and Levi, G. (1982) Selective release of glutamate from cerebellar granule cells differentiating in culture, *Proceedings of the National Academy of Sciences of the United States of America 79*, 7919-7923.

[7] Nelson, S. B., Hempel, C., and Sugino, K. (2006) Probing the transcriptome of neuronal cell types, *Current opinion in neurobiology 16*, 571-576.

[8] Birnbaumer, L., Campbell, K. P., Catterall, W. A., Harpold, M. M., Hofmann, F., Horne, W. A., Mori, Y., Schwartz, A., Snutch, T. P., Tanabe, T., and et al. (1994) The naming of voltage-gated calcium channels, *Neuron 13*, 505-506.

[9] Meldrum, B. S. (2000) Glutamate as a neurotransmitter in the brain: review of physiology and pathology, *J Nutr 130*, 1007S-1015S.

[10] Palmada, M., and Centelles, J. J. (1998) Excitatory amino acid neurotransmission. Pathways for metabolism, storage and reuptake of glutamate in brain, *Front Biosci 3*, d701-718.

[11] Reimer, R. J., Chaudhry, F. A., Gray, A. T., and Edwards, R. H. (2000) Amino acid transport system A resembles system N in sequence but differs in mechanism, *Proceedings of the National Academy of Sciences of the United States of America 97*, 7715-7720.

[12] Norenberg, W., Gobel, I., Meyer, A., Cox, S. L., Starke, K., and Trendelenburg, A. U. (2001) Stimulation of mouse cultured sympathetic neurons by uracil but not adenine nucleotides, *Neuroscience 103*, 227-236.

[13] Laube, B., Kuhse, J., and Betz, H. (1998) Evidence for a tetrameric structure of recombinant NMDA receptors, *The Journal of neuroscience : the official journal of the Society for Neuroscience 18*, 2954-2961.

[14] Dingledine, R., and Conn, P. J. (2000) Peripheral glutamate receptors: molecular biology and role in taste sensation, *J Nutr 130*, 1039S-1042S.

[15] Henley, J. M., and Wilkinson, K. A. (2013) AMPA receptor trafficking and the mechanisms underlying synaptic plasticity and cognitive aging, *Dialogues Clin Neurosci 15*, 11-27.

[16] Riedel, G., Platt, B., and Micheau, J. (2003) Glutamate receptor function in learning and memory, *Behav Brain Res 140*, 1-47.

[17] Mody, I., and MacDonald, J. F. (1995) NMDA receptor-dependent excitotoxicity: the role of intracellular Ca2+ release, *Trends Pharmacol Sci 16*, 356-359.

[18] Hollmann, M., O'Shea-Greenfield, A., Rogers, S. W., and Heinemann, S. (1989) Cloning by functional expression of a member of the glutamate receptor family, *Nature 342*, 643-648.

[19] Lerma, J., and Marques, J. M. (2013) Kainate receptors in health and disease, *Neuron 80*, 292-311.

[20] Niswender, C. M., and Conn, P. J. (2010) Metabotropic glutamate receptors: physiology, pharmacology, and disease, *Annu Rev Pharmacol Toxicol 50*, 295-322.

[21] Grueter, B. A., McElligott, Z. A., Robison, A. J., Mathews, G. C., and Winder, D. G. (2008) In vivo metabotropic glutamate receptor 5 (mGluR5) antagonism prevents cocaine-induced disruption of postsynaptically maintained mGluR5-dependent long-term depression, *The Journal of neuroscience : the official journal of the Society for Neuroscience 28*, 9261-9270.

[22] Kammermeier, P. J., and Worley, P. F. (2007) Homer 1a uncouples metabotropic glutamate receptor 5 from postsynaptic effectors, *Proceedings of the National Academy of Sciences of the United States of America 104*, 6055-6060.

[23] Mitchell, S. J., and Silver, R. A. (2000) Glutamate spillover suppresses inhibition by activating presynaptic mGluRs, *Nature 404*, 498-502.

[24] Levy, L. M., Warr, O., and Attwell, D. (1998) Stoichiometry of the glial glutamate transporter GLT-1 expressed inducibly in a Chinese hamster ovary cell line selected for low

endogenous Na⁺-dependent glutamate uptake, *The Journal of neuroscience : the official journal of the Society for Neuroscience 18*, 9620-9628.

[25] Shigeri, Y., Seal, R. P., and Shimamoto, K. (2004) Molecular pharmacology of glutamate transporters, EAATs and VGLUTs, *Brain Res Brain Res Rev 45*, 250-265.

[26] Perego, C., Vanoni, C., Bossi, M., Massari, S., Basudev, H., Longhi, R., and Pietrini, G. (2000) The GLT-1 and GLAST glutamate transporters are expressed on morphologically distinct astrocytes and regulated by neuronal activity in primary hippocampal cocultures, *Journal of neurochemistry 75*, 1076-1084.

[27] Ota, Y., Zanetti, A. T., and Hallock, R. M. (2013) The role of astrocytes in the regulation of synaptic plasticity and memory formation, *Neural Plast 2013*, 185463.

[28] Auld, D. S., and Robitaille, R. (2003) Glial cells and neurotransmission: an inclusive view of synaptic function, *Neuron 40*, 389-400.

[29] Benediktsson, A. M., Marrs, G. S., Tu, J. C., Worley, P. F., Rothstein, J. D., Bergles, D. E., and Dailey, M. E. (2012) Neuronal activity regulates glutamate transporter dynamics in developing astrocytes, *Glia 60*, 175-188.

[30] Tanaka, K., Watase, K., Manabe, T., Yamada, K., Watanabe, M., Takahashi, K., Iwama, H., Nishikawa, T., Ichihara, N., Kikuchi, T., Okuyama, S., Kawashima, N., Hori, S., Takimoto, M., and Wada, K. (1997) Epilepsy and exacerbation of brain injury in mice lacking the glutamate transporter GLT-1, *Science 276*, 1699-1702.

[31] Murphy-Royal, C., Dupuis, J. P., Varela, J. A., Panatier, A., Pinson, B., Baufreton, J., Groc, L., and Oliet, S. H. (2015) Surface diffusion of astrocytic glutamate transporters shapes synaptic transmission, *Nature neuroscience 18*, 219-226.

[32] Lu, S. C. (2013) Glutathione synthesis, *Biochim Biophys Acta 1830*, 3143-3153.

[33] Bridges, R., Lutgen, V., Lobner, D., and Baker, D. A. (2012) Thinking outside the cleft to understand synaptic activity: contribution of the cystine-glutamate antiporter (System xc-) to normal and pathological glutamatergic signaling, *Pharmacological reviews 64*, 780-802.

[34] Sato, H., Tamba, M., Ishii, T., and Bannai, S. (1999) Cloning and expression of a plasma membrane cystine/glutamate exchange transporter composed of two distinct proteins, *The Journal of biological chemistry 274*, 11455-11458.

[35] Lewerenz, J., Hewett, S. J., Huang, Y., Lambros, M., Gout, P. W., Kalivas, P. W., Massie, A., Smolders, I., Methner, A., Pergande, M., Smith, S. B., Ganapathy, V., and Maher, P. (2012)

The Cystine/Glutamate Antiporter System x(c)(-) in Health and Disease: From Molecular Mechanisms to Novel Therapeutic Opportunities, *Antioxid Redox Signal*.

[36] Sato, H., Tamba, M., Okuno, S., Sato, K., Keino-Masu, K., Masu, M., and Bannai, S. (2002) Distribution of cystine/glutamate exchange transporter, system x(c)-, in the mouse brain, *The Journal of neuroscience : the official journal of the Society for Neuroscience 22*, 8028-8033.

[37] Pochini, L., Scalise, M., Galluccio, M., and Indiveri, C. (2014) Membrane transporters for the special amino acid glutamine: structure/function relationships and relevance to human health, *Front Chem 2*, 61.

[38] Verrey, F., Closs, E. I., Wagner, C. A., Palacin, M., Endou, H., and Kanai, Y. (2004) CATs and HATs: the SLC7 family of amino acid transporters, *Pflugers Archiv : European journal of physiology 447*, 532-542.

[39] Baker, D. A., Xi, Z. X., Shen, H., Swanson, C. J., and Kalivas, P. W. (2002) The origin and neuronal function of in vivo nonsynaptic glutamate, *The Journal of neuroscience : the official journal of the Society for Neuroscience 22*, 9134-9141.

[40] Baker, D. A., McFarland, K., Lake, R. W., Shen, H., Tang, X. C., Toda, S., and Kalivas, P. W. (2003) Neuroadaptations in cystine-glutamate exchange underlie cocaine relapse, *Nature neuroscience 6*, 743-749.

[41] Kalivas, P. W. (2009) The glutamate homeostasis hypothesis of addiction, *Nature reviews. Neuroscience 10*, 561-572.

[42] Knackstedt, L. A., Melendez, R. I., and Kalivas, P. W. (2010) Ceftriaxone restores glutamate homeostasis and prevents relapse to cocaine seeking, *Biological psychiatry 67*, 81-84.

[43] Rothstein, J. D., Patel, S., Regan, M. R., Haenggeli, C., Huang, Y. H., Bergles, D. E., Jin, L., Dykes Hoberg, M., Vidensky, S., Chung, D. S., Toan, S. V., Bruijn, L. I., Su, Z. Z., Gupta, P., and Fisher, P. B. (2005) Beta-lactam antibiotics offer neuroprotection by increasing glutamate transporter expression, *Nature 433*, 73-77.

[44] Sari, Y., Prieto, A. L., Barton, S. J., Miller, B. R., and Rebec, G. V. (2010) Ceftriaxone-induced up-regulation of cortical and striatal GLT1 in the R6/2 model of Huntington's disease, *J Biomed Sci 17*, 62.

[45] Rothstein, J. D., Van Kammen, M., Levey, A. I., Martin, L. J., and Kuncl, R. W. (1995) Selective loss of glial glutamate transporter GLT-1 in amyotrophic lateral sclerosis, *Ann Neurol 38*, 73-84.

[46] Rothstein, J. D., Martin, L. J., and Kuncl, R. W. (1992) Decreased glutamate transport by the brain and spinal cord in amyotrophic lateral sclerosis, *The New England Journal of Medicine 326*, 1464-1468.

[47] Andre, V. M., Cepeda, C., and Levine, M. S. (2010) Dopamine and glutamate in Huntington's disease: A balancing act, *CNS Neurosci Ther 16*, 163-178.

[48] Wei, J., Pan, X., Pei, Z., Wang, W., Qiu, W., Shi, Z., and Xiao, G. (2012) The beta-lactam antibiotic, ceftriaxone, provides neuroprotective potential via anti-excitotoxicity and anti-inflammation response in a rat model of traumatic brain injury, *J Trauma Acute Care Surg*.

[49] Lipski, J., Wan, C. K., Bai, J. Z., Pi, R., Li, D., and Donnelly, D. (2007) Neuroprotective potential of ceftriaxone in in vitro models of stroke, *Neuroscience 146*, 617-629.

[50] Pekna, M., and Pekny, M. (2012) The neurobiology of brain injury, *Cerebrum 2012*, 9.

[51] Kantrowitz, J., and Javitt, D. C. (2012) Glutamatergic transmission in schizophrenia: from basic research to clinical practice, *Curr Opin Psychiatry 25*, 96-102.

[52] Moghaddam, B., and Javitt, D. (2012) From revolution to evolution: the glutamate hypothesis of schizophrenia and its implication for treatment, *Neuropsychopharmacology : official publication of the American College of Neuropsychopharmacology 37*, 4-15.

[53] Javitt, D. C. (2007) Glutamate and schizophrenia: phencyclidine, N-methyl-D-aspartate receptors, and dopamine-glutamate interactions, *Int Rev Neurobiol 78*, 69-108.

[54] Aan Het Rot, M., Zarate, C. A., Jr., Charney, D. S., and Mathew, S. J. (2012) Ketamine for depression: where do we go from here?, *Biological psychiatry 72*, 537-547.

[55] Drevets, W. C. (2001) Neuroimaging and neuropathological studies of depression: implications for the cognitive-emotional features of mood disorders, *Current opinion in neurobiology 11*, 240-249.

[56] Zarate, C. A., Jr., Singh, J. B., Carlson, P. J., Brutsche, N. E., Ameli, R., Luckenbaugh, D. A., Charney, D. S., and Manji, H. K. (2006) A randomized trial of an N-methyl-D-aspartate antagonist in treatment-resistant major depression, *Arch Gen Psychiatry 63*, 856-864.

[57] Leshner, A. I., and Koob, G. F. (1999) Drugs of abuse and the brain, *Proc Assoc Am Physicians 111*, 99-108.

[58] Traynor, B. J., Bruijn, L., Conwit, R., Beal, F., O'Neill, G., Fagan, S. C., and Cudkowicz, M. E. (2006) Neuroprotective agents for clinical trials in ALS: a systematic assessment, *Neurology 67*, 20-27.

[59] Trantham-Davidson, H., LaLumiere, R. T., Reissner, K. J., Kalivas, P. W., and Knackstedt, L. A. (2012) Ceftriaxone normalizes nucleus accumbens synaptic transmission, glutamate transport, and export following cocaine self-administration and extinction training, *The Journal of neuroscience : the official journal of the Society for Neuroscience 32*, 12406-12410.

[60] Alajaji, M., Bowers, M. S., Knackstedt, L., and Damaj, M. I. (2013) Effects of the beta-lactam antibiotic ceftriaxone on nicotine withdrawal and nicotine-induced reinstatement of preference in mice, *Psychopharmacology (Berl)*.

[61] Tallarida, C. S., Corley, G., Kovalevich, J., Yen, W., Langford, D., and Rawls, S. M. (2013) Ceftriaxone attenuates locomotor activity induced by acute and repeated cocaine exposure in mice, *Neurosci Lett 556*, 155-159.

[62] Abulseoud, O. A., Miller, J. D., Wu, J., Choi, D. S., and Holschneider, D. P. (2012) Ceftriaxone upregulates the glutamate transporter in medial prefrontal cortex and blocks reinstatement of methamphetamine seeking in a condition place preference paradigm, *Brain Res 1456*, 14-21.

[63] Ward, S. J., Rasmussen, B. A., Corley, G., Henry, C., Kim, J. K., Walker, E. A., and Rawls, S. M. (2011) Beta-lactam antibiotic decreases acquisition of and motivation to respond for cocaine, but not sweet food, in C57Bl/6 mice, *Behav Pharmacol 22*, 370-373.

[64] Lee, S. G., Su, Z. Z., Emdad, L., Gupta, P., Sarkar, D., Borjabad, A., Volsky, D. J., and Fisher, P. B. (2008) Mechanism of ceftriaxone induction of excitatory amino acid transporter-2 expression and glutamate uptake in primary human astrocytes, *The Journal of biological chemistry 283*, 13116-13123.

[65] Lewerenz, J., Albrecht, P., Tien, M. L., Henke, N., Karumbayaram, S., Kornblum, H. I., Wiedau-Pazos, M., Schubert, D., Maher, P., and Methner, A. (2009) Induction of Nrf2 and xCT are involved in the action of the neuroprotective antibiotic ceftriaxone in vitro, *Journal of neurochemistry 111*, 332-343.

[66] Zhang, Y., Zhang, X., and Qu, S. (2015) Ceftriaxone Protects Astrocytes from MPP(+) via Suppression of NF-kappaB/JNK/c-Jun Signaling, *Mol Neurobiol 52*, 78-92.

[67] LaCrosse, A. L., Hill, K., and Knackstedt, L. A. (2016) Ceftriaxone attenuates cocaine relapse after abstinence through modulation of nucleus accumbens AMPA subunit expression, *Eur Neuropsychopharmacol 26*, 186-194.

[68] Ruzza, P., Siligardi, G., Hussain, R., Marchiani, A., Islami, M., Bubacco, L., Delogu, G., Fabbri, D., Dettori, M. A., Sechi, M., Pala, N., Spissu, Y., Migheli, R., Serra, P. A., and Sechi, G. (2014) Ceftriaxone blocks the polymerization of alpha-synuclein and exerts neuroprotective effects in vitro, *ACS chemical neuroscience 5*, 30-38.

[69] Ruzza, P., Vitale, R. M., Hussain, R., Biondi, B., Amodeo, P., Sechi, G., and Siligardi, G. (2016) Interactions of GFAP with ceftriaxone and phenytoin: SRCD and molecular docking and dynamic simulation, *Biochim Biophys Acta 1860*, 2239-2248.

[70] Fisher, J. F., Meroueh, S. O., and Mobashery, S. (2005) Bacterial resistance to beta-lactam antibiotics: compelling opportunism, compelling opportunity, *Chem Rev 105*, 395-424.

[71] Davies, J. (1996) Origins and evolution of antibiotic resistance, *Microbiologia 12*, 9-16.

[72] Dever, L. A., and Dermody, T. S. (1991) Mechanisms of bacterial resistance to antibiotics, *Arch Intern Med 151*, 886-895.

[73] Bush, K. (1998) Metallo-beta-lactamases: a class apart, *Clinical infectious diseases : an official publication of the Infectious Diseases Society of America 27 Suppl 1*, S48-53.

[74] Bush, K., and Jacoby, G. A. (2010) Updated functional classification of beta-lactamases, *Antimicrobial agents and chemotherapy 54*, 969-976.

[75] Meini, M. R., Llarrull, L. I., and Vila, A. J. (2014) Evolution of Metallo-beta-lactamases: Trends Revealed by Natural Diversity and in vitro Evolution, *Antibiotics (Basel) 3*, 285-316.

[76] Drawz, S. M., and Bonomo, R. A. (2010) Three decades of beta-lactamase inhibitors, *Clin Microbiol Rev 23*, 160-201.

[77] Page, M. I., and Badarau, A. (2008) The mechanisms of catalysis by metallo beta-lactamases, *Bioinorg Chem Appl*, 576297.

[78] Carfi, A., Pares, S., Duee, E., Galleni, M., Duez, C., Frere, J. M., and Dideberg, O. (1995) The 3-D structure of a zinc metallo-beta-lactamase from Bacillus cereus reveals a new type of protein fold, *EMBO J 14*, 4914-4921.

[79] Pettinati, I., Brem, J., Lee, S. Y., McHugh, P. J., and Schofield, C. J. (2016) The Chemical Biology of Human Metallo-beta-Lactamase Fold Proteins, *Trends Biochem Sci*.

[80] Hardaway, J. A., Hardie, S. L., Whitaker, S. M., Baas, S. R., Zhang, B., Bermingham, D. P., Lichtenstein, A. J., and Blakely, R. D. (2012) Forward genetic analysis to identify determinants of dopamine signaling in Caenorhabditis elegans using swimming-induced paralysis, *G3 2*, 961-975.

[81] Hardaway, J. A., Sturgeon, S. M., Snarrenberg, C. L., Li, Z., Xu, X. Z., Bermingham, D. P., Odiase, P., Spencer, W. C., Miller, D. M., 3rd, Carvelli, L., Hardie, S. L., and Blakely, R. D. (2015) Glial Expression of the Caenorhabditis elegans Gene swip-10 Supports Glutamate Dependent Control of Extrasynaptic Dopamine Signaling, *The Journal of neuroscience : the official journal of the Society for Neuroscience 35*, 9409-9423.

[82] Tzschentke, T. M., and Schmidt, W. J. (2003) Glutamatergic mechanisms in addiction, *Mol Psychiatry 8*, 373-382.

[83] Seeman, P. (2009) Glutamate and dopamine components in schizophrenia, *J Psychiatry Neurosci 34*, 143-149.

[84] Xu, Y., and Chen, X. (2006) Glyoxalase II, a detoxifying enzyme of glycolysis byproduct methylglyoxal and a target of p63 and p73, is a pro-survival factor of the p53 family, *The Journal of biological chemistry 281*, 26702-26713.

[85] Van Boeckel, T. P., Gandra, S., Ashok, A., Caudron, Q., Grenfell, B. T., Levin, S. A., and Laxminarayan, R. (2014) Global antibiotic consumption 2000 to 2010: an analysis of national pharmaceutical sales data, *Lancet Infect Dis 14*, 742-750.

[86] Kong, K. F., Schneper, L., and Mathee, K. (2010) Beta-lactam antibiotics: from antibiosis to resistance and bacteriology, *APMIS 118*, 1-36.

[87] Davies, J., and Davies, D. (2010) Origins and evolution of antibiotic resistance, *Microbiol Mol Biol Rev 74*, 417-433.

[88] Khan, A. U., Ali, A., Danishuddin, Srivastava, G., and Sharma, A. (2017) Potential inhibitors designed against NDM-1 type metallo-beta-lactamases: an attempt to enhance efficacies of antibiotics against multi-drug-resistant bacteria, *Sci Rep 7*, 9207.

[89] Tikka, T., Usenius, T., Tenhunen, M., Keinanen, R., and Koistinaho, J. (2001) Tetracycline derivatives and ceftriaxone, a cephalosporin antibiotic, protect neurons against apoptosis induced by ionizing radiation, *Journal of neurochemistry 78*, 1409-1414.

[90] Chu, K., Lee, S. T., Sinn, D. I., Ko, S. Y., Kim, E. H., Kim, J. M., Kim, S. J., Park, D. K., Jung, K. H., Song, E. C., Lee, S. K., Kim, M., and Roh, J. K. (2007) Pharmacological Induction of Ischemic Tolerance by Glutamate Transporter-1 (EAAT2) Upregulation, *Stroke 38*, 177-182.

[91] Jelenkovic, A. V., Jovanovic, M. D., Stanimirovic, D. D., Bokonjic, D. D., Ocic, G. G., and Boskovic, B. S. (2008) Beneficial effects of ceftriaxone against pentylenetetrazole-evoked convulsions, *Exp Biol Med (Maywood) 233*, 1389-1394.

[92] Sondheimer, I., and Knackstedt, L. A. (2011) Ceftriaxone prevents the induction of cocaine sensitization and produces enduring attenuation of cue- and cocaine-primed reinstatement of cocaine-seeking, *Behav Brain Res 225*, 252-258.

[93] Leung, T. C. H., Lui, C. N. P., Chen, L. W., Yung, W. H., Chan, Y. S., and Yung, K. K. L. (2011) Ceftriaxone Ameliorates Motor Deficits and Protects Dopaminergic Neurons in 6-Hydroxydopamine-Lesioned Rats, *ACS chemical neuroscience*, 9.

[94] Hota, S. K., Barhwal, K., Ray, K., Singh, S. B., and Ilavazhagan, G. (2008) Ceftriaxone rescues hippocampal neurons from excitotoxicity and enhances memory retrieval in chronic hypobaric hypoxia, *Neurobiol Learn Mem 89*, 522-532.

[95] Thone-Reineke, C., Neumann, C., Namsolleck, P., Schmerbach, K., Krikov, M., Schefe, J. H., Lucht, K., Hortnagl, H., Godes, M., Muller, S., Rumschussel, K., Funke-Kaiser, H., Villringer, A., Steckelings, U. M., and Unger, T. (2008) The beta-lactam antibiotic, ceftriaxone, dramatically improves survival, increases glutamate uptake and induces neurotrophins in stroke, *J Hypertens 26*, 2426-2435.

[96] Rao, P. S., and Sari, Y. (2014) Effects of Ceftriaxone on Chronic Ethanol Consumption: a Potential Role for xCT and GLT1 Modulation of Glutamate Levels in Male P Rats, *Journal of molecular neuroscience : MN*.

[97] Rao, P. S., Saternos, H., Goodwani, S., and Sari, Y. (2015) Effects of ceftriaxone on GLT1 isoforms, xCT and associated signaling pathways in P rats exposed to ethanol, *Psychopharmacology (Berl) 232*, 2333-2342.

[98] Kussrow, A., Enders, C. S., and Bornhop, D. J. (2012) Interferometric Methods for Label-Free Molecular Interaction Studies, *Anal Chem 84*, 779-792.

[99] Bornhop, D. J., Kammer, M. N., Kussrow, A., Flowers, R. A., and Meiler, J. (2016) Origin and prediction of free-solution interaction studies performed label-free, *P Natl Acad Sci USA 113*, E1595-E1604.

[100] Baksh, M. M., Kussrow, A. K., Mileni, M., Finn, M. G., and Bornhop, D. J. (2011) Label-free quantification of membrane-ligand interactions using backscattering interferometry, *Nat Biotechnol 29*, 357-U173.

[101] Kost, G. C., Selvaraj, S., Lee, Y. B., Kim, D. J., Ahn, C. H., and Singh, B. B. (2012) Clavulanic acid inhibits MPP(+)-induced ROS generation and subsequent loss of dopaminergic cells, *Brain Res 1469*, 129-135.

[102] Schroeder, J. A., Tolman, N. G., McKenna, F. F., Watkins, K. L., Passeri, S. M., Hsu, A. H., Shinn, B. R., and Rawls, S. M. (2014) Clavulanic acid reduces rewarding, hyperthermic and locomotor-sensitizing effects of morphine in rats: a new indication for an old drug?, *Drug and alcohol dependence 142*, 41-45.

[103] Zumkehr, J., Rodriguez-Ortiz, C. J., Cheng, D., Kieu, Z., Wai, T., Hawkins, C., Kilian, J., Lim, S. L., Medeiros, R., and Kitazawa, M. (2015) Ceftriaxone ameliorates tau pathology and cognitive decline via restoration of glial glutamate transporter in a mouse model of Alzheimer's disease, *Neurobiol Aging 36*, 2260-2271.

[104] Matos-Ocasio, F., Hernandez-Lopez, A., and Thompson, K. J. (2014) Ceftriaxone, a GLT-1 transporter activator, disrupts hippocampal learning in rats, *Pharmacology, biochemistry, and behavior 122C*, 118-121.

[105] Lee, S. Y., Brem, J., Pettinati, I., Claridge, T. D., Gileadi, O., Schofield, C. J., and McHugh, P. J. (2016) Cephalosporins inhibit human metallo beta-lactamase fold DNA repair nucleases SNM1A and SNM1B/apollo, *Chem Commun (Camb) 52*, 6727-6730.

[106] Zimmer, E. R., Parent, M. J., Leuzy, A., Aliaga, A., Moquin, L., Schirrmacher, E. S., Soucy, J. P., Skelin, I., Gratton, A., Gauthier, S., and Rosa-Neto, P. (2015) Imaging in vivo glutamate fluctuations with [(11)C]ABP688: a GLT-1 challenge with ceftriaxone, *J Cereb Blood Flow Metab 35*, 1169-1174.

[107] Abulseoud, O. A., Camsari, U. M., Ruby, C. L., Kasasbeh, A., Choi, S., and Choi, D. S. (2014) Attenuation of Ethanol Withdrawal by Ceftriaxone-Induced Upregulation of Glutamate Transporter EAAT2, *Neuropsychopharmacology : official publication of the American College of Neuropsychopharmacology 39*, 1674-1684.

[108] Amin, B., Hajhashemi, V., Abnous, K., and Hosseinzadeh, H. (2014) Ceftriaxone, a beta-lactam antibiotic, modulates apoptosis pathways and oxidative stress in a rat model of neuropathic pain, *Biomed Res Int 2014*, 937568.

[109] Weng, J. C., Tikhonova, M. A., Chen, J. H., Shen, M. S., Meng, W. Y., Chang, Y. T., Chen, K. H., Liang, K. C., Hung, C. S., Amstislavskaya, T. G., and Ho, Y. J. (2016) Ceftriaxone prevents the neurodegeneration and decreased neurogenesis seen in a Parkinson's disease rat model: An immunohistochemical and MRI study, *Behav Brain Res 305*, 126-139.

[110] Mineur, Y. S., Picciotto, M. R., and Sanacora, G. (2007) Antidepressant-like effects of ceftriaxone in male C57BL/6J mice, *Biological psychiatry 61*, 250-252.

[111] Sari, Y., Smith, K. D., Ali, P. K., and Rebec, G. V. (2009) Upregulation of GLT1 attenuates cue-induced reinstatement of cocaine-seeking behavior in rats, *The Journal of neuroscience : the official journal of the Society for Neuroscience 29*, 9239-9243.

[112] Miller, B. R., Dorner, J. L., Shou, M., Sari, Y., Barton, S. J., Sengelaub, D. R., Kennedy, R. T., and Rebec, G. V. (2008) Up-regulation of GLT1 expression increases glutamate uptake and attenuates the Huntington's disease phenotype in the R6/2 mouse, *Neuroscience 153*, 329-337.

[113] Uyanikgil, Y., Ozkeskek, K., Cavusoglu, T., Solmaz, V., Tumer, M. K., and Erbas, O. (2016) Positive effects of ceftriaxone on pentylenetetrazol-induced convulsion model in rats, *Int J Neurosci 126*, 70-75.

[114] Chotibut, T., Davis, R. W., Arnold, J. C., Frenchek, Z., Gurwara, S., Bondada, V., Geddes, J. W., and Salvatore, M. F. (2013) Ceftriaxone increases glutamate uptake and reduces striatal tyrosine hydroxylase loss in 6-OHDA Parkinson's model, *Molecular neurobiology*.

[115] Sari, Y., Sakai, M., Weedman, J. M., Rebec, G. V., and Bell, R. L. (2011) Ceftriaxone, a beta-lactam antibiotic, reduces ethanol consumption in alcohol-preferring rats, *Alcohol Alcohol 46*, 239-246.

[116] Alajaji, M., Bowers, M. S., Knackstedt, L., and Damaj, M. I. (2013) Effects of the beta-lactam antibiotic ceftriaxone on nicotine withdrawal and nicotine-induced reinstatement of preference in mice, *Psychopharmacology (Berl) 228*, 419-426.

[117] Adinoff, B. (2004) Neurobiologic processes in drug reward and addiction, *Harv Rev Psychiatry 12*, 305-320.

[118] Kalivas, P. W. (2004) Glutamate systems in cocaine addiction, *Curr Opin Pharmacol 4*, 23-29.

[119] Cooper, S., Robison, A. J., and Mazei-Robison, M. S. (2017) Reward Circuitry in Addiction, *Neurotherapeutics 14*, 687-697.

[120] Volkow, N. D., Wang, G. J., Fowler, J. S., Tomasi, D., and Telang, F. (2011) Addiction: beyond dopamine reward circuitry, *Proceedings of the National Academy of Sciences of the United States of America 108*, 15037-15042.

[121] Rawls, S. M., Baron, D. A., and Kim, J. (2010) beta-Lactam antibiotic inhibits development of morphine physical dependence in rats, *Behav Pharmacol 21*, 161-164.

[122] Vanderschuren, L. J., and Kalivas, P. W. (2000) Alterations in dopaminergic and glutamatergic transmission in the induction and expression of behavioral sensitization: a critical review of preclinical studies, *Psychopharmacology (Berl) 151*, 99-120.

[123] Steketee, J. D., and Kalivas, P. W. (2011) Drug wanting: behavioral sensitization and relapse to drug-seeking behavior, *Pharmacological reviews 63*, 348-365.

[124] Carlezon, W. A., Jr., and Nestler, E. J. (2002) Elevated levels of GluR1 in the midbrain: a trigger for sensitization to drugs of abuse?, *Trends in neurosciences 25*, 610-615.

[125] Retzlaff, C. L., Kussrow, A., Schorkopf, T., Saetear, P., Bornhop, D. J., Hardaway, J. A., Sturgeon, S. M., Wright, J., and Blakely, R. D. (2017) Metallo-beta-lactamase Domain-Containing Protein 1 (MBLAC1) Is a Specific, High-Affinity Target for the Glutamate Transporter Inducer Ceftriaxone, *ACS chemical neuroscience*.

[126] Mergy, M. A., Gowrishankar, R., Davis, G. L., Jessen, T. N., Wright, J., Stanwood, G. D., Hahn, M. K., and Blakely, R. D. (2014) Genetic targeting of the amphetamine and methylphenidate-sensitive dopamine transporter: On the path to an animal model of attention-deficit hyperactivity disorder, *Neurochemistry international 73C*, 56-70.

[127] Lauderback, C. M., Hackett, J. M., Huang, F. F., Keller, J. N., Szweda, L. I., Markesbery, W. R., and Butterfield, D. A. (2001) The glial glutamate transporter, GLT-1, is oxidatively modified by 4-hydroxy-2-nonenal in the Alzheimer's disease brain: the role of Abeta1-42, *Journal of neurochemistry 78*, 413-416.

[128] Wiedenheft, B., Sternberg, S. H., and Doudna, J. A. (2012) RNA-guided genetic silencing systems in bacteria and archaea, *Nature 482*, 331-338.

[129] Qi, L. S., Larson, M. H., Gilbert, L. A., Doudna, J. A., Weissman, J. S., Arkin, A. P., and Lim, W. A. (2013) Repurposing CRISPR as an RNA-guided platform for sequence-specific control of gene expression, *Cell 152*, 1173-1183.

[130] Quig, D. (1998) Cysteine metabolism and metal toxicity, *Altern Med Rev 3*, 262-270.

[131] Segovia, G., Del Arco, A., and Mora, F. (1997) Endogenous glutamate increases extracellular concentrations of dopamine, GABA, and taurine through NMDA and AMPA/kainate receptors in striatum of the freely moving rat: a microdialysis study, *Journal of neurochemistry 69*, 1476-1483.

[132] Sun, W., and Rebec, G. V. (2006) Repeated cocaine self-administration alters processing of cocaine-related information in rat prefrontal cortex, *The Journal of neuroscience : the official journal of the Society for Neuroscience 26*, 8004-8008.

[133] Reissner, K. J., and Kalivas, P. W. (2010) Using glutamate homeostasis as a target for treating addictive disorders, *Behav Pharmacol 21*, 514-522.

[134] David, C. N., Frias, E. S., Szu, J. I., Vieira, P. A., Hubbard, J. A., Lovelace, J., Michael, M., Worth, D., McGovern, K. E., Ethell, I. M., Stanley, B. G., Korzus, E., Fiacco, T. A., Binder, D. K., and Wilson, E. H. (2016) GLT-1-Dependent Disruption of CNS Glutamate Homeostasis and Neuronal Function by the Protozoan Parasite Toxoplasma gondii, *PLoS Pathog 12*, e1005643.

[135] Mesci, P., Zaidi, S., Lobsiger, C. S., Millecamps, S., Escartin, C., Seilhean, D., Sato, H., Mallat, M., and Boillee, S. (2015) System xC- is a mediator of microglial function and its deletion slows symptoms in amyotrophic lateral sclerosis mice, *Brain 138*, 53-68.

[136] Bridges, R. J., Natale, N. R., and Patel, S. A. (2012) System xc(-) cystine/glutamate antiporter: an update on molecular pharmacology and roles within the CNS, *Br J Pharmacol 165*, 20-34.

[137] Lewerenz, J., Klein, M., and Methner, A. (2006) Cooperative action of glutamate transporters and cystine/glutamate antiporter system Xc- protects from oxidative glutamate toxicity, *Journal of neurochemistry 98*, 916-925.

[138] Coyle, J. T., and Puttfarcken, P. (1993) Oxidative stress, glutamate, and neurodegenerative disorders, *Science 262*, 689-695.

[139] Beal, M. F. (1996) Mitochondria, free radicals, and neurodegeneration, *Current opinion in neurobiology 6*, 661-666.

[140] Lu, S. C. (2009) Regulation of glutathione synthesis, *Mol Aspects Med 30*, 42-59.

[141] Drew, R., and Miners, J. O. (1984) The effects of buthionine sulphoximine (BSO) on glutathione depletion and xenobiotic biotransformation, *Biochem Pharmacol 33*, 2989-2994.

[142] Markovic, J., Mora, N. J., Broseta, A. M., Gimeno, A., de-la-Concepcion, N., Vina, J., and Pallardo, F. V. (2009) The depletion of nuclear glutathione impairs cell proliferation in 3t3 fibroblasts, *PLoS One 4*, e6413.

[143] Shrieve, D. C., and Harris, J. W. (1986) Effects of glutathione depletion by buthionine sulfoximine on the sensitivity of EMT6/SF cells to chemotherapy agents or X radiation, *Int J Radiat Oncol Biol Phys 12*, 1171-1174.

[144] Seib, T. M., Patel, S. A., and Bridges, R. J. (2011) Regulation of the system x(C)-cystine/glutamate exchanger by intracellular glutathione levels in rat astrocyte primary cultures, *Glia 59*, 1387-1401.

[145] Volterra, A., Trotti, D., Floridi, S., and Racagni, G. (1994) Reactive oxygen species inhibit high-affinity glutamate uptake: molecular mechanism and neuropathological implications, *Ann N Y Acad Sci 738*, 153-162.

[146] Volterra, A., Trotti, D., and Racagni, G. (1994) Glutamate uptake is inhibited by arachidonic acid and oxygen radicals via two distinct and additive mechanisms, *Molecular Pharmacology 46*, 986-992.

[147] Kim, Y. A., Kim, M. Y., and Jung, Y. S. (2013) Glutathione Depletion by L-Buthionine-S,R-Sulfoximine Induces Apoptosis of Cardiomyocytes through Activation of PKC-delta, *Biomol Ther (Seoul) 21*, 358-363.

[148] Armstrong, J. S., Steinauer, K. K., Hornung, B., Irish, J. M., Lecane, P., Birrell, G. W., Peehl, D. M., and Knox, S. J. (2002) Role of glutathione depletion and reactive oxygen species generation in apoptotic signaling in a human B lymphoma cell line, *Cell Death Differ 9*, 252-263.

[149] Kramer, R. A., Soble, M., Howes, A. E., and Montoya, V. P. (1989) The effect of glutathione (GSH) depletion in vivo by buthionine sulfoximine (BSO) on the radiosensitization of SR 2508, *Int J Radiat Oncol Biol Phys 16*, 1325-1329.

[150] Lee, H. R., Cho, J. M., Shin, D. H., Yong, C. S., Choi, H. G., Wakabayashi, N., and Kwak, M. K. (2008) Adaptive response to GSH depletion and resistance to L-buthionine-(S,R)-sulfoximine: involvement of Nrf2 activation, *Mol Cell Biochem 318*, 23-31.

[151] Kuhn, H., Angehrn, P., and Havas, L. (1986) Autoradiographic evidence for penetration of 3H-ceftriaxone (Rocephin) into cells of spleen, liver and kidney of mice, *Chemotherapy 32*, 102-112.

[152] Sutton, M. A., Karanian, D. A., and Self, D. W. (2000) Factors that determine a propensity for cocaine-seeking behavior during abstinence in rats, *Neuropsychopharmacology : official publication of the American College of Neuropsychopharmacology 22*, 626-641.

[153] Inui, T., Alessandri, B., Heimann, A., Nishimura, F., Frauenknecht, K., Sommer, C., and Kempski, O. (2013) Neuroprotective effect of ceftriaxone on the penumbra in a rat venous ischemia model, *Neuroscience 242*, 1-10.

[154] Araque, A., Parpura, V., Sanzgiri, R. P., and Haydon, P. G. (1999) Tripartite synapses: glia, the unacknowledged partner, *Trends in neurosciences 22*, 208-215.

[155] Araque, A., and Navarrete, M. (2010) Glial cells in neuronal network function, *Philos Trans R Soc Lond B Biol Sci 365*, 2375-2381.

[156] Zhang, J. M., Wang, H. K., Ye, C. Q., Ge, W., Chen, Y., Jiang, Z. L., Wu, C. P., Poo, M. M., and Duan, S. (2003) ATP released by astrocytes mediates glutamatergic activity-dependent heterosynaptic suppression, *Neuron 40*, 971-982.

[157] Kosir, M., and Podbregar, M. (2017) Advances in the Diagnosis of Sepsis: Hydrogen Sulfide as a Prognostic Marker of Septic Shock Severity, *EJIFCC 28*, 134-141.

[158] Verma, R., Mishra, V., Sasmal, D., and Raghubir, R. (2010) Pharmacological evaluation of glutamate transporter 1 (GLT-1) mediated neuroprotection following cerebral ischemia/reperfusion injury, *Eur J Pharmacol 638*, 65-71.